ADVANCES IN INORGANIC CHEMISTRY, VOL. 46

MANGANESE REDOX ENZYMES AND MODEL SYSTEMS: PROPERTIES, STRUCTURES, AND REACTIVITY

NEIL A. LAW, M. TYLER CAUDLE, and VINCENT L. PECORARO

Department of Chemistry, The University of Michigan, Ann Arbor, Michigan 48109

I. Introduction

Manganese is one of several first-row transition elements that have been employed by biological systems to assist in varied metabolic and structural roles. Manganese is used to give structural support to pro-

0898-8838/99 $25.00

teins and is a cofactor in chemical transformations that include hydrolytic and redox reactions. Perhaps the best known function, and the one of greatest importance to aerobic life, is in the oxygen-evolving complex, which oxidizes water to dioxygen during photosynthesis. Some representative reactions catalyzed by manganese-containing enzymes are shown in Scheme 1.

Oxygen Evolving Complex

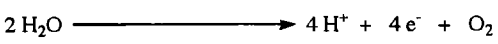

Manganese Catalase

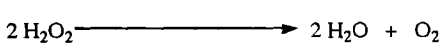

Manganese Superoxide Dismutase

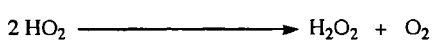

Arginase

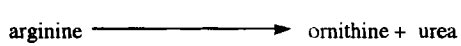

Manganese Ribonucleotide Reductase

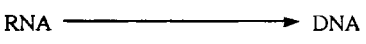

SCHEME 1.

Several enzymes are known that naturally contain manganese. Most of these employ manganese in nonredox roles (*1*), for example conducting hydrolytic reactions, a Lewis acid role, or utilizing Mn^{II} to provide structural support to a protein so that it may maintain a specific conformation. For example, pyruvate carboxylase binds Mn^{II} tightly, but the Mn^{II} is not involved in the enzyme's catalytic process, thus playing a structural role (*2*). Several binuclear metallohydrolases are known that contain a binuclear Mn^{II}_2 site (*3–5*). Many of these may be categorized as phosphohydrolases, hydrolyzing phosphate groups from a substrate molecule. Hydrolases are often activated by more than one M^{II} element, although at least one is specific for manganese.

One particularly key metallohydrolase that contains manganese is the enzyme arginase (*4–7*), an enzyme for which a crystal structure

at 2.1-Å resolution has recently been solved for the arginase enzyme from rat liver (Fig. 1) (*8*). This enzyme catalyzes the hydrolytic conversion of arginine to urea and ornithine. Arginase is found in a great variety of organisms for the removal of nitrogen-containing wastes and is therefore integral to the biological cycle of nitrogen. Many of the binuclear hydrolases may be active with metals other than Mn at their active sites, but arginase has been shown to specifically require manganese to be fully functional (*5*). The active site contains a binuclear Mn_2^{II} dimer bridged by a bidentate carboxylate and two μ_2-"O" donor bridges, a monodentate carboxylate, and a solvent molecule derived hydroxide (or perhaps water at lower pH, the crystals were grown at pH 8.5). The catalysis of this reaction involves a bridging μ-OH unit, which is formed according to a mechanistic proposal by loss of a proton from a water molecule upon binding of substrate. This hydroxide is believed to be ideally situated for forming the intermediates required for arginase hydrolysis (*8*). Finally, arginase has recently been reported to exhibit some redox activity, catalyzing the disproportionation of hydrogen peroxide and peroxidase activity (discussed later) (*9*, *10*).

Manganese(II) ions may also be employed in the hydrolases that compose the ribonuclease H domain of reverse transcriptases (*3*, *4*). Many of these enzymes, which may employ either Mn^{II} or Mg^{II}, are found in a variety of organisms where they may or may not be essential (e.g., *Escherichia coli*) (*3*, *4*). This class of enzymes catalyzes the hydrolysis of DNA–RNA hybrids. However, retroviral reverse transcriptases are critical for the replication of retroviruses, and Mn^{II} may be the required cofactor for these ribonuclease hydrolases to function (*3*, *4*). One example of this family of hydrolase enzymes is the RNase H enzyme from HIV-I. This enzyme has been crystallographically characterized (*11*). In the crystal structure at 2.4-Å resolution, the two Mn^{II} ions are separated by a distance of about 4 Å. They are bound to carboxylate residues that are located near the surface of the enzyme. One of these carboxylates bridges the two manganese

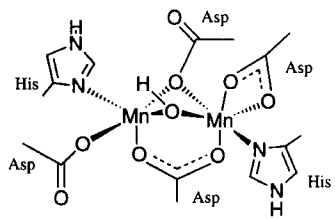

FIG. 1. Structure of the active site of the rat liver arginase enzyme based on (*8*).

ions in a motif that is now recognized as a common structural element in many binuclear metalloenzyme active sites (discussed later). Some controversy with respect to the active sites of ribonuclease enzymes does exist, with some reports suggesting that there may be only one metal ion present (or perhaps required) in the active enzyme (*12*, *13*).

Concanavalin A, a lectin, is another interesting nonredox manganese-containing enzyme that is found in various forms in plants and animals (*14*, *15*). Lectins are a class of enzymes known to bind small carbohydrate molecules (*16*, *17*). The active site of crystallographically characterized concanavalin A enzyme shows a six-coordinate Mn^{II} bridged via two carboxylate-bearing protein residues to an approximately seven-coordinate Ca^{II} ion (Fig. 2) (*14*, *15*, *18*). The calcium and manganese ions are separated by about 4.2 Å. Concanavalin A is an interesting case of a mixed metal active site in a biological system. If the Ca^{II} is replaced by another Mn^{II} ion, an EPR spectrum consistent with a weakly coupled Mn_2^{II} system is observed (*19*, *20*). Newer crystal structures of concanavalin A with the substrate methyl-α-D-mannopyranoside have been reported. The more recent structure in 1994 has a resolution of 2.0 Å. These structures show that methyl-α-D-mannopyranoside is bound near the metal binding site, about 8.7 Å from the calcium and about 12.8 Å from manganese (*21*). The 1994 structure also indicates that a water bound to the calcium may be involved in hydrogen bonding to the carboxylate-bearing protein residues, which are in turn hydrogen bond to the methyl-α-D-mannopyranoside (*18*). Finally, a new crystal structure for concanavalin A at 0.94-Å resolution has been solved (*22*).

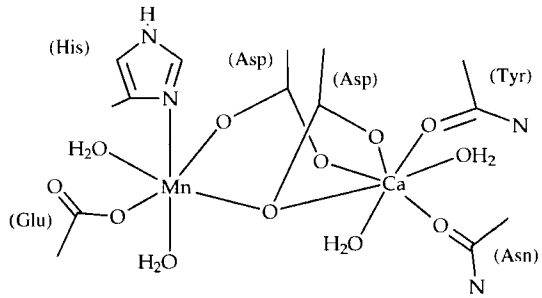

FIG. 2. Structure of the manganese and calcium dimer in concanavalin A, based on (*14*, *15*, *18*, *22*).

Redox chemistry is another facet of the biological chemistry of manganese, and various enzymes employ manganese at mono-, bi-, and tetranuclear sites. Three mononuclear manganese enzymes are currently known that catalyze redox-based chemical transformations. These are manganese superoxide dismutase, manganese peroxidase, and manganese^{II} dioxygenase. Catalase and the manganese ribonucleotide reductase are two known manganese enzymes that undertake redox transformations that utilize a binuclear manganese site, and a tetranuclear cluster of four manganese is found in the oxygen evolving complex (OEC) of Photosystem II (PS II), the site where water is oxidized during the photosynthetic process to yield dioxygen.

The focus of this review will be on mono- and multinuclear redox active manganese systems, and in particular, the relation of bi-, tri-, and tetranuclear manganese complexes as models for the multinuclear manganese-containing enzymes. Aspects of the structurally characterized compounds, spectroscopic features of synthetic compounds and magnetochemistry will also be discussed. The reactivity of complexes will also be addressed, with respect to epoxidation and catalase models, for example. Throughout, discussion will relate our current knowledge of manganese chemistry to the broader area of biological systems. Before addressing the synthetic complexes and their properties in detail, a brief overview of some of the redox-active manganese enzymes will be presented. Finally, several reviews of manganese coordination complex chemistry have appeared in recent years. Among these are reviews by Wieghardt, Pecoraro and co-workers, Vincent and Christou, Brudvig and Crabtree, and Dismukes and co-workers, which have focused on a wide range of model systems, manganese–dioxygen interactions, mechanistic considerations of reactivity studies, and single systems such as the OEC (*5*, *23–50*). The 1992 book "Manganese Redox Enzymes" (*28*) also contains much relevant information about biological manganese chemistry by a variety of researchers. A 1996 issue of *Chemistry Reviews* focusing on bioinorganic chemistry contains several reviews that are pertinent to the biological role of manganese (*3*, *33*, *37*). In addition, several reviews aimed solely at the OEC are also available, including reviews by Debus (*42*) and the recent book "Oxygenic Photosynthesis: The Light Reactions" edited by Ort and Yocum (*48*). Finally, the Proceedings of the Photosynthesis Conference, held periodically, presents short updates from research groups around the world as they work to comprehend this intricate system (*51*).

II. The Enzymes

A. Manganese Superoxide Dismutase, MnSOD

Manganese superoxide dismutase (MnSOD) is a redox-active manganese enzyme that employs a mononuclear manganese ion at its active site. Discovered in 1970 (*52*), this enzyme catalyzes the dismutation of superoxide (HO_2), to dioxygen and hydrogen peroxide, as shown in Scheme 2. Superoxide is the radical, one-electron-reduced

$$Mn^{3+} + HO_2^{\cdot} \longrightarrow Mn^{2+} + O_2 + H^+$$
$$Mn^{2+} + HO_2^{\cdot} + H^+ \longrightarrow Mn^{3+} + H_2O_2$$

Scheme 2.

form of dioxygen. MnSOD is found in a broad range of species that run the gamut from bacteria to humans (*53*). It is a member of one of the two families of superoxide dismutase enzymes, the first of which is the family that contains MnSOD and the analogous iron superoxide dismutase, FeSOD. A high degree of sequence homology exists between the two types of enzymes, and the active sites of both enzymes employ the same types and orientations of protein residues to generate a trigonal bipyramidal geometry about the active site metal (*54–61*). The second family contains the structurally distinct copper/zinc superoxide dismutase, CuZnSOD (*62*, *63*). Recent reports have indicated that a new group of nickel superoxide dismutase enzymes might also exist (*64*). Superoxide and superoxide dismutases have been the subject of a variety of reviews (*5*, *29*, *53*, *65*).

Superoxide, HO_2, is produced naturally by several enzymes and was first recognized as an intermediate of aerobic respiration in 1968 (*62*, *66–68*). Although it may be utilized beneficially, for example by macrophages to fight an infection (*69*), it is generally not a benign byproduct. Therefore, SODs are critical to aerobic life forms, in which they perform the important role of protecting an organism from the deleterious effects of superoxide. Although HO_2 may not be the direct cause of oxidative damage to an organism due to its relatively short life span (self dismutation occurs at a rate of $2.0–3.2 \times 10^5$ $M^{-1} \cdot s^{-1}$) (*52*), it is sufficiently long-lived to allow it to engender chemical compounds such as hydrogen peroxide or hydroxyl radical, $HO\cdot$, which readily cause oxidative damage to cellular components (*70*). Another aspect of superoxide chemistry is the growing research into peroxynitrite (*71–74*), which can be formed from nitrite and superoxide. Thus, superoxide has been implicated as a participant in a vari-

ety of destructive processes affecting DNA, cell membranes, arteriosclerosis and the damage that is caused to cells deprived of oxygen, ischemia, during a stroke or heart attack due to an increased output of superoxide once oxygen is restored to the affected cells and their enzymes (*69*, *71*, *72*).

MnSOD is often found as a homodimer or homotetramer, with approximately one manganese per monomer subunit (*53*). A few of these enzymes have been crystallographically characterized, including the enzyme from human mitochondria (*75*) and the enzyme from the bacterium *Thermus thermophilus* (*76*). The active sites of these enzymes have been shown to contain a single manganese bound by three histidines, one aspartate, and either a water or hydroxide in a trigonal bipyramidal geometry as shown in Fig. 3, based on the *T. thermophilus* structure (*76*). In this structure, two of the histidine residues and the aspartate form the equatorial plane, and the third histidine and water/hydroxide occupy the axial positions. Other structures of this enzyme with azide in the active site indicate that the coordination number of the manganese may be expanded to accommodate a sixth ligand, for example, superoxide during turnover (*58*).

MnSOD catalyzes the dismutation of HO_2 into dioxygen and hydrogen peroxide. As a redox enzyme, it shuttles between the Mn^{II} and the Mn^{III} oxidation states (*77*). This process has been studied, and the enzyme has been shown to catalyze this reaction at a rate of $1–2.2 \times 10^9$ $M^{-1} \cdot s^{-1}$, which is at the diffusion limit (*52*). A representation of the proposed catalytic cycle is shown in Scheme 3 (*78*). Several studies on MnSOD kinetics have been published (*78–82*). Early studies on the reaction of MnSOD from *Escherichia coli* and *Bacillus thermophilus* indicated evidence for a four-step process involving two fast and

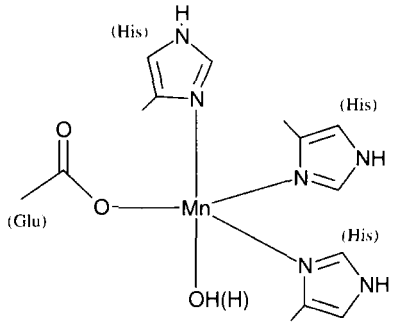

FIG. 3. Structure of the active site of manganese superoxide dismutase, based on (*76*).

two slower steps (*79*, *80*). Later studies utilizing stopped-flow techniques refined this further. Saturation kinetics were observed for the *T. thermophilus* MnSOD, and the data showed that there were three phases to this reaction: a fast "burst" phase of quick HO_2 dismutation, a slower second phase, and a final fast phase (*78*). A "dead-end" form of the enzyme was implicated to account for the slow phase (*78*). This has been formulated as a side-on-bound Mn^{III}–peroxo species based on spectroscopic similarities to manganese model complexes with side-on-bound peroxy groups (*83*). Such phases are not observed for FeSOD (*84*).

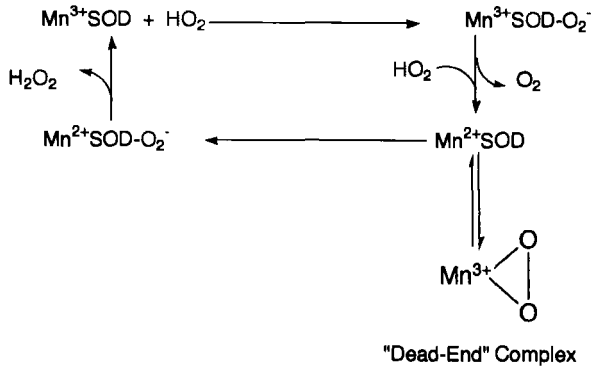

SCHEME 3.

B. MANGANESE(II) DIOXYGENASE

There now exist three reported Mn(II) dioxygenase enzymes. The most extensively studied of these is the Mn(II) dioxygenase from *Arthrobacter globoformis* CM-2 (*85*). The first Mn(II) dioxygenase was reported in 1981 from *Bacillus brevis* (*86*). Dioxygenases catalyze the incorporation of dioxygen into an organic substrate (*87*). In this case, the substrate is an aromatic compound that contains a catechol *cis*-diol structure. These reactions are important in that they catalyze the degradation of aromatic compounds to simpler carbon components for action by other enzymes. In addition, the ability of dioxygenase enzymes to initiate the decomposition of aromatic compounds may be useful in the bioremediation of sites contaminated with aromatic organics of this type (*88*).

Most of the known dioxygenases contain iron, and these enzymes tend to be very specific in their function (*87*, *89*). For example, the

Fe(III) dioxygenases have generally been shown to be intradiol dioxygenases, meaning that they cleave the aromatic ring between the *cis*-diols. The Fe(II) dioxygenases are classified as extradiol dioxygenases and cleave to the aromatic ring to one side of the diol moiety. Substrate specificity is also exhibited to various degrees, with many dioxygenases preferentially cleaving one substrate over others (*89*). The Mn(II) dioxygenases characterized to date belong to the class of extradiol dioxygenases (*86*, *90*).

Although none of the Mn(II) dioxygenases have been structurally characterized, a recent structure has appeared for an Fe(II) dioxygenase (*91*). Whereas the Fe^{III} enzymes have phenolate and histidine ligands, the Fe^{II} was bound to the protein by two histidines and a glutamate, with two waters completing the first coordination sphere. The geometry about the iron atom is square pyramidal, with one of the histidines occupying the axial position (Fig. 4). Finally, some evidence for an Fe^{II}/Mn^{II} dioxygenase correspondence similar to that observed for MnSOD/FeSOD might also exist, as evidenced by the conserved residues that form the metal binding sites of these dioxygenases (*92*). Thus, this manganese enzyme may have a structure similar to the iron site.

The details of the reactions of the iron dioxygenases have been extensively probed for the Fe(III) enzymes and more recently for the Fe(II) dioxygenases (*87*, *89*). These two groups of enzymes exhibit different catalytic processes. For both of these types of enzymes, though, it has been shown that although the reaction catalyzed is redox in nature, the central metal does not cycle between discrete oxidation states during the reaction. A resonance form of an intermediate, however, has been proposed to exist briefly as Fe^{III} for the Fe(II) dioxygenases. A recent proposal for the catalytic cycle of an Fe(II) dioxygenase is presented in Scheme 4 (*89*, *93*). The catechol substrate is thought to bind as a monoanion to the central metal ion followed by the coordi-

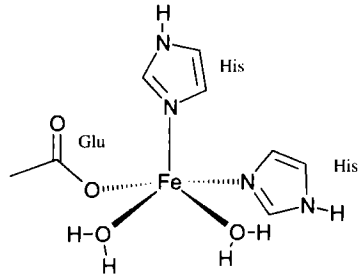

FIG. 4. Structure of the active site of an extradiol iron(II) dioxygenase, based on (*91*).

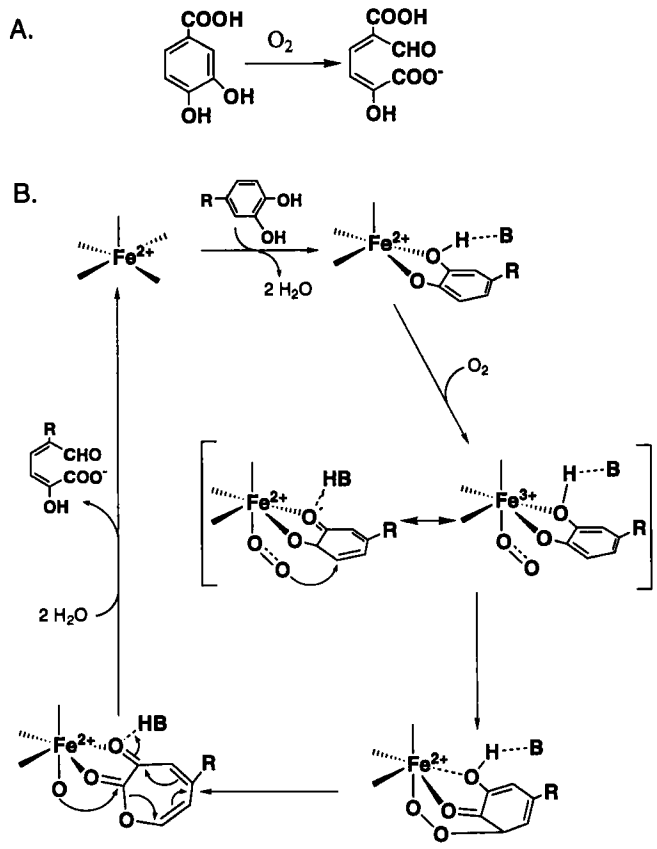

SCHEME 4. A proposed mechanism for extradiol Fe(II)dioxygenases. [Adapted with permission from (*89*). Copyright 1996 the American Chemical Society.]

nation of a dioxygen molecule to the metal, which might be formally considered to be a superoxide bound to an Fe^{III}. It is believed that substrate binding activates the metal center for binding dioxygen, based on the increased affinity for binding nitrosyl to the active site iron in the presence of substrate (*89*). Attack of the "superoxide group" on the carbon adjacent to the catechol moiety followed by rearrangement to give the product and the product's release complete the catalytic cycle. This mechanism contrasts with the Fe(III) dioxygenase mechanism, wherein the iron activates the substrate for direct attack of dioxygen on the aromatic ring of the substrate. The reaction rate of the manganese containing *A. globoformis* enzyme, with its primary substrate 3,4-dihydroxyphenylacetate, has been measured, yielding values of k_{cat} = 1400 min^{-1}, and K_m = 7 μM (*85*). It is likely

that a similar mechanism exists between the Fe^{II} and Mn^{II} enzymes (*89*, *90*).

1. Modeling Features, MnSOD and Mn(II) Dioxygenase

These two enzymes present a unique challenge for the synthesis of small-molecule model complexes. First, the MnSOD has been shown to have an active site with a trigonal bipyramidal geometry about the manganese ion, whereas the Mn(II) dioxygenase most likely contains a square pyramidal geometry about the manganese ion in accord with the Fe(II) dioxygenase structure. Few complexes of manganese in a trigonal bipyramidal geometry are known, and these are predominately of Mn^{II}, whereas the MnSOD enzyme has been crystallographically characterized with a trigonal bipyramidal geometry about the manganese in both the Mn^{II} and Mn^{III} oxidation states. In the case of the Mn(II) dioxygenase, the structure is probably square pyramidal by analogy with the Fe(II) dioxygenase structure. Square pyramidal complexes are the more common form for five-coordinate manganese complexes, but this geometry is most often observed for the Mn^{III} oxidation state due to the presence of the pseudo-Jahn–Teller distortion axis, and not Mn^{II}.

The reactivity of model compounds is also key to gaining a better understanding of an enzyme. The MnSOD presents a number of challenges, the first of which is catalytic dismutation of superoxide. Many Mn compounds are known to interact (discussed later) with superoxide, but few have been shown to be catalytic in nature. The unique characteristics of the catalytic cycle, with the "dead-end" complex, also provides challenges for synthesis. Further, there has been some interest in recent years in the use of manganese complexes as pharmaceutical superoxide dismutase agents to aid in reducing cellular damage by superoxide, for example in the wake of a heart attack, which opens questions of the biological compatibility interactions of the complexes and their solution behavior at physiological pH values.

C. Manganese Peroxidase, MnP

Manganese peroxidase (MnP) is an unique enzyme in many respects. It is an extracellular enzyme that involves a heme protoporphyrin IX for the oxidation of Mn^{II} to Mn^{III} (*94*, *95*). A crystal structure at 2.06-Å resolution of the manganese peroxidase from the white rot basidiomycete *Phanerocaete chrysosporium*, which utilizes this enzyme to degrade lignin, appeared in 1994 (*96*). The active site (Fig. 5) and the overall structure are quite similar to lignin peroxidase (LiP),

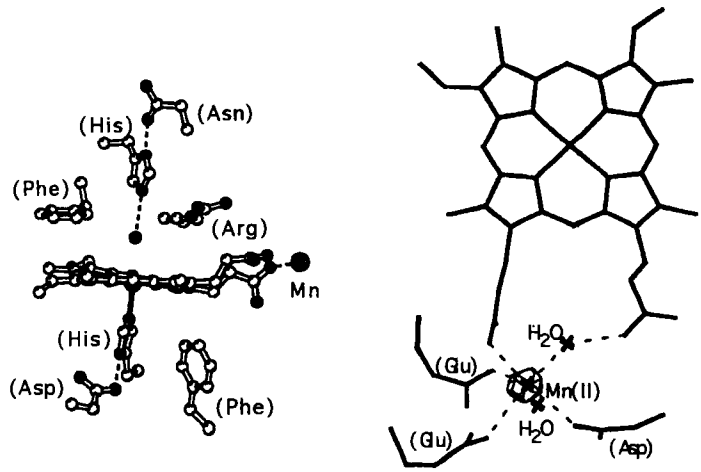

FIG. 5. Structure of the active site of MnP. The left half is a side-on view of the active site showing the protoporphyrin IX, the bound proximal histidine, and the water and histidine poised on the opposite face. The right half is a "top"-down view showing the heme and the bound Mn^{II}, and the additional protein residues that act as ligands to Mn^{II}. [Adapted with permission from (*96*). Copyright 1994, The American Society for Biochemistry and Molecular Biology.]

an enzyme with which MnP shares a significant sequence homology (*96*). The white rot fungi are some of the only species known that are able to degrade lignin (*97–99*). Furthermore, MnP itself is one of only two, or perhaps three, enzymes that are known to degrade lignin. The related LiPs are the other lignin-degrading enzymes that have been known since the early 1980s (*98*, *99*). Meanwhile, a few more recent reports have suggested that some fungi may also utilize a laccase in addition to MnP and LiP to facilitate lignin degradation (*100*, *101*). The MnP and LiP enzymes catalyze the biodegradation of lignin to phenolic residues that can then be further decomposed. Lignin, found predominantly in plant cell walls, is a random three-dimensional polymeric material composed of phenolic residues that is thought to be the second most common biopolymer after cellulose. Lignin comprises a significant portion of woody plants, with lignin content values ranging from 15 to 36% (*97–99*, *102*). Lignin is also found in a variety of other vascular plants. The major role of lignin in the plant is to provide support and protection for plant tissue (*98*, *99*). The lignin-degrading peroxidases act on lignin by initiating one-electron oxidations that lead to the breakdown of the linkages that connect the building blocks of this material. It has been shown that the decomposition of cellulose is retarded by lignin, probably as a result of lignin

interfering with access to the cellulose (*98*, *99*). [As has been pointed out, the importance of the degradation of lignin is underscored by the extensive amounts of carbon employed in lignin and cellulose manufacture by plants and the interplay that this may have with respect to the cycling of carbon on the globe (*97–99*).] Thus, the Mn-catalyzed degradation of lignin may be designed to allow the fungus access to the cellulose (*98*, *99*).

MnP functions by the oxidation of the heme by hydrogen peroxide to form compound I, $Fe^{IV}=O(P^{+\cdot})$ (Scheme 5). (*95*, *103–106*). The oxidized heme then oxidizes a Mn^{II} that is bound to at least one of the

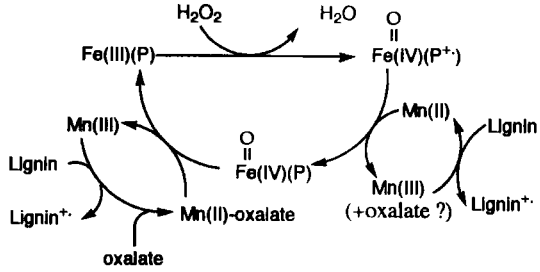

SCHEME 5.

two propionate arms of the heme group in a site located near the edge of the enzyme, an observation based on the recently solved crystal structure of the *P. chrysosporium* enzyme (*96*). This forms a Mn^{III} ion and Compound II, Fe(IV)=O. The Mn^{III} then diffuses away from the enzyme to oxidize lignin. In this way, the enzyme can work on the random structured polymer, where structural specificity may be a problem for an enzyme and where Mn^{III} may diffuse more easily into the substrate than a larger enzyme would be able to do. The Mn^{III} initiates a one-electron oxidation, most likely forming an initial phenoxy radical cation, that triggers a cascade of oxidations that eventually break down the linkages between the lignin subunits. Compound II is then reduced to the resting Fe^{III} oxidation state by oxidizing a second equivalent of Mn^{II}. This step absolutely requires manganese, preferentially a Mn^{II}–oxalate complex (*105*), unlike the first step, which will function with substrates other than manganese (*103*). A new addition to the chemistry of lignin peroxidases is the observation that LiPs are also capable of oxidizing Mn^{II} to Mn^{III} in the presence of oxalate (*107*). Thus, some LiPs may also act as a manganese peroxidase.

Oxalate and similar small molecule chelators play a key role in the

function of MnP (*104–109*). Oxalate and malonate have been observed to be excreted in active MnP-producing cultures (*104*), and they have been shown to promote enzyme activity (*105*, *106*, *108*, *109*). One of the roles proposed for the small molecules is to aid in the diffusion process of Mn^{III} and to stabilize the Mn^{III} from disproportionating to Mn^{II} and Mn^{IV} so that it may reach the target lignin and initiate the depolymerization of lignin (*95*, *103*). It is not known whether oxalate binds with manganese to the enzyme during the reduction of Compound I to Compound II or whether a small molecule is taken up to assist departure of Mn^{III} from the enzyme. No evidence for oxalate or other small molecules bound to manganese were observed in the crystal structure other than water. It is known, however, that without the oxalate or a related small chelating molecule, turnover is reduced (*104–106*). Furthermore, studies suggest that the manganese required for the reduction of Compound II must bind with the exogenous ligand oxalate (*105*, *106*). Experiments with α-hydroxy acids such as lactic acid or small organic acids such as malonic acid, showed that such compounds also appeared to promote the activity of MnP (*95*, *103*). However, related compounds that could form stronger complexes with manganese were found to inhibit the enzyme, presumably by out-competing the enzyme system for binding Mn^{II}. It was proposed that these compounds might facilitate the diffusion of Mn from the enzyme and in that way lead to enhanced reactivity. Roles for oxalate beyond the reduction of Compound II (e.g., assisting in the diffusion of Mn^{III}) remain controversial (*104–107*, *109*). Oxalate is known to be decarboxylated in the presence of Mn^{III}, so it may not be utilized in Mn^{III} diffusion, although that may be a role for the malonate. One other proposal for the role of oxalate was the reduction of Mn^{IV} O_2, which is known to form near these enzymes, to return the manganese to a functional oxidation state. Some model work has addressed these points, and although unstable, such Mn^{III}-oxalate complexes may have lifetimes sufficient for them to reach the substrate and initiate oxidation before they would completely decompose.

Finally, there is a functional similarity between the MnP and LiP enzymes (*110*). LiP has been shown to be able to oxidize Mn^{II} (*107*). Further, it has been shown that a veratryl alcohol is produced in conjunction with LiP, and it has been suggested that this compound may serve LiP in a capacity similar to that served by Mn^{II} in MnP (*109*).

Functional mimic systems for the MnP enzyme will be discussed in Section V, "Reactivity." An example of monomeric complexes prepared with α-hydroxy acids as functional mimics is presented in Section III.A.3 on monomeric structures.

D. Manganese Ribonucleotide Reductase, MnRR

The conversion of ribonucleotides into deoxyribonucleotides for the synthesis of DNA is key to the survival of any DNA-based life form. This process is completed by one of a variety of ribonucleotide reductases that reduce the furanose ring of a ribonucleic diphosphate acid monomer by replacing a hydroxyl functional group at the 2′-position with a hydrogen (Scheme 6) to generate the deoxyribonucleic acid

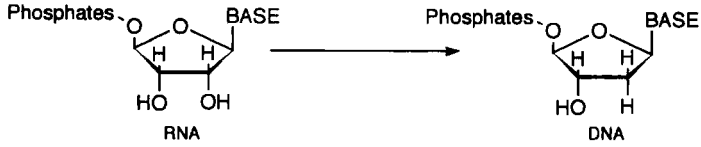

Scheme 6.

monomers necessary for DNA synthesis (*111–114*). Ribonucleotide reductases have been identified with a wide variety of protein structures and active site compositions. Many are known that contain a diiron core (in the oxidized form of FeRR, the active site contains an Fe_2^{III} dimer bridged by a μ-oxo and a μ-carboxylato), a stable tyrosine radical, and potentially redox active thiols in the form of cysteines at the active site (*114*, *115*). The role of the diiron dimer is to generate the stable tyrosyl radical, which in turn initiates a transient thiyl radical at the active site (*114*, *115*). Two other classes of ribonucleotide reductases have also been identified; one is based on adenosylcobalamin (*114*, *116*) and the other, which is found in strictly anaerobic microorganisms, likely utilizes a glycyl radical in conjunction with *S*-adenosylmethionine to reduce RNA. These enzymes have been grouped as Class I, Class II, and Class III ribonucleotide reductases, respectively (*116*). A fourth segment of these enzymes is represented by the manganese-based ribonucleotide reductases, which probably function in a manner similar to the iron ribonucleotide reductases (discussed later) and, therefore, may fall under the Class I umbrella (*116*). The MnRR enzyme is a bacterial enzyme, and is widely distributed among the Coryneform and related bacteria (*111*, *117*, *118*). Several members of this group of bacteria have been shown to absolutely require manganese for the transformation of RNA into DNA. The MnRR enzyme from *Corynebacterium* (formerly *Brevibacterium*) *ammoniagenes* has been the most studied member of this group (*111*).

The FeRR system has been extensively studied (*112*, *114*). For this type of ribonucleotide reductase, the enzyme is comprised of two subunits, known as R1 and R2 (or occasionally B1 and B2). The R1 and

R2 subunits are each comprised of a homodimer of the α- and β-polypeptides, respectively (*112*, *114*), and both the R1 and R2 subunits have been crystallographically characterized (*119–122*). The active site for RNA reduction is located on the R1 subunit. The oxidized diiron site and the stable tyrosine radical are located in the R2 subunit. The diiron site is comprised of two Fe^{III} ions, bridged by an oxo and a carboxylate, with an Fe–Fe distance of 3.3 Å. The reduction of RNA begins with the abstraction of a hydrogen atom from the 3′-position of the furanose ring by a transient thiyl radical. This is believed to be generated via an electron-transfer mechanism that allows the tyrosyl radical to form a thiyl radical from one of the cysteines located at the active site. In addition to that cysteine, a pair of redox-active cysteines is located at the active site. This pair of cysteines is then proposed to be oxidized to a disulfide-linked moiety in conjunction with substrate reduction. In the first step, a hydrogen atom is abstracted by the thiyl radical from the 3′-position on the furanose ring. A proton from one of the redox-active cysteines is transferred to the hydroxyl group of the 2′-position to form a water-molecule-leaving group. Completion of the oxidation to the disulfide and the regeneration of the initial thiyl radical by H-atom transfer to the 3′-position of the furanose yields the DNA monomer product (Scheme 7) (*114*, *115*). The disulfide linkage is then believed to be reduced by another enzyme system to regenerate the active site (*115*). For several of the MnRR systems, a thioredoxin/NADPH-dependent thioredoxin reductase system is thought to complete this phase of the process (*123*).

Although an X-ray crystal structure of MnRR has not been solved to date, a structure with Mn substituted into the iron ribonucleotide reductase has been reported (Fig. 6) (*124*). In this case, the two manganese(III) ions were bridged by two carboxylates from protein residues, but without the oxo bridge postulated for the active Fe_2^{III} form of the FeRR enzyme. This inactive enzyme with manganese was proposed as a model for the inactive Fe_2^{II} form of the iron enzyme and is

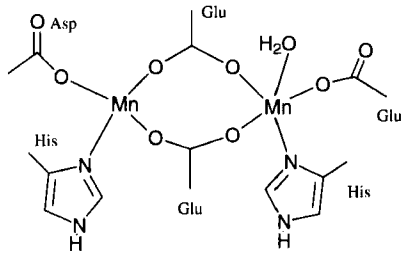

FIG. 6. Structure of the Mn^{II}-substituted FeRR enzyme, based on (*124*).

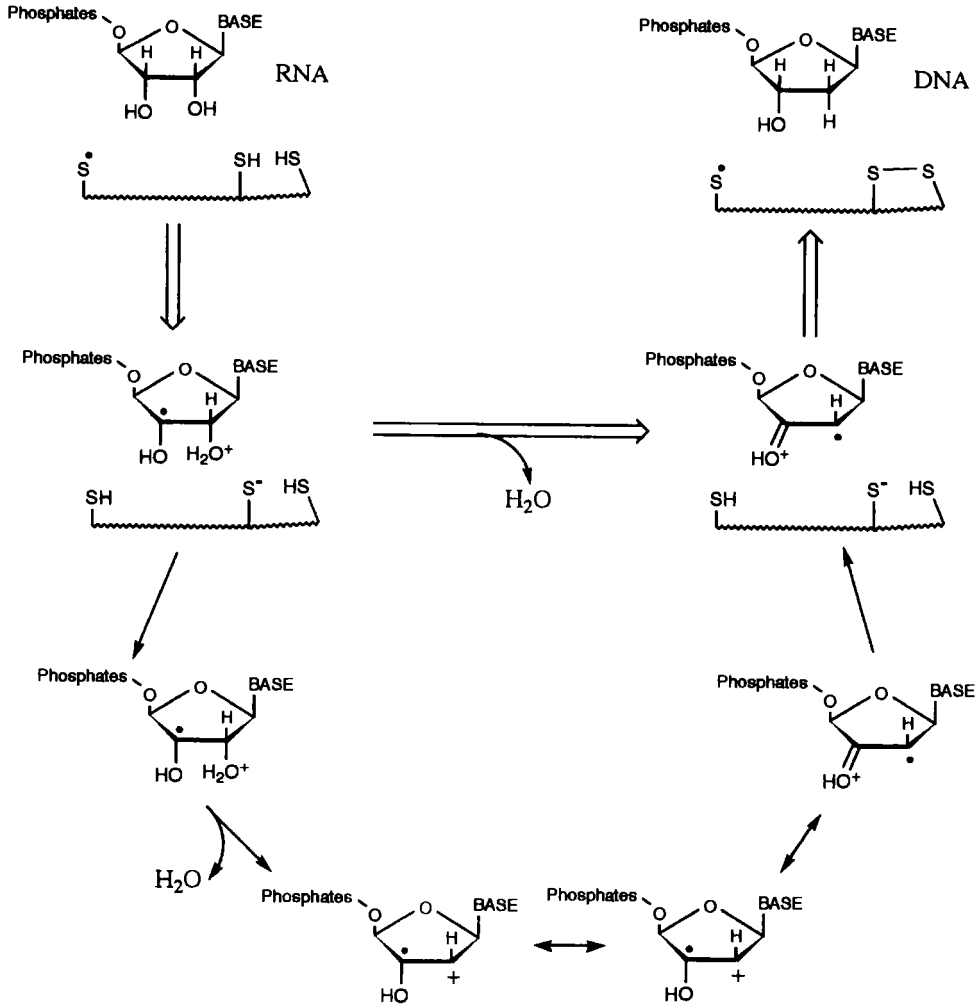

SCHEME 7. A partial proposed mechanism for the functioning of iron ribonucleotide reductase. Manganese ribonucleotide reductase may function in a similar manner. [Adapted with permission from (*113*) and (*111*). Copyright 1994, Current Biology Publishers, and Copyright 1994 Marcel-Dekker, Inc., respectively.]

quite similar to the structure of the reduced Fe_2^{II} active site which has since been crystallographically determined. Based on UV-visible spectroscopy of MnRR and the similarity that this spectrum bears to that observed for catalase and to model oxo-, carboxylato-bridged Mn^{III} dimer complexes, the active site structure of MnRR is proposed to include the Mn–O–Mn structural motif (*111*). This would also be similar to the active site structures observed for FeRR. This proposal is

further bolstered by the recent crystal structure of the catalase from the bacterium *Thermus thermophilus* (*125*) (discussed later), which generally corroborates the postulated catalase μ-carboxylato-, μ-oxo-bridged Mn dimer motif for the catalase active site structure. In addition, the assignment of a Mn_2^{III} oxidation state is supported by the EPR silence of this enzyme with respect to the observation of any signal arising from a manganese dimer (*111*).

MnRR converts all four RNA bases into their corresponding DNA products (*111*, *123*), and the overall enzyme is considered to be structurally similar to FeRR (*111*). For example, MnRR is comprised of R1 and R2 subunits that are analogous to those of FeRR. A mechanistic similarity between these two systems, however, was not certain. No radical signal equivalent to the FeRR tyrosyl radical had been observed for MnRR prior to 1996 (*126*). One tantalizing piece of evidence was the hydroxyurea sensitivity of MnRR, a trait also observed for FeRR. Hydroxyurea is known to quench the FeRR tyrosyl radical (*118*). In the meantime, proposals for this lack of a radical signal had been put forward. One proposal suggested that the coupling of a stable protein radical to the Mn of MnRR might account for the lack of any observed radical by EPR in MnRR (*111*). Another suggested that the manganese dimer might engage more directly in the RNA-to-DNA conversion process, perhaps by abstracting the initial hydrogen atom itself to initiate the reduction process, in a role distinctly different from that proposed for the diiron site of FeRR (*111*). Proposals that mirror FeRR, however, may now, in light of the radical signal that has recently been observed in the MnRR R2 subunit, be reasonably considered (*126*). Unlike the relatively stable FeRR enzyme radical, though, the MnRR radical only has a half-life of 1.5 h. It was only after developing a "fast" isolation technique for this subunit that Auling and co-workers were able to observe this radical signal in the EPR. By analogy, this radical is proposed to be located on tyrosine residue. Finally, the presence and concentration of the radical signal were shown to correlate with the activity of an MnRR sample (*126*). Otherwise, little is known about the exact identity or proximity of this radical to either the manganese dimer or the substrate binding sites.

E. Manganese Catalase

Catalase is yet another manganese-containing enzyme that interacts with dioxygen or its reduced forms. The role of this manganese enzyme is to protect the organism from oxidative damage that may be caused or initiated by the presence of hydrogen peroxide, such as in the interaction of hydrogen peroxide with Fe^{II} in Fenton-like chem-

istry to generate HO·63. To date, manganese-containing catalases have only been found in bacteria—for example, the enzymes from *Lactobacillus plantarum* (*127*, *128*), *Thermoleophilum album* (*129*), and *T. thermophilus* (*130*, *131*). Several reviews with respect to the catalase itself and the modeling chemistry of this enzyme have appeared in recent years (*3*, *5*, *23*, *25*, *26*, *29*, *30*, *38*).

The catalase enzyme that utilizes manganese instead of a heme group to catalyze the disproportionation of hydrogen peroxide to dioxygen and water was known for several years before the presence of manganese was confirmed in 1983 (*128*). A low-resolution crystal structure in 1985 indicated that the enzyme from *T. thermophilus* contained a binuclear manganese site, with a Mn–Mn separation of about 3.6 Å (*130*, *131*). This was further supported by evidence from optical spectroscopy that suggested that the active site contained two manganese ions that were bridged by one oxo, μ-O^{2-}, and at least one carboxylate ligand based on spectroscopic comparisons to oxo- and carboxylato-bridged manganese model complexes (*30*, *132*, *133*). Extended X-ray absorption fine structure (EXAFS) studies of this enzyme suggested that the first coordination sphere about the manganese of the catalase consisted of O/N donors (*134*, *135*). The presence of the dimer was further bolstered by the observation of EPR spectra consistent with a coupled manganese dimer, for example the $Mn^{III}Mn^{IV}$ EPR spectrum of the "superoxidized" enzyme (*136*). EXAFS showed that this "superoxidized" catalase has a Mn–Mn vector of 2.7 Å, consistent with a $Mn_2(\mu_2\text{-}O^{2-})_2$ core. Very recent reports of crystal structures at resolutions of 1.6 Å for the reduced, Mn_2^{II}, and 1.4 Å for the oxidized, Mn_2^{III}, forms of the enzyme from *T. thermophilus* confirm much of what had been proposed for the structure of the catalase's active site (*125*). A representation of these results is shown in Fig. 7. The active site assembly contains two five- or six-coordinate

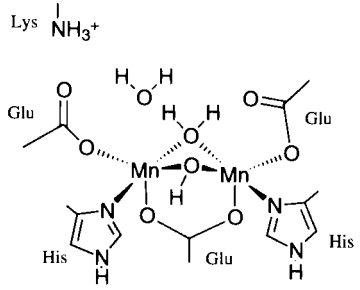

FIG. 7. Structure of the active site of the *T. thermophilus* catalase enzyme, based on (*125*).

manganese ions bridged by one carboxylate from a protein residue, one water molecule, and a hydroxide ion in the reduced enzyme. The hydroxide is suggested to be converted to an oxo bridge in the oxidized form of the enzyme. One additional water molecule, carboxylates, and imidazoles complete the first coordination spheres of the Mn ions. The geometry about both Mn ions has been described in terms of square pyramidal (*125*). The Mn–Mn vectors are 3.18 Å in the reduced form and 3.14 Å for the oxidized form of the enzyme. Finally, this binuclear manganese site is bound within a bundle of four α-helices. The *T. thermophilus* enzyme itself is a homohexamer, composed of six identical subunits (*125*, *131*).

During its catalytic cycle, the Mn catalases shuttle between the Mn_2^{II} and the Mn_2^{III} oxidation states in 2 two-electron reactions (*137*). Overall this process converts two hydrogen peroxide molecules into one molecule of dioxygen and two water molecules. A proposal for the catalytic cycle of catalase is presented in Scheme 8 (*23*). When the

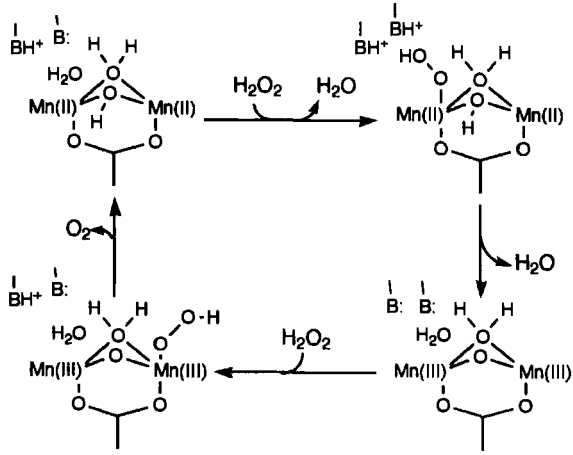

SCHEME 8. A proposed mechanism for the disproportionation of hydrogen peroxide by manganese catalase, based on the mechanism proposed by Penner-Hahn in 1992, and the *T. thermophilus* catalase crystal structure. [Adapted with permission from (*24*). Copyright 1992 WILEY-VCH Verlag.]

T. thermophilus enzyme is isolated, a mixture of enzyme oxidation states including Mn_2^{II}, $Mn^{II}Mn^{III}$, Mn_2^{III}, and $Mn^{III}Mn^{IV}$ is observed (*138*, *139*). The $Mn^{II}Mn^{III}$ and $Mn^{III}Mn^{IV}$ oxidation states are catalytically inactive but can be reduced to active oxidation states, $Mn^{II}Mn^{II}$ or $Mn^{III}Mn^{III}$, by hydroxylamine (*23*). The $Mn^{III}Mn^{IV}$ oxidation state is quite intriguing because it is thought to contain a bis-(μ_2-O^{2-}), core which previously has been implicated in the oxygen-evolving complex

(*23*). The products of the "superoxidized" state may be explained if one considers the possibility that occasionally during turnover an active site at Mn_2^{III} is reduced by only one electron to $Mn^{II}Mn^{III}$. The following two-electron oxidation step would then yield the $Mn^{III}Mn^{IV}$ form of the enzyme, which is only slowly reduced back to an active Mn_2^{III} form. Such chemistry was shown to be viable by the introduction of the one-electron reductant hydroxylamine to catalase followed by the addition of hydrogen peroxide (*23*). These catalases exhibit saturation kinetics and complete the disproportionation of hydrogen peroxide at a rate of 5.75×10^5 $M^{-1} \cdot s^{-1}$ for *L. plantarum* (*23*), 1.7×10^6 $M^- \cdot s^{-1}$ for *T. album* (*129*) and 3.2×10^6 $M^{-1} \cdot s^{-1}$ for *T. thermophilus* (*131, 140*). Finally, the catalase enzymes have been shown to be inhibited by azide, chloride, fluoride, and thiocyanate (*23*). In the case of fluoride inhibition, there is significant controversy both for the number of fluorides that are bound and whether or not the anion acts as a terminal ligand or a bridging μ_2-F^- species.

Numerous model complexes that model one or more traits of the catalase enzyme have been prepared over the years (discussed later). Several systems that mimic the function of this enzyme have been reported, and a selection of these will be discussed in Section V, "Reactivity." Other models with respect to structures or physical properties of the catalase enzyme will be presented in the ensuing sections of this review.

F. Binuclear Manganese Enzymes: A Comparison of Three Enzymes

One of the striking features of the two redox-active binuclear enzymes described earlier, MnRR and catalase, and the hydrolytically active enzyme arginase is the apparent similarity of their active site structures. Yet all three exhibit vastly different reactivities. Both the MnRR and catalase exhibit UV-vis spectra consistent with carboxylato- and oxo-, hydroxo-, or aquo-bridged cores. This would indicate that both have similar Mn–Mn core structures. An EXAFS study by Stemmler, *et al.* (*9*) compared the active sites of these three enzymes. Those studies suggested that arginase and the iron ribonucleotide reductase substituted with Mn had similar structures that tended to be six coordinate. Their data for catalase suggested that the manganese of this enzyme were likely five coordinate. No crystal structure for MnRR has been solved to allow for a specific identification of ligands or a direct comparison of distance parameters and ligand orientations. However, it is possible to compare the arginase (*8*) and catalase crystal structures in this manner (*125*). Other comparisons have ap-

peared in the literature (*9*, *10*). These environments are quite similar, as can be seen from Figs. 1 and 7, and the potential correlation between the two sites is strengthened by the low level of catalase activity exhibited by arginase (*9*, *10*). The similarity of the bridging motifs and protein residues as ligands is striking. Both have enzyme-active sites that contain dimers of Mn ions bridged by a bidentate carboxylate and two μ_2-"O" donor bridges: a monodentate carboxylate and a hydroxide (crystals grown at pH) in arginase, and a water molecule and hydroxide in the reduced catalase. The remaining ligands to the metal ions on each side of the dimer are identical in terms of type, carboxylates, and imidazoles, and in terms of their general positions about the manganese dimer. In the case of arginase, one Mn ion is five coordinate, the other is six coordinate due to a bidentate carboxylate. The catalase contains a water in the area of what would be the corresponding open site on the five-coordinate arginase Mn, and the carboxylate donor on the second manganese is monodentate instead of bidentate. The Mn–Mn vector for arginase is 3.3 Å compared to 3.14 Å and 3.18 Å for the Mn_2^{II} and Mn_2^{III} oxidation states of catalase. Presumably, the native MnRR will also have a Mn–Mn vector in the 3.0- to 3.5-Å range.

The broader structure about the Mn cores of these sites of the arginase and catalase enzymes, however, does vary considerably from one enzyme to the other. Both of these enzymes are located within hydrophobic pockets. However, in the case of the active-site structure of catalase, there is an additional glutamate that may hydrogen bond to two of the imidazoles that are bound to the manganese and a lysine NH_3^+ group is also hydrogen bonded to a manganese ligand carboxylate (*125*). In arginase, there are only two other polar residues reported to be near the active site beyond those that are bound to manganese (*8*). One of these is a histidine imidazole, which may function in a proton shuttle capacity. The other is a glutamate, which probably salt-bridges to the guanidinium functional group of the arginine substrate. The protein structures near the active sites are also quite different. In catalase, the binuclear active site is located within a four-helix bundle about 18 Å from the surface at the bottom of a channel. Overall, the catalase enzyme is composed mostly of helical structural motifs. Meanwhile, the arginase enzyme's active site is not located within a four-helix bundle, and this enzyme contains several helix and β-sheet structures. The active site of arginase sits at the bottom of 15-Å-deep cleft that is located within an area of turns and loops between helices and β-sheets.

The reactivity of catalase enzymes and rat liver arginase may also now be directly compared. Arginase has recently been reported to dis-

proportionate hydrogen peroxide, albeit much less effectively than the actual manganese catalases (in a buffered solution at pH 9.5) (*9*, *10*), albeit much less effective than the actual manganese catalases, exhibiting a rate of reaction on the order of 30 s^{-1} versus 200,000 s^{-1} for *L. plantarum* (*10*). It was also reported that evidence for the manganese-substituted iron ribonucleotide reductase exhibiting a low level of catalase activity might also exist (*9*). No "superoxidized" form of arginase could be formed in the presence of hydrogen peroxide and hydroxylamine, but it did show hydroxylamine inhibition. Another difference between these systems was a lowered sensitivity of arginase to the inhibitory effects of halides (*10*). A final point of comparison is the reported peroxidase activity of arginase. The catalase from *T. album* has been shown to complete a peroxidase reaction on *p*-phenylenediamine (*129*). Arginase was shown to perform peroxidase activity on this compound and *o*-phenylenediamine (*10*). Thus, as one might expect from their structural similarities, these enzymes can in some cases catalyze similar chemistry.

Thus, despite the initial similarities of the immediate active site dimers, a broader inspection of the enzyme begins to suggest potential explanations for the differences in their reactivity. For example, the existence and type of residues near the active site, with respect to acid/base chemistry, that may attenuate the overall reactivity of the core will play a role. The types of bridging μ-"O" moieties, monodenate carboxylate and hydroxide in arginase versus hydroxide and water in catalase, probably play a significant role. The hydroxide and the proposed oxo (or perhaps two hydroxides) of the Mn_2^{III} form of the enzyme may be better able to support the higher oxidation state on manganese versus the carboxylate/hydroxide bridges of arginase. The two five-coordinate manganese of catalase may play a role, too, if rearrangement were required for the activation of arginase.

Overall, these enzymes exemplify a growing theme in bioinorganic chemistry, that of nature utilizing an active site structural motif in more than one enzyme to catalyze quite similar or dissimilar chemistries. Such reapplication of a structural motif has been observed in the recurring themes of binuclear iron (*141*), for example. For manganese, it appears that a general binuclear manganese active site design has been reapplied three times in separate settings for at least three different purposes.

G. The Oxygen-Evolving Complex, OEC

Dioxygen is important to all aerobic life forms. It is required for respiration and, therefore, the release of energy required to sustain

biological processes. Dioxygen is a by-product of photosynthesis and is produced by the oxidation of two molecules of water to dioxygen in conjunction with the release of four equivalents of protons and four equivalents of electrons, which will be processed into reducing equivalents suitable for eventual carbohydrate biosynthesis. The catalytic site for water oxidation is known as the oxygen-evolving complex (OEC) of Photosystem II (PS II), located in the chloroplasts of green plants and algae (*42*, *48*). The OEC, sometimes referred to as the WOC, water oxidation complex, or water oxidase, contains a group of four manganese ions at its active site (*42*). Calcium and chloride are also required for the proper function of the OEC (*35*). Part of a complex system of several polypeptides and cofactors, which are membrane-bound in the thylakoid membrane of green plants, the OEC's role is to provide the reducing equivalents necessary to rereduce a specific photoexcited chlorophyll *a* molecule that initiates the chain of events leading to the production of reducing equivalents. The polypeptides of PS II and those surrounding the OEC serve in various roles, many of which have been probed and elucidated (*42*, *48*, *51*). Some of these roles relate directly to the manganese cluster of the OEC and the other inorganic cofactors. Based on the wealth of research in this field related to PS II, a gross structural similarity of green plant and algal PS IIs is believed to exist with that of the crystallographically characterized (*142*) bacterial (Rhodopseudomonas) PS IIs (*42*, *143*) that do not employ the OEC. The commonalities between these systems has led to a proposed orientation of the various components of PS II (Fig. 8) (*24*). The OEC is located near the "base" of two polypeptides known as D1 and D2 and is surrounded and stabilized by several additional polypeptide units (*42*, *144*).

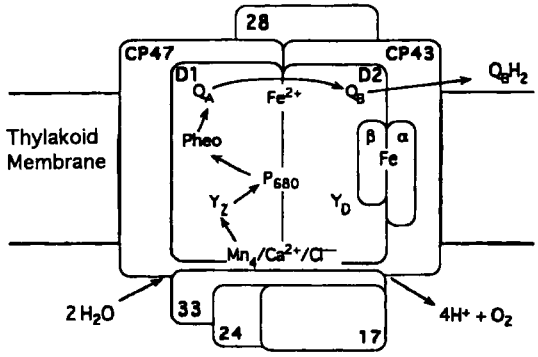

FIG. 8. A scheme of the generally proposed layout of the components of Photosystem II. The polypeptides are labeled, too. The electron flow in PS II follows the arrows shown. [Reproduced with permission from (*24*). Copyright 1998 Springer-Verlag.]

For more detailed discussions of the biochemical aspects of the PS II, such as the role of the various polypeptides or differences between the PS IIs, the reader is directed to one of several reviews and compilations. The OEC and PS II have been extensively reviewed over the past several years. The review by Debus in 1992 sums up much of the knowledge obtained on PS II to that point (*42*). The Photosynthetic Congress, held every few years, has produced several volumes of material from a broad spectrum of researchers covering the whole of photosynthesis with current results to the time of that Congress (*51*). A 1996 book edited by Ort and Yocum (*48*) contains several chapters covering various aspects of photosynthesis, from PS II to PS I. Manganese modeling chemistry has also been extensively covered by reviews (*24*, *26–31*, *34*, *37*, *45*, *50*).

The OEC is involved in the earliest stages of the overall photosynthetic process, which produces NADPH for carbohydrate biosynthesis. Overall, the photosynthetic system is composed of two halves, PS II and PS I (*48*). PS II provides reducing equivalents that are transferred to PS I and are eventually converted into the reducing energy of NADPH. Both PS I and PS II absorb light energy to initiate their respective electron flows. The protons released during these steps are likely utilized in the generation of a proton gradient for the synthesis of ATP, which is also required for carbohydrate biosynthesis (*48*).

It has been established that the OEC contains a tetranuclear cluster of manganese ions, and that it requires at least one calcium ion (*39*, *145*, *146*) and at least one chloride ion (*147*, *148*) to complete its catalytic cycle. This catalytic cycle involves four successive oxidations of the OEC (*42*, *48*) to eventually yield a highly oxidized system that then completes the oxidation of two molecules of water with the concomitant release of dioxygen and the return of the OEC to an overall oxidation state four levels lower. The sequential oxidation process starts when light energy is harvested by antennae chlorophyll molecules, which transfer this energy to the P_{680} chlorophyll *a* molecule of the reaction center. This photoexcited P_{680} then reduces Pheophytin A to give a charge-separated state of P_{680}^{+} and $Pheo^{-}$. Pheophytin A then reduces a bound plastoquinone molecule, Q_A, which then reduces a dissociable plastoquinone molecule, known as Q_B. Once Q_B has been doubly reduced and doubly protonated, it departs to carry the collected reducing equivalents further into the photosynthetic system (Fig. 8). Once oxidized, $P_{680}+$ needs to be "reset" so that new reducing equivalents may be initiated, and to prevent charge recombination, or back-reactions, from occurring. This is accomplished by oxidizing the OEC. This oxidation is mediated by a particular tyrosine residue, known as Tyrosine Z, Y_Z, residue 161 of the D1 polypeptide (*149*, *150*).

This tyrosine is initially oxidized by P_{680}^{+}, and then it in turn oxidizes the OEC by one electron. In this manner, the OEC is oxidized successively four times, whereupon dioxygen release occurs, the OEC returns to its initial oxidation state, and the successive oxidation cycle begins anew. Four protons are generated in conjunction with the electron withdrawal and dioxygen release, and these are likely utilized in the generation of a proton gradient for ATP synthesis (*42*, *144*). The cycle of four progressive oxidations followed by release of dioxygen with the concomitant reduction of the manganese center of the OEC has been termed the S cycle, or S clock (*151–153*) (Scheme 9). This

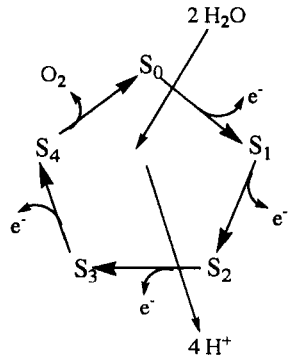

SCHEME 9.

clock is a five-stage cycle that proceeds from S_0 to S_4, with S_0 being the most reduced form of the enzyme whereas S_4 represents the most oxidized form. Dioxygen release occurs during the S_3–S_4–S_0 phase of the cycle, presumably once S_4 is reached (*152*, *153*). S_4 is relatively unstable and rapidly returns to the S_0 state (*46*). The initial evidence for the S cycle was reported by Joliot (*151*). Those experiments were reproduced and reinterpreted by Kok and co-workers (*153*), who showed that, for photosynthetic centers given a sequence of single flashes of light, a burst of dioxygen occurred with the third flash of light and a burst of dioxygen then occurred with every fourth flash thereafter (Fig. 9). The initial burst came on the third flash, indicating that PS IIs stored in the dark will equilibrate to the S_1 state, which is one step oxidized from the OEC's lowest overall oxidation state. Further research has tied at least some S-state progressions to an increase in the overall oxidation of the manganese cluster of the OEC (discussed later).

In the absence of crystallographic data, all of the structural infor-

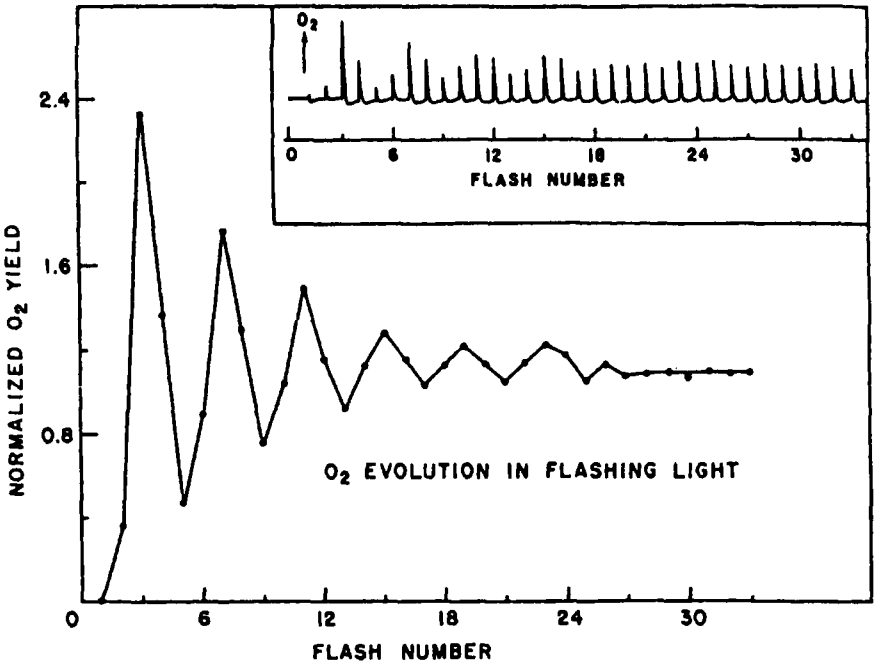

FIG. 9. The Four Flash experiment. The peaks in the plot represent the dioxygen bursts that occur with every fourth flash of light administered to a PS II sample. This cycle peaks on the third flash due to the resting state of the enzyme being at S_1. The process is eventually dampened by double hits of light leading, for example, to an inhomogenous sample with respect to the S state. [Reproduced with permission from (*46*), Chapter 9. Copyright 1996 Kluwer Academic Publishers.]

mation known about the OEC has been gathered by the use of spectroscopy (*24*, *28*, *33*, *42*, *46*). The use of X-ray absorption spectroscopy (XAS) has provided some particularly useful quantitative structural information. EXAFS (extended X-ray absorption fine structure) is an X-ray absorption spectroscopic technique that provides distance information and some idea about the nature of the first coordination sphere of the element in question. EXAFS studies have shown that the OEC manganese ions are present in a predominantly O/N-donor coordination environment (*24*, *154*). Furthermore, EXAFS data show that there exists at least one Mn–Mn vector, and probably two, of 2.7 Å, and a third significant vector is at a distance of 3.3 Å (*155–159*, *477*), which may result from a Mn–Mn or Mn–Ca interaction (discussed later).

EPR spectroscopy has been another extremely important means for exploring the OEC (*24*, *28*, *42*, *46*). The S_1 state is readily prepared

by dark-adapting preparations of PS IIs, from which S_2 is achieved by flashing the sample with one pulse of light (*42*). The S_2 state exhibits at least two distinct EPR signals, which have been the focus of extensive research and controversy, too. The first, the multiline, is a multiline signal centered around $g = 2$ (*160*, *161*), and the second, which depends on sample preparation technique and conditions, appears at $g = 4.1$ (*162–166*). These EPR signals may be interconverted, and are shown in Fig. 10. The multiline signal is indicative of magnetically coupled manganese ions, with at least 18–20 resolved lines being observed. It also indicates that at least two of the manganese are involved in a multinuclear cluster. Based on the expected manganese oxidation states, and more lines than the 12–16 traditionally observed for a $Mn^{III}Mn^{IV}$ dimer, a cluster of at least three manganese ions is probable (*46*). The second EPR signal at first appeared similar to that generated by an isolated Mn^{IV}, leading to trinuclear/mononuclear proposals for the structure of the OEC. Later EPR evidence showed that this signal did not result from a monomeric Mn^{IV} ion, but rather most likely arose from a multinuclear manganese structure itself (*167*, *168*). In ammonia-treated, oriented PS II samples, a multiline signal was observed in the $g = 4.1$ EPR spectrum. Further-

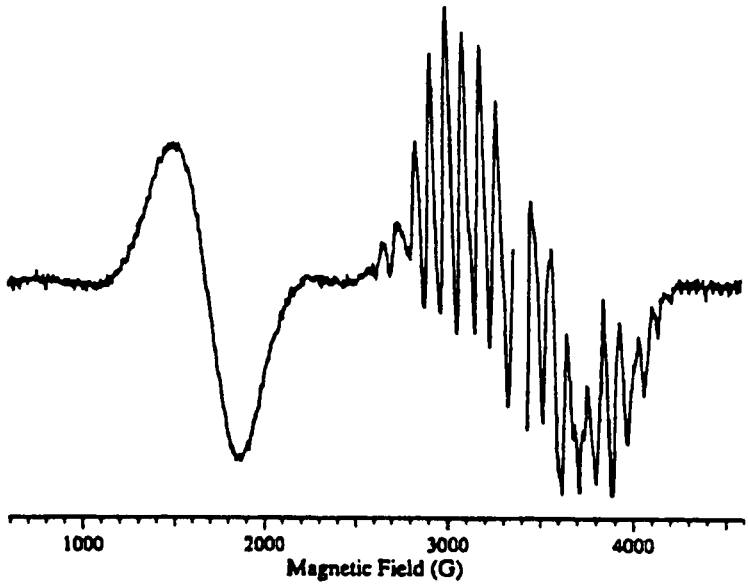

FIG. 10. The $g = 4.1$ EPR signal from the S_3 state of the OEC (left) and the $g = 2$ multiline signal (right). [Reproduced with permission from (*46*), Chapter 9. Copyright 1996 Kluwer Academic Publishers.]

more, another study on this signal suggested that it arose from an $S = 5/2$ ground state (*169*), which would be inconsistent with a Mn^{IV} ion, but not a multinuclear array of manganese. The appearance of the multiline EPR signal upon going from S_1 to S_2 also supports the existence of metal-centered oxidation (*160*, *161*). For a more detailed discussion on these two signals and the conditions affecting their respective formation, the reader is again directed to one of the various reviews and compilations (*42*, *46*).

In 1997, new EPR data on the S_0 state was reported by Messinger and co-workers (*170*, *171*). Until these reports, no EPR spectra had been recorded for this S state. The first set of experiments took dark-adapted PS IIs to S_0 by the addition of reductants (*171*). This S state is labeled S_0^* to account for potential alterations to the manganese structure. A multiline signal EPR signal was observed for this S_0^* state that exhibits 24–26 lines centered near $g = 2$ [Fig. 11(a)]. This signal is wider than the S_2 multiline and exhibits more lines, many of which do not line up with transitions observed in the S_2 multiline. The authors suggest that this added breadth is a result of the lower overall oxidation state of the manganese ions composing S_0 and that this may be indicative of the presence of a $Mn^{II}Mn^{III}$ couple based on model complex data. A second set of experiments reported by Messinger, Sauer, Klein, and co-workers (*170*) took dark-adapted samples through one S-state cycle to poise them at S_0. This preparation also presented a multiline signal, which did not appear to differ significantly from that observed for S_0^* [Fig. 11(b)]. For both of these spectra, the presence of methanol (0.5–1.5%) in the sample was required to observe the multiline signals. Without methanol, a broad EPR signal is still observed for the S_0 preparation. The authors theorize that methanol may be binding to the manganese cluster and that this facilitates the observed spectra, perhaps by altering the coupling of the manganese ions. Simulations conducted to ascertain what the possible oxidation states of the manganese ions in S_0 might be have not yet clarified this point, because the overall oxidation states $Mn^{II}Mn_3^{III}$, $Mn^{II}Mn^{III}Mn_2^{IV}$, or $Mn_3^{III}Mn^{IV}$ all gave similar spectral widths consistent with the data. However, the simulations did suggest that neither binuclear species nor a tetranuclear cluster arranged as $Mn^{II}Mn^{IV}$/$Mn^{III}Mn^{IV}$ would not yield comparable spectral widths. Also in 1997, Styring and co-workers (*172*) reported a multiline signal for S_0. Their study showed that by administering light flashes to PS II samples, they could produce a multiline signal that they believed to arise from S_0 after 3 flashes from S_2 samples. This spectrum is also wider than that observed for S_2, similar to that reported earlier. A second se-

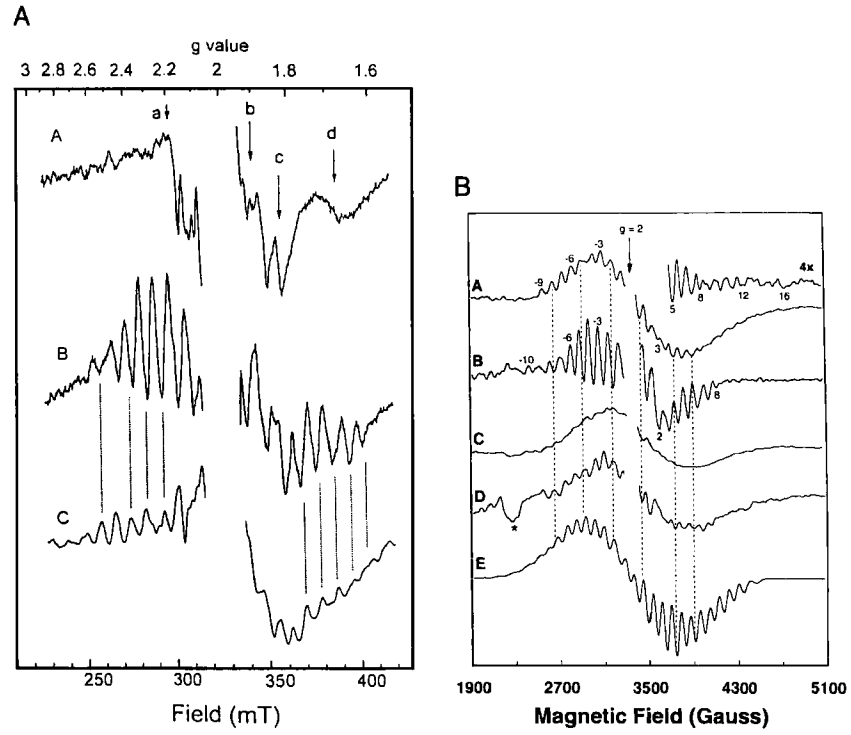

FIG. 11. S_0^* and S_0 EPR signals. (a) EPR Spectrum of the S_0^* state. The top spectrum, A, represents the S_{-1} state that was formed by reducing PS II samples with hydrazine. This was illuminated to yield a new multiline signal, C. B is the spectrum of the S_2 state multiline from control experiments. Details of sample preparation may be found in the references provided. (b) A and B. Difference spectra of prepared S_0 minus residual S_1 signal. B. For comparison, the S_2 multiline under the same conditions. Note that S_0 is a broader signal and is shifted with respect to the S_2 signal. C. S_0 spectrum without added methanol. D. S_0^* Spectrum produced by reducing S_1 samples with hydroxylamine. E. Simulated spectrum of S_0. [(a) and (b) reproduced with permission from (*171*) and (*170*), respectively. Copyright 1997 the American Chemical Society, respectively.]

quence of light flashes regenerated the S_0 signal. They also utilized methanol in their samples.

EPR signals have also been reported for the S_1 state (*173*). A very intriguing article (*174*) has recently appeared in which Britt, Debus, and co-workers showed, via the application of parallel polarization EPR studies, that a multiline EPR signal can be observed for the S_1 state (Fig. 12). When illuminated, the amplitude of this signal was "greatly reduced," and a conventional perpendicular polarization $g = 2$ multiline signal consistent with the formation of the S_2 state was

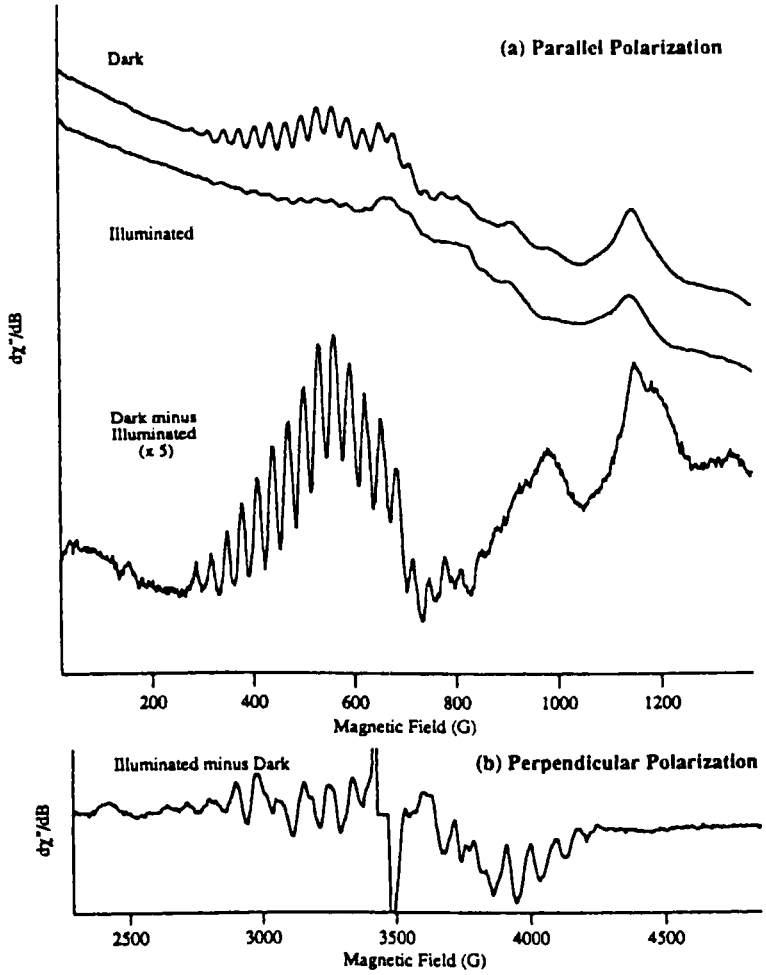

FIG. 12. S_1 multiline signal. In (a) the spectrum (parallel polarization EPR) labeled Dark represents a dark-adapted PS II sample; thus, it is in the S_1 state. The second trace represents the sample following illumination with light to generate S_2. The top, Dark, spectrum minus the middle, Illuminated, spectrum yields the third spectrum in (a). This represents a well-resolved multiline signal arising from a "multinuclear exchange coupled paramagnetic Mn cluster" (*174*) in the S_1 state of the OEC. If the subtraction is reversed and the spectra are recorded using perpendicular polarization, then when the Dark spectrum is subtracted from the Illuminated spectrum, an S_2 multiline signal is readily observed (b). [Reproduced with permission from (*174*). Copyright 1998 the American Chemical Society.]

observed. This S_1 multiline signal is consistent with the interaction of multinuclear clusters of manganese ions, and these authors proposed that it arises from a cluster of manganese ions. This proposal would minimally require that a trimeric cluster of coupled manganese ions exists, versus an arrangement invoking two distinct dimers, one a Mn_2^{III} dimer and the other a Mn_2^{IV}, an arrangement based on the assumed overall integer spin of this S state. Furthermore, because S_1 is expected to be integer spin, a trimer/monomer motif would suggest that the monomeric manganese should be in the Mn^{III} oxidation state. If that were true, then a six-line spectrum consistent with a Mn^{III} should be observable under the conditions employed to observe this new S_1 multiline signal. The lack of such a signal is suggestive that this new multiline signal actually arises from a tetranuclear cluster of manganese ions.

Application of the X-ray Absorption Spectroscopy (XAS) to the observation of Mn K-edge data (*24*, *32*, *33*, *156*, *175*), via X-ray Absorption Near Edge Structure (XANES), has provided insight into the overall oxidation state of various S states. The inflection point of the edge shifts for the various oxidation states of manganese (*24*, *33*). Studies of the OEC show changes in edge energies consistent with an increase in the overall oxidation state of the manganese cluster. Thus, at least some of the oxidations of the OEC occur on the tetranuclear cluster of manganese ions. Numerous XAS studies in conjunction with EPR data have lead to proposals of the oxidation levels of the OEC S states (*24*, *33*, *42*, *46*). Two of these proposals are presented in Scheme 10. The S-state oxidation levels of the manganese are not

S-state			
S_0	III/III/III/IV	III/III/III/IV	II/III/IV/IV
S_1	III/III/IV/IV	III/III/IV/IV	
S_2	III/IV/IV/IV	III/IV/IV/IV	
S_3	IV/IV/IV/IV	IV/IV/IV/IV	
S_4	IV/IV/IV/V	IV/IV/IV/IV$Y_z^{\bullet}$	

SCHEME 10.

clear-cut, and some controversy does remain (*24*, *33*, *42*, *46*). Much of this controversy revolves around defining oxidation states for the S states from spectroscopic techniques. For example, the transitions from S_0 to S_1 and S_1 to S_2 have strong evidence for manganese-based oxidation state changes. However, the nature of the S_2 to S_3 transition is quite controversial because there is no clear-cut alteration to the observed XANES edge energies. Proposals to explain this have invoked oxidized protein residues or structural rearrangements of the

tetranuclear cluster (*176*). The imidazole oxidation that had been suggested, however, is unlikely. The signals that were attributed to the oxidized imidazole have now been shown to arise from $Y_Z^{\cdot}$ (*177*, *178*). In the final S_3 to S_4 to S_0 phase, little is certain due to the instability of the S_3 and the transient nature of the S_4 state. Again the oxidation state controversy is centered on whether oxidation occurs on a protein residue, such as $Y_Z^{\cdot}$, or on a manganese of the OEC.

The results of the XAS and EPR data, combined with knowledge from model complexes, (discussed later) allow for the formulation of structural models of the OEC. Many manganese compounds have been proposed as structural models for the OEC, ranging from butterfly arrangements to adamantanes to cubanes (*26*, *27*, *29–34*, *50*). Most of those proposals, however, are inconsistent with the known structural data for the OEC. Currently the most widely favored model is the "dimer of dimers" model (Scheme 11), first suggested by Klein,

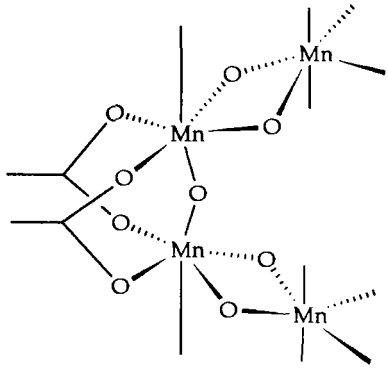

SCHEME 11.

Sauer, and co-workers (*32*, *154*). This model proposes that two manganese dimers that interact with one another exist in the OEC. The dimers are suggested to contain $Mn_2(\mu_2\text{-}O^{2-})_2$ cores and to be bridged to one another by oxo and carboxylato units. This model is supported by several pieces of current data on the OEC. First, the 2.7-Å Mn–Mn vectors of the OEC are most consistent with crystallographically characterized dimeric manganese model complexes that contain $Mn_2(\mu_2\text{-}O^{2-})_2$ cores, and two such vectors are observed for the OEC. Second, such a model would provide the potential for magnetically coupled Mn–Mn interactions to occur. Bridging two $Mn_2(\mu_2\text{-}O^{2-})_2$ cores to one another by carboxylates and a single $(\mu_2\text{-}O^{2-})$ unit would provide for an approximately 3.3-Å distance, a formulation consistent with known model compounds (discussed later). Furthermore, the

EPR data from S_0, S_1, and S_2 indicate that there are coupled Mn ions. In particular, the multiline signals are suggestive of coupled manganese structures that require clusters of greater than two manganese ions.

The related Electron Nuclear Double Resonance (ESEEM) and Electron Spin Echo Envelope Modulation (ENDOR) spectroscopies have also proven useful in elucidating information about protein residues near the OEC. One of these residues is the important protein radical Tyrosine Z, $Y_Z^{\cdot}$, which is usually found in an oxidized radical form (*42*). Study of this protein residue via ENDOR and ESEEM spectroscopies has been enlightening. The presence and protein residue associated with this radical signal was defined several years ago, and $Y_Z^{\cdot}$ was originally assigned the role of an electron-transfer mediator for the electrons moving between the OEC and P_{680}^{+} (*150*, *179*). More recent work has been modifying this view. Tyrosine Z has been shown by Britt and co-workers to be located in close proximity to the manganese cluster, probably within 5 Å (*180*). Probes of the nature of this tyrosyl radical by Babcock's group have suggested that this tyrosine may play a more active role than solely to act in an electron-transfer capacity (*181*, *182*). It does not bear the hallmarks of a protein residue whose sole purpose is to participate in an electron-transfer chain—for example, it does not retain a nearly rigid orientation with respect to its surroundings. Other similarities between this redox-active tyrosine and other metalloenzyme systems that employ radical components suggested that this tyrosine might also act in such as role (*47*, *183*). These observations have lead to recent proposals by Britt and Babcock that involve $Y_Z^{\cdot}$ more intimately in the water oxidation mechanism (*182*, *184*, *185*). Instead of merely acting as an electron transfer agent between the OEC and P_{680}^{+}, it is now proposed to perform a hydrogen atom abstraction. New models for the function of the OEC have been formulated based on this proposal (discussed later). The role of Y_Z is still not settled, of course, as evidenced by a recent article arguing against a hydrogen atom abstraction role (*186*). Finally, spectroscopic studies have also focused on identifying potential protein residues that might be ligands to the OEC. Through ESEEM spectroscopy, the presence of at least one imidazole ligand to the OEC manganese cluster has been established (*187*).

Studies involving calcium and chloride have shown these ions to be critical to the proper functioning of the OEC (*35*, *146*, *188*), although their exact roles have yet to be elucidated. Without either of these, dioxygen evolution is halted and the OEC cannot complete one full cycle. It has recently been reported, for example, that the OEC can reach S_2 without chloride, but cannot be further oxidized to S_3 or pro-

ceed from S_3 to S_4 without the addition of chloride (*188*). There has been speculation that the chloride's role may be to prevent premature loss of oxidizing equivalents, perhaps by preventing the premature loss of oxidation equivalents in the formation of hydrogen peroxide (*189*). Another suggestion may relate chloride to substrate binding, an idea that has received some support from small-molecule-binding studies, which indicate that there is a site for a small molecule such as amnonia to bind to the OEC in a process that displaces chloride (*35*, *190*). Calcium may be bound near the manganese and has been proposed to be the source for the Mn–X 3.3-Å distance observed by EXAFS (*191*). One possible role for the calcium may be to act as a water-binding site from which water is transferred at some point to one of the four Mn ions of the OEC (*192*, *193*). Various researchers have studied the effects of substituting for these critical ions. Only strontium has been successfully inserted in place of calcium with retention of any level of function, albeit severely attenuated (*35*, *194*). Substitution for chloride is less sensitive. The addition of bromide does not appreciably alter the ability of the OEC to generate dioxygen (*35*, *42*). The OEC is also functional, but at reduced levels in the presence of iodide and nitrate. Fluoride strongly inhibits the OEC and has been suggested to alter the structure of the manganese cluster structure based on EXAFS data (*195*). Amines also replace the chloride and inhibit the function of the OEC (*35*, *190*). Ammonia is a particularly interesting case in this regard, in that it appears to bind at two different sites within the OEC, suggesting that there may exist a second chloride-inaccessible site, which has been proposed to be a water-binding site to a manganese (*35*, *196*).

Water is of course key to this whole process. Water-binding studies have been attempted to establish when the two water molecules that are oxidized to dioxygen become bound to the OEC and whether they are bound directly to manganese. Early water-binding studies suggested that the water converted to dioxygen is still exchangeable until at least S_3. From isotopic labeling studies, it appears that the waters that are oxidized are not bound or highly restricted with respect to exchange until the late S states (*197*). A recent water-binding study suggested that there were two waters in exchange with the bulk water, but that these waters were exchanging at different rates (*198*). One proposal put forward to explain this observation was the existence of an Mn=O moiety. A review based on the thermodynamics of water oxidation was published in 1996 (*37*).

Pulling the data together again, a larger picture of some to the structural and reactivity details of the OEC begins to emerge. The new hydrogen atom abstraction role proposed for Y_Z coupled with the

dimer of dimers model has led to some intriguing new hypotheses for the potential manner in which the OEC functions (*46*, *47*, *177*, *178*, *181*, *182*, *184*, *185*). A synthesis of these new concepts is presented in Scheme 12 (*182*). If the OEC functions in the newly suggested manner, then it would join a growing class of enzymes that utilize protein

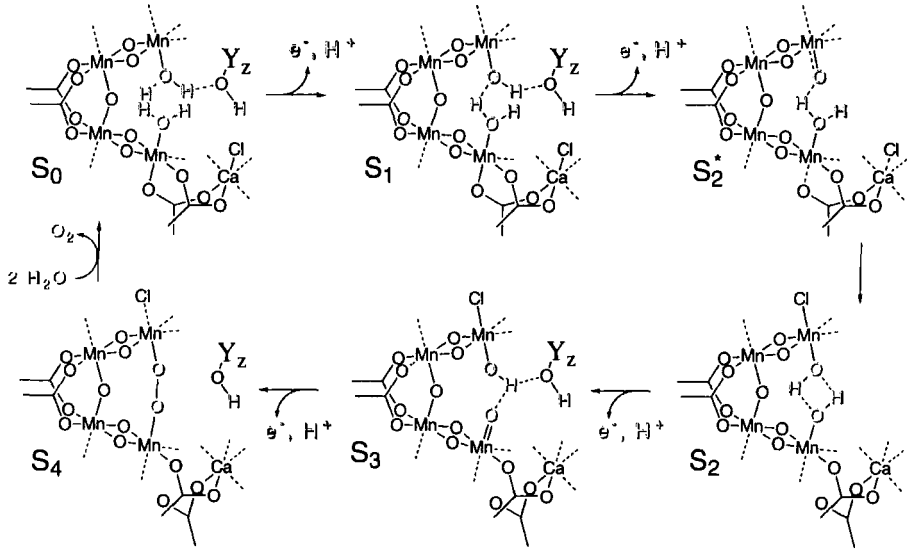

SCHEME 12. A mechanism for dioxygen evolution by the OEC as proposed by Babcock that employs the hydrogen atom abstraction concept. [Reproduced with permission from (*182*). Copyright 1998, the American Chemical Society.]

residue radicals to complete their catalytic processes (*47*, *183*). The dimer of dimers structural model has been modified to include hydrogen atom abstraction from a water bound to a manganese by $Y_Z^{\cdot}$, which is equivalent to proton loss being coupled to the stepwise oxidation of the OEC. This proposal eventually leads to the generation of a high-valent manganese (IV) or (V) with an oxo bound, Mn=O, that then combines with a second water-derived oxygen atom bound to a nearby manganese to form dioxygen during the S_4–S_0 step. Another feature of these new models is the retention of charge neutrality throughout the process. Scheme 13 shows the Babcock proposal as modified by our group. For any functional proposal to gain validity, one needs to consider whether or not the energetics of the process involved would be favorable. Recent studies by Pecoraro and co-workers suggest that the energies required for this process to occur are likely to be favorable (discussed later).

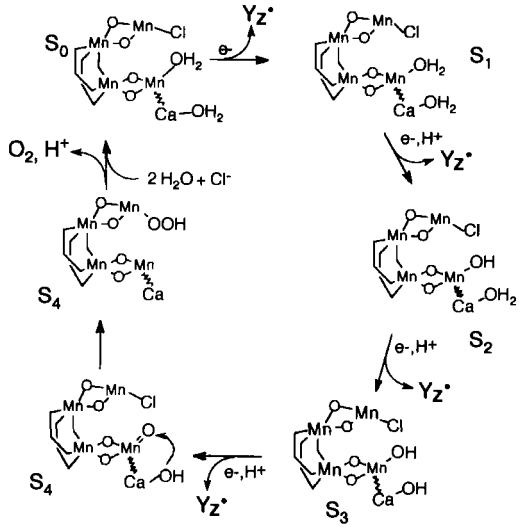

SCHEME 13. A mechanism for dioxygen evolution by the OEC involving hydrogen atom abstraction as proposed by Pecoraro.

The OEC provides perhaps the most complicated manganese enzyme system yet known and thus is rich with possibilities for the exploration of manganese chemistry. Overall, the OEC and PS II are among the more intricate enzymatic systems that are currently being explored. Structural models, spectroscopic models, and reactivity model complexes are all integral to insights that have been attained and those yet to be gained. The following paragraphs detail some of the work in this area. Models related to water oxidation are presented in the Section V, "Reactivity." A selection of the newer multinuclear complexes will be discussed in Sections III.B to III.D. Again, many reviews have dealt with model complexes for the OEC (*29–31*, *34*, *45*, *50*).

Many bioinorganic chemists have prepared speculative structural models over the past several years to gain an insight into this system—for example, with respect to possible arrangement of manganese ions—or to provide characterized materials as reference compounds for spectroscopic examinations. The agreement between EXAFS data and the Mn–Mn vector of a $Mn_2(\mu\text{-}O)_2$ core is one prime example of structural modeling chemistry and spectroscopy combining to elucidate critical data on this system (discussed earlier). Multinuclear clusters are always of interest in this field, and several have been prepared (*28–31*, *34*, *45*). The adamantane and cubane structures led to proposals for the possible oxidation of water to dioxygen

that involved rearrangement of a manganese cubane to adamantane upon incorporation of water molecules, and another proposal invoked a butterfly structure that was converted to a cubane during the catalytic cycle (*199*, *200*). These proposals, among others, have been extensively reviewed, and the reader is directed to one of the referenced sources noted earlier. New examples of dimers of alkyl-bridged $Mn_2(\mu_2\text{-}O)_2$ cores have been prepared and structurally characterized in recent years (discussed later). A few of these also include waters bound to the manganese. One of the more interesting tetranuclear manganese structures in this class of compounds was reported in 1992 by Armstrong and co-workers, who then further probed its complicated magnetic couplings (*201*).

A variety of other complexes have been prepared that have proven useful in the area of the spectroscopic understanding of the OEC. Many have been used as models for XAS studies to establish what is to be expected from the various oxidation states of Mn. Others have been probed to gain a better understanding of the interactions between manganese nuclei—for example, most $Mn^{III}Mn^{IV}$ complexes that are known exhibit 16-line EPR signals (*140*). However, the $Mn^{III}Mn^{IV}$ complex prepared with the 2-OHsalpn ligand (*202*) only exhibits a 12-line spectrum. Another area that model complexes may help to address is the effects of water binding to a manganese cluster. Small molecules such as water can be bound to the complexes derived from 2-OHsalpn, and these have been probed by ENDOR spectroscopy to ascertain what perturbations might arise from that bound molecule versus the complex without such an additional ligand (*203*).

The energetics of water oxidation is another key point to address. This topic includes the interesting question of how the oxidizing equivalents are stored in the OEC without being released too soon, and how the requisite 3.6 V versus NHE for water oxidation can be built up when $Y_Z^{\cdot}$ is thought to maximally be able to provide oxidations at a level of 1.1 V per oxidation (*41*). In addition, the proposal of hydrogen atom abstraction has led to the exploration of how the homolytic bond dissociation energy of a water bound to a manganese dimer might be altered from the values observed for an individual water molecule in solution. To abstract a hydrogen atom from water would require more energy than is available to $Y_Z^{\cdot}$ (Table I). However, Pecoraro and co-workers have shown that the ΔG value for removing a proton from a protonated μ-oxo bridge is within a reasonable range for the $Y_Z^{\cdot}$ to be able to abstract a hydrogen atom (Table I) (*204*, *205*). These studies employ a concept worked out by Mayer for the oxidation of, for example, toluene by permanganate (*206*). Studies of water

TABLE I

HYDROGEN BOND DISSOCIATION ENERGIES[a]

Complex	HBDE (kcal/mol)	Reference
Tyrosine	86	*457*
Water	119	*458*
$[Mn^{IV}(salpn)(\mu\text{-}O)]_2$	76	*204*
$[Mn^{IV}(3,5\text{-di-Cl-salpn})(\mu\text{-}O)]_2$	77	*204*
$[Mn^{IV}(3,5\text{-di-}(NO_2)salpn)(\mu\text{-}O)]_2$	79	*204*
$[Mn^{III/IV}(bpy)(\mu\text{-}O)]_2^{3+}$	84	*204, 459, 460*
$[Mn_2^{III}(2\text{-OH}(3,5\text{-diCl})salpn)_2(OH_2)]$	89	*205*
$[Mn^{III}Mn^{IV}(2\text{-OH}(3,5\text{-diCl})salpn)_2(OH_2)]^+$	94	*205*
$[Mn_2^{III}(2\text{-OH})salpn)_2(OH_2)]$	85	*205*
$[Mn^{III}Mn^{IV}(2\text{-OH})salpn)_2(OH_2)]^+$	89	*205*
$[Mn_2^{III}(2\text{-OH}(3,5\text{-di-}t\text{-Bu})salpn)_2(OH_2)]$	82	*205*
$[Mn^{III}Mn^{IV}(2\text{-OH}(3,5\text{-di-}t\text{-Bu})salpn)_2(OH_2)]^+$	86	*205*

[a] For complete details, including complex pK_a's and electrochemical reduction potentials, the reader is directed to (*204*) and (*205*).

bound to complexes derived from the 2-OHsalpn ligand show that hydrogen atom abstraction from these complexes is also in a reasonable energy range, theoretically, for H-atom abstraction by $Y_Z^{\cdot}$ (*205*). In addition, the normally observed increase in reduction potential of this complex with an hydroxide bound is attenuated. This also suggests that if H-atom abstraction is occurring in the OEC, this might favorably affect the redox potential of the manganese dimer to which that water is bound, further stabilizing the system against early loss of its oxidizing equivalents before water oxidation can occur and thus allowing the potential for oxidation of the manganese cluster to remain in a range accessible to $Y_Z^{\cdot}$. A report of quantum chemical calculations in 1997 supports these data (*207*).

Other topics of importance to the OEC will be discussed in greater detail later. Water oxidation models will be addressed in Section V, "Reactivity," and models for the catalase-like reaction of the OEC will be addressed in Section V.B.3., "Catalase."

III. Structural Models

Manganese redox enzymes exhibit a range of structural motifs involving mononuclear or bi- and tetranuclear aggregates of manganese ions. There has been a great deal of research in the area of structur-

ally modeling the active sites of manganese enzymes such as the MnSOD, catalase, and the OEC. These small-active-site analogs have been prepared in the hope that structural mimics will also mimic (i) the spectroscopy and (ii) the reactivity of the biological center. Some success has been achieved in modeling the reactivity of catalase and SOD with these models, but there is no structural analog for the OEC that exhibits water-oxidizing activity. The following is an overview of additions in the field of manganese chemistry since the superior review by Wieghardt in 1989 (*30*). This section will provide a compendium of the structure types that have appeared in the literature over the past eight years but is not meant to be an exhaustive recapitulation of every structure that has been generated during that time.

A. Mononuclear

1. Mn(II)

Mononuclear complexes of manganese are quite common and have been prepared in all of the currently recognized biologically relevant oxidation states of manganese, II–V. Mononuclear Mn^{II} complexes exhibit a range of polyhedra about the metal, with coordination numbers of 5–8 dominating. The lack of coordination number specificity is understandable, as this d^5 ion does not, in theory, exhibit specific geometric preferences. Numerous complexes have been prepared with predominantly N_xO_y-donor atom sets, which are often augmented by halide or pseudohalide ligands and the occasional sulfur donor. In general, this represents the known biologically relevant donor atoms to manganese. Several of these complexes have been generated with the target of mimicking or modeling MnSOD.

A variety of five-coordinate complexes of Mn^{II} have been prepared. Crystallographically characterized Mn complexes with a trigonal bipyramidal geometry are still relatively rare, however. Kitajima and co-workers (*208*) reported two trigonal bipyramidal complexes utilizing hydrotris(3,5-diisopropylpyrazol-1-yl)borate, HB-*i*-Pr, a facially binding tridentate ligand (*209*, *210*) (Fig. 13). The coordination sphere of the first complex was completed by a bidenate benzoate; the other complex contains a monodentate benzoate and one equivalent of 3,5-diisopropylpyrazole. Another variation that has recently appeared is composed of tbp complexes of Mn^{II} with tris(benzimidazoyl-2-methyl)-amine bound to the manganese (*211*, *212*) (Fig. 14). The tris(benzimidazoyl-2-methyl)amine is a tetradentate tripodal amine ligand that provides four N-donor atoms. The first coordination sphere of these complexes was completed by a chloride. However, these products are

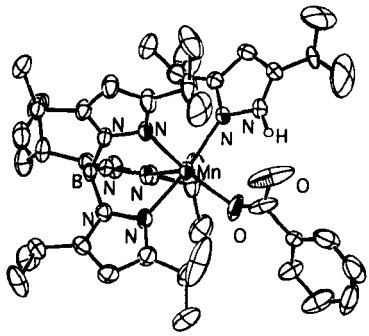

FIG. 13. [Mn^{III}(hydrotris(3,5-diisopropylpyrazol-1-yl)borate)(3,5-diisopropylpyrazole)(benzoate)] perchlorate. [Reproduced with permission from (*208*). Copyright 1993 the American Chemical Society.]

not purely five-coordinate compounds. The crystal structure of each bears both a five-coordinate form with one Cl^- bound to the central Mn and one Cl^- counterion, and a six-coordinate complex with two chlorides bound to the central Mn (Fig. 14). Another five-coordinate complex appeared in 1990 (*213*) with a single bis(benzyimidazolyl-1-methyl)amine ligand and two acetate molecules (Fig. 15). The amine ligand binds meridionally, with the two acetate ions completing the equatorial plane of the structure. A few Mn^{II} complexes with square pyramidal geometry were also reported. In one case, the basal plane is occupied by two dihydrobis(pyrazol-1-yl)borate ligands with an axial chloride (Fig. 16) (*214*). In another, the axial position is occupied by an axial THF molecule with two THF molecules and two phenoxy donor groups in the basal plane (*215*).

The greatest number of complexes characterized are those that are six coordinate. One general structure type involves multidentate li-

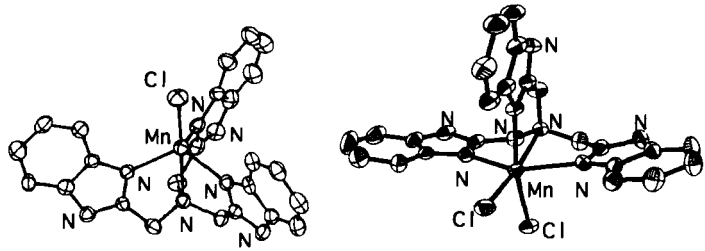

FIG. 14. Crystal structure (left) of [Mn^{II}(tris(benzimidazoyl-2-methyl)amino)Cl]$^+$, the trigonal bipyramidal complex. Crystal structure (right) of the neutral six-coordinate [Mn^{II}(tris(benzimidazoyl-2-methyl)amine)Cl_2]. [Reproduced with permission from (*211*) and (*212*), respectively. Copyright 1997 the American Chemical Society and copyright 1995 Elsevier Science, respectively.]

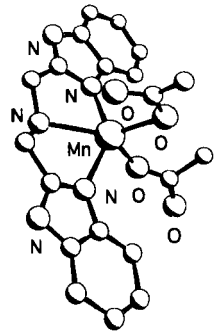

FIG. 15. [Mn^{II}(bis(benzyimidazolyl-1-methyl)amine)$(OAc)_2$]. [Reproduced with permission from (*213*). Copyright 1990 the Royal Society of Chemistry.]

gands that fill four of the six available coordination sites, allowing monodentate ligands such as halides or water to occupy the two remaining positions in the first coordination sphere. In complexes that involve bidentate ligands such as phenanthroline, bipyridine, or acetylacetone, which often do not bind opposite to each other in the "equatorial" plane of these compounds, a structural type in which the two remaining coordination sites are *cis* to one another is promoted. One example of these bis bidentate chelate complexes is the complex (ditriflato)bis(bipyridino) Mn^{II} (*216*) and bis (phenanthrolino)(dithiocyanato) Mn^{II} (Fig. 17) (*217*). One of the more unique examples in this group involves a fused-ring system, which provides a tetradentate N_4-donor ligand that occupies three coordination sites on one face and one addition site on the other. The two remaining *cis* positions were filled by bromides and chlorides, ultimately leading to distorted octahedral structures (Fig. 18) (*218*). This group also includes complexes derived from the tris(benzimidazoyl-2-methyl)amine ligand mentioned earlier (Fig. 14) (*211*, *212*).

When the chelating ligands are able to occupy the "equatorial plane" of a Mn^{II} complex at the same time, the monodentate ligands

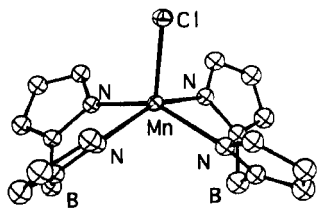

FIG. 16. Square pyramidal [Mn^{II}(dihydorobis(pyrazol-1yl)borate)Cl]$^+$. [Reproduced with permission from (*214*). Copyright 1990 the Royal Society of Chemistry.]

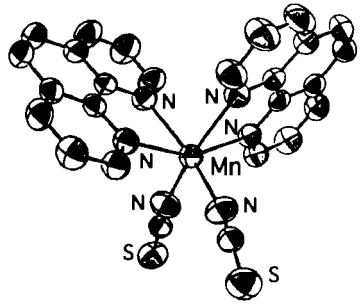

FIG. 17. [Mn^{II}(phenanthroline)$_2$(SCN)$_2$]. [Reproduced with permission from (*217*). Copyright 1993 International Union of Crystallography.]

will bind to the central Mn^{II} ion on the remaining two *trans* "axial" positions. Variations on this theme include charged chelating ligands with a pair of neutral ligands axial or equatorial neutral chelates, such as a tetraazamacrocyle, for example, with charged axial ligands, such as halide ions (Fig. 19) (*219*). Yet another variation found for these complexes is one in which all of the ligands about the central Mn^{II} are neutral, for example the complex [bis(bis(2-pyridylmethyl) amino)Mn^{II}]$^{2+}$ (Fig. 19) (*220*).

A less common but rapidly growing family of Mn^{II} complexes are those that are seven coordinate. These complexes may be built up from a variety of ligand systems that range from multiple ligands to a single septadentate ligand. Some of these systems have been tested as MnSOD mimics. Most of the seven-coordinate complexes that were structurally characterized in recent years have adopted a pentagonal bipyramidal geometry. One motif is based on a pentadentate macrocylic ligand with two unidentate ligands in the axial positions. One particular family of pentagonal bipyramidal complexes was prepared by Riley and co-workers from the macrocyclic ligand 1,4,7,10,13-pen-

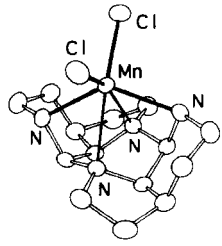

FIG. 18. Mn^{II}(2,5,8,10,13,16-hexaazapentacyclo[8.6.1.1^{2,5}.0^{9,18}.0^{13,17}]octadecane)Cl_2. [Reproduced with permission from (*218*). Copyright 1989 Verlag der Zeitschriften für Naturforschung.]

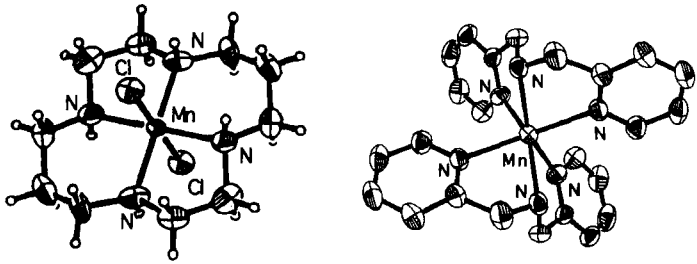

FIG. 19. [Mn^{II}(1,4,7,10-tetraazadodecane)Cl_2], left, and [Mn^{II}(bis(2-pyridylmethyl) amine)$_2$]$^{2+}$, right. [Reproduced with permission from (*219*) and (*220*), respectively. Copyright 1996 International Union of Crystallography and Copyright 1992 American Chemical Society, respectively.]

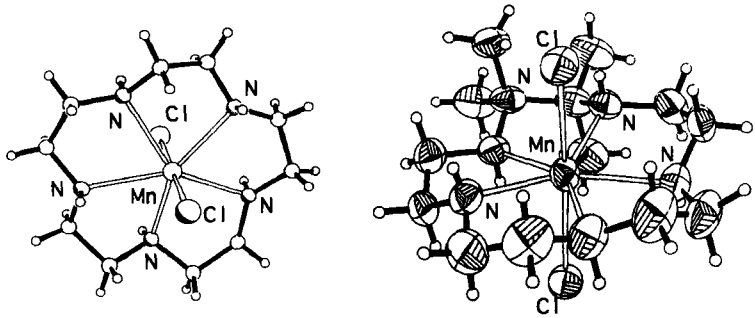

FIG. 20. Two seven-coordinate Mn^{II} complexes that have been tested as MnSOD mimics. [Mn^{II}(1,4,7,10,13-pentaazacyclopentadecane)Cl_2] (left) and [Mn^{II}(trans-2,3-cyclohexano-1,4,7,10,13-pentaazacyclopentadecane)Cl_2] (right). [Reproduced with permission from (*221*) and (*222*). Copyright 1994 and 1996 the American Chemical Society, respectively.]

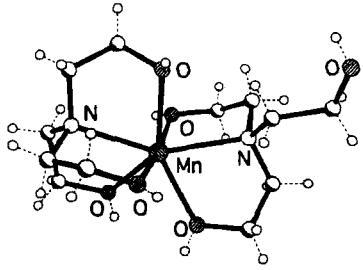

FIG. 21. [Mn^{II}(tris(ethanol)amine)$_2$]. [Reproduced with permission from (*217*). Copyright 1993 Verlag der Zeitschriften für Naturforschung.]

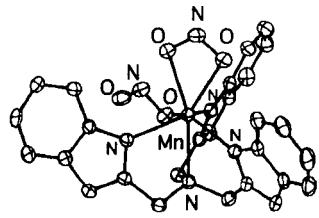

FIG. 22. [Mn^{II}(tris(benzimidazoyl-2-methyl)amino)$(NO_2)_2$]. [Reproduced with permission from (*211*). Copyright 1997 the American Chemical Society.]

taazacyclopentadecane (*221*, *222*) (Fig. 20). The first coordination sphere in these complexes is completed by two axial chlorides. This work was specifically focused on the development of MnSOD mimics, and these workers have generated a wide range of complexes by preparing a series of ligands in which the macrocyclic ligand was modified by additions to the ring's carbon skeleton (*222*). Another example involves a modified 15-C-5 ligand with axial di-*t*-butylnaphthylsulfonates (*223*), and a related complex has been prepared with two axial trifluoromethylsulfonates (*224*). Pentagonal bipyramidal complexes do not, however, require macrocyles to form. Other pentadentate but open-ended ligands have also proved to be well suited for the generation of seven-coordinate complexes (*225–227*). Figure 21 shows an example of a complex with an MnL_2 motif, wherein one tris(ethanol) amine ligand binds as a tetradentate ligand, while the other binds as a tridentate ligand with one unbound ethanol arm. Another example of CN 7 is that of the tetradentate ligand tris(benzimidazoyl-2-methyl) amine and Mn^{II} (Fig. 22) (*211*), wherein the other three binding sites are occupied by one monodentate nitrite and one bidentate nitrite molecule. A final example is provided by the complex of Mn^{II} with quaterypyridine, one water, and a bidentate acetate (Fig. 23) (*226*).

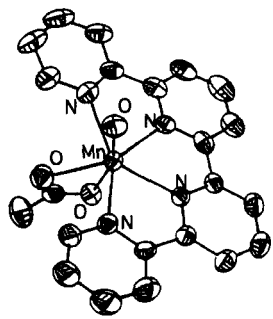

FIG. 23. [Mn^{II}(quaterpyridine)(OAc)(H_2O)]$^+$. [Reproduced with permission from (*226*). Copyright 1993 Elsevier Science.]

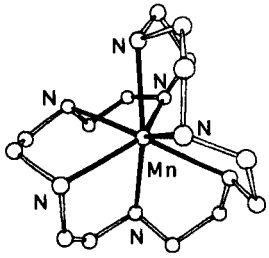

FIG. 24. $[Mn^{II}(1,4,7,10,13,16,19\text{-septaazacyclouneicosane})]^{2+}$. [Reproduced with permission from (*228*). Copyright 1990 the American Chemical Society.]

Two seven-coordinate complexes were attained by utilizing single septadentate ligands. The first involved 1,4,7,10,13,16,19-septaazacyclouneicosane, but no specific geometric orientation about the Mn^{II} was reported (Fig. 24) (*228*). The second structure is of a monocapped trigonal antiprism, prepared by using the septadentate ligand formed by Schiff-base condensation from tris(2-aminoethyl)amine and 2-pyridinecarboxaldehyde to give tris(2-aminoethyl)amine-pendant pyridyl-2-methyl functional groups (Fig. 25) (*229*). This complex was tested for MnSOD activity (discussed later).

A final structural motif for Mn^{II} is represented by a few eight coordinate structures. One of these was a product of tetraazacyclododecane with pyrazolylyl-1-methyl groups appended to the ring nitrogens

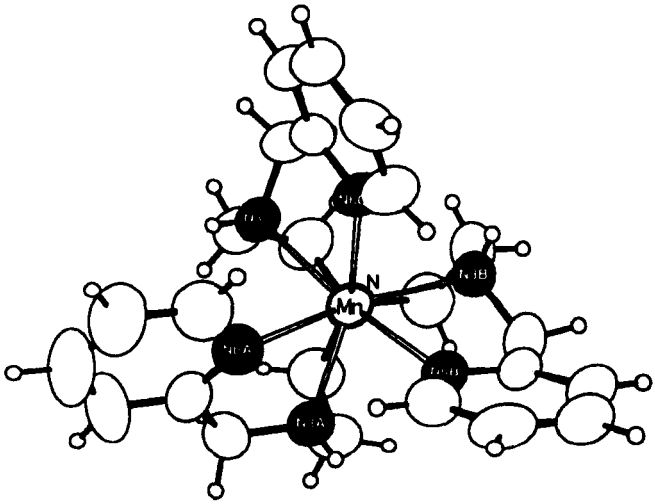

FIG. 25. $[Mn^{II}(tpaa)]^{2+}$. [Reproduced with permission from (*229*). Copyright 1996 the American Chemical Society.]

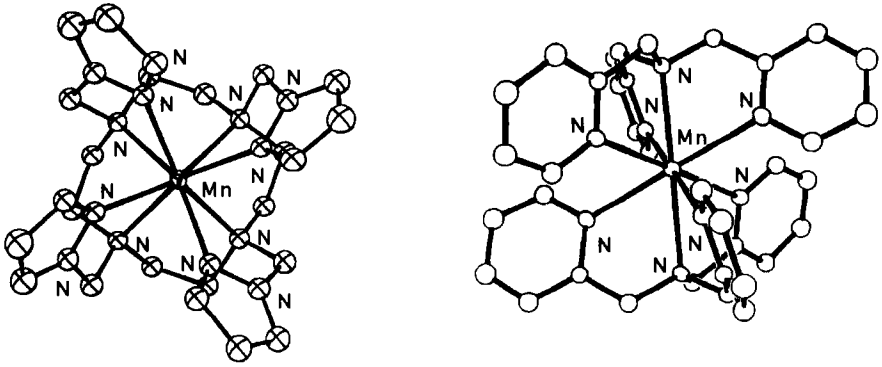

FIG. 26. $[Mn^{II}(1,4,7,10\text{-}(1\text{-pyrazolylmethyl})tetraazacyclododecane)]^{2+}$ (left) and $[Mn^{II}$(tris(2-pyridylmethyl)amine)$]^{2+}$ (right). [Reproduced with permission from (*230*) and (*232*). Copyright 1992 the Royal Society of Chemistry and copyright 1993 Elsevier Science, respectively.]

(Fig. 26) (*230*). This led to a Mn^{II} complex having a square prismatic geometry. The second complex is composed of a cryptate ligand that yields a complex with a cubic symmetry (Fig. 27) (*231*). The third structure is built up from two tetradentate tripodal amine ligands about the Mn^{II} ions (Fig. 26) (*232*).

One final note is of interest. Most of the structurally characterized and otherwise isolated complexes of Mn^{II} tend to be high spin. The structure of at least one low-spin complex was reported during the past few years. This is a six-coordinate complex composed of two methyl-4,5-dihydro-5-{[imino(methylthio)methyl]azo}-3,5-dimethyl-1*H*-pyrazole-1-carboximidothioato ligands, which provide an N_6 first coordination sphere via one aza-nitrogen and two carboximido-nitrogens (Fig. 28) (*233*).

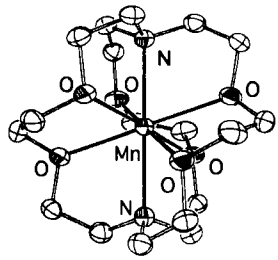

FIG. 27. $[Mn^{II}([2.2.2]cryptand)]^{2+}$ [2.2.2]cryptand = 4,7,13,16,21,24-hexaoxa-1,10-diazabicyclo[8.8.8]hexaxosane. [Reproduced with permission from (*231*). Copyright 1992 Wiley-VCH Verlag.]

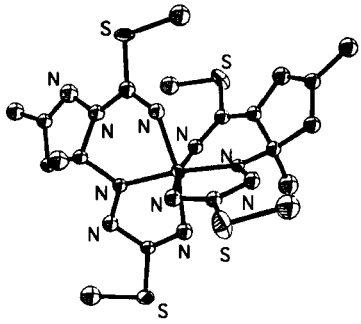

FIG. 28. Low-spin [Mn^{II}(methyl-4,5-dihydro-5-{[imino(methylthio)methyl]azo}-3,5-dimethyl-1*H*-pyrazole-1-carboximidothioate)]. [Reproduced with permission from (*233*). Copyright 1993 the Royal Chemical Society.]

2. *Mn(III)*

Five- and six-coordinate structures dominate the crystallographically characterized structures reported for Mn^{III}. Here the pseudo-Jahn–Teller axis of this d^4 ion plays a role in the overall structure of the Mn^{III} coordination complex, so these complexes tend to adopt either a square pyramidal or octahedral geometry. Most of the five-coordinate complexes that have been structurally characterized are found to adopt a square pyramidal geometry. A prime example of such products are the myriad of Mn^{III} complexes that utilize a tetradentate Schiff-base ligand (*234*), for example H_2-Salpn or H_2Salen, with a fifth donor in the axial position to complete a square pyramidal structure. Such structures are also observed in the Mn^{III} porphyrin complexes with a single axial ligand (*470*). This structure ably supports the pseudo-Jahn–Teller axis along the axial, or *z*, axis. Specific examples of this group of complexes are the complexes utilized for exploring epoxidation chemistry (*235*). One of these complexes is shown in Fig. 29 (*236*), with a structure similar to the other members of this type of complex (*237*). For this type of complex, the Mn^{III} ion tends to be located out of the equatorial plane toward the axial ligand. Another area of Mn^{III} complexes are those that utilize a variety of porphyrins as ligands. Five-coordinate complexes were not limited to the square pyramidal geometry. At least two reports of structurally characterized trigonal bipyramidal complexes have appeared in the literature in recent years. The first is of a complex in which the Mn^{III} is surrounded by an O_5 first coordination sphere composed of two bidentate 2,2′-biphenoxide ligands and one monodentate 2,2′-biphenoxide to create a distorted trigonal bipyramidal geometry (Fig. 30) (*238*). The

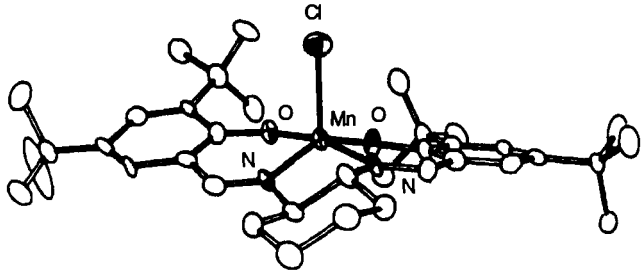

FIG. 29. {Mn^{III}[3,5-(di-*t*-butyl)Salicylidenimino-(*R*,*R*)-(1,2-diaminocyclohexane)]}. [Reproduced with permission from (*236*). Copyright 1996 Wiley-VCH Verlag.]

second is a very intriguing structure with a tegradentate tripodal amine ligand (*239*). Three of the five donor atoms are nitrogens from amide functional groups (Fig. 31). The unique feature of this complex is the hydroxide bound to the Mn^{III} ion. In general, structurally characterized complexes of manganese with hydroxide tend to be rare.

Six-coordinate complexes of Mn^{III} are also quite common. Many of these, again, were prepared with tetradentate Schiff-base ligands that occupy the equatorial plane of the complex while two other ligands bind to the central manganese ion on the remaining *trans* axial positions (*234*, *240*). Structures with Mn^{III} were not, of course, exclusively prepared with tetradentate Schiff bases or similar ligands, however (*241*). A unique six-coordinate structure was reported in 1992 for a Mn^{III}–OH complex, another rare example of a structurally characterized Mn^{III}–OH complex (Fig. 31) (*242*).

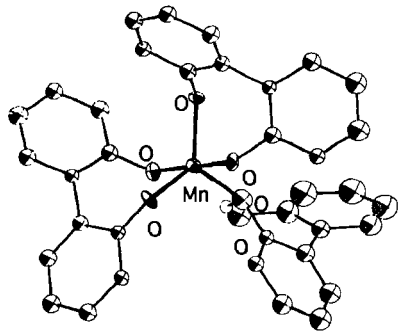

FIG. 30. [Mn^{III}(2,2′-bisphenoxide)(2,2′-bisphenoxideH)]. [Reproduced with permission from (*238*). Copyright 1991 the American Chemical Society.]

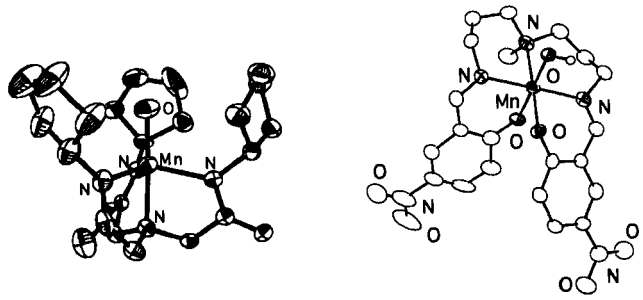

FIG. 31. Rare examples of Mn^{III}–OH-complexes: [Mn^{III}(tris(cyclopropylcarbanoylmethyl)amine)OH]$^-$ (left) and [Mn^{III}(bis(2-hydroxy-5-nitrobenzoiminopropyl)methylamine)OH]. [Reproduced with permission from (*239*) and (*242*). Copyright 1997 and 1992 the Royal Society of Chemistry, respectively.]

The structure of one rather key six-coordinate Mn^{III} complex in this area was reported by Kitajima and co-workers in 1994. This complex is composed of the hydrotris(3,5-diisopropylpyrazol-1-yl)borate ligand, one monodentate 3,5-diisopropylpyrazole, and a side-on-bound peroxide molecule (Fig. 32) (*243*). This structure is important with respect to the question of the "dead-end" complex that is proposed to occur during turnover in MnSOD. It is also a rare example of a structurally characterized Mn–peroxide moiety. One of the key features of this system is the two differing structures that were isolated. In the second structure (Fig. 32), the peroxide is presumed to be hydrogen bonding to the extra pyrozole ligand, based on the shortened interaction between the hydrogen on the nitrogen of the pyrazole ring and the oxygens of the peroxide.

3. *Mn(IV)*

A less common but growing class of complexes are the mononuclear complexes of Mn^{IV}. The structurally characterized Mn^{IV}, d^3, complexes tend to adopt six-coordinate structures that are octahedral in nature. Typically, these Mn^{IV} structures require charged ligands to support the higher oxidation states. This is also true of the Mn^{V} complexes. In most of these complexes, phenolato, alkoxo, or amido donors have been employed to stabilize these higher oxidation states. Among these are the complexes of Mn^{IV} salpn(acac)(PF_6) (*244*) (Fig. 33), which is octahedral with the $salpn^{2-}$ ligand in a *cis*-beta conformation, and a Mn^{IV}(salpn)Cl_2 (*245*) complex with an equatorial $salpn^{2-}$ and two axial chlorides (Fig. 33). An example of an O_6 first coordination sphere is

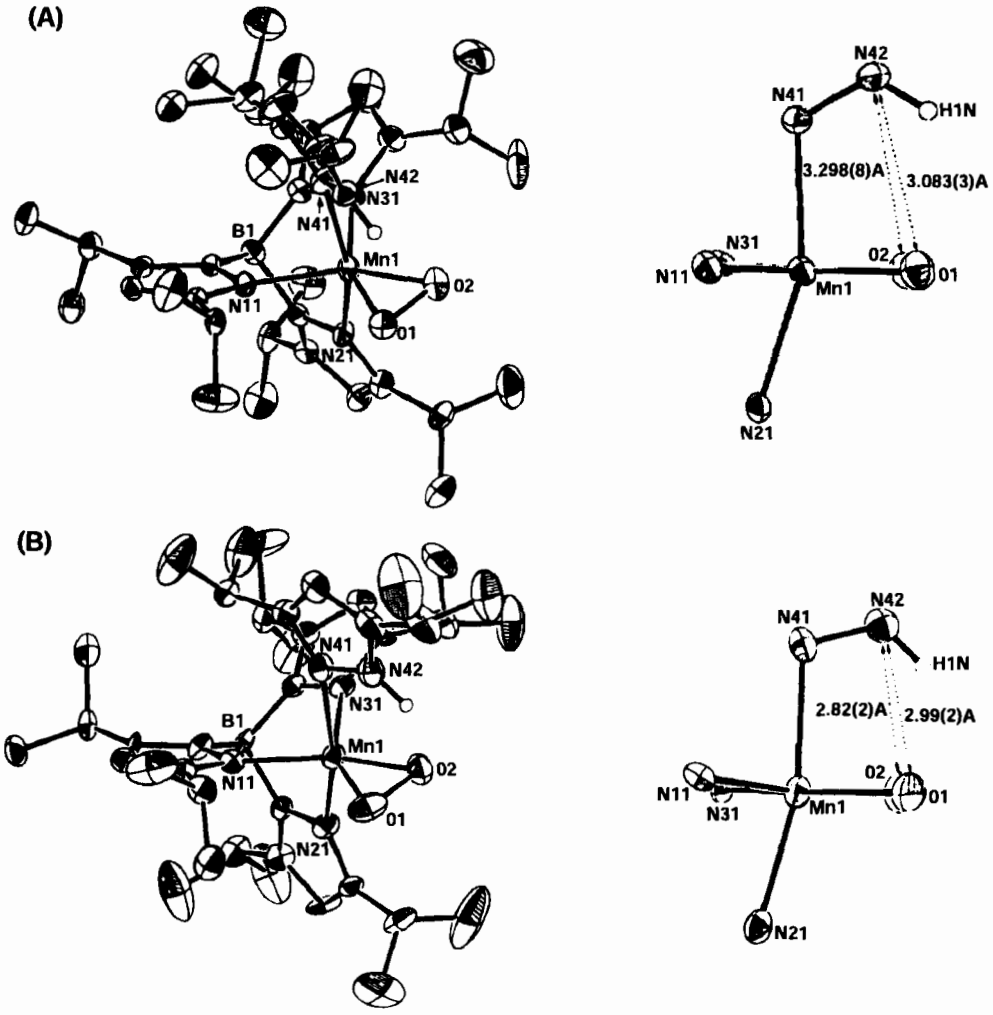

FIG. 32. [Mn^{III}(hydrotris(3,5-diisopropylpyrazol-1-yl)borate)(3,5-diisopropylpyrazole) peroxide]$^+$ Two different structures were grown at low temperatures. In one structure (bottom) there is a hydrogen-bonding interaction between the 3,5-diisopropylpyrazole ligand and the peroxide moiety. The hydrogen-bonding interactions are indicated in the expanded figures to the right. This is an important complex with respect to modeling manganese redox enzymes. [Reproduced with permission from (*243*). Copyright 1994 the American Chemical Society.]

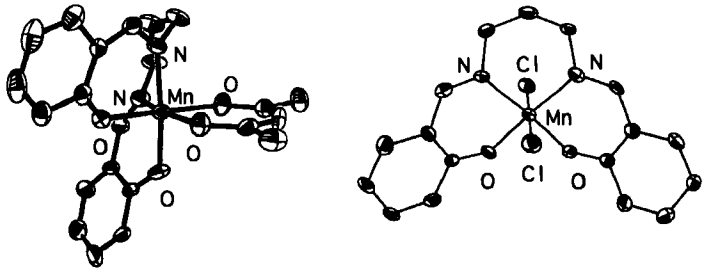

FIG. 33. $[Mn^{IV}(salpn)(acac)](PF_6)$ (left) and $Mn^{IV}(salpn)Cl_2$ (right). [Reproduced with permission from (*244*) and (*245*). Copyright 1991 the American Chemical Society and copyright 1995 the Royal Society of Chemistry, respectively.]

provided by the Mn^{IV} complexes with α-hydroxy acids that were prepared to model manganese peroxidases (Fig. 34) (*246*). A unique hexadentate ligand, based on octamethyltetraamine with salicylic acid moieties appended to the terminal nitrogens to form amide functionalities, produces the mononuclear Mn^{IV} complex shown in Fig. 35 (*247*).

The macrocycle 1,4,7-triazacyclononane (*248*), tacn, has been a popular ligand in the manganese community in recent years. Two interesting complexes based on this ligand with N_3O_3 first coordination spheres have been reported. One Mn^{IV} example is the Mn^{IV}tacn $(OCH_3)_3PF_6$ complex (*249*), which has been suggested as able to epoxidize olefins. This complex adopts a structure with a facial array of methoxides due to the nature of the other, facially binding tacn-based ligand. The second is one in which the alkoxides are appended by alkyl arms to the tacn ligand, similar to the structure in Fig. 36. That structure is represented by the complex with an N_6 first coordination

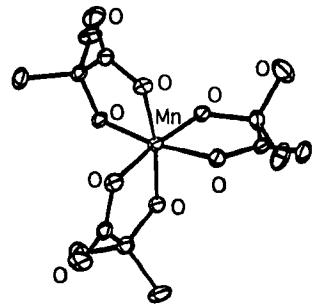

FIG. 34. $[Mn^{IV}(2\text{-hydroxyethylbutyric acid})_3]^-$. [Reproduced with permission from (*246*). Copyright 1991 the American Chemical Society.]

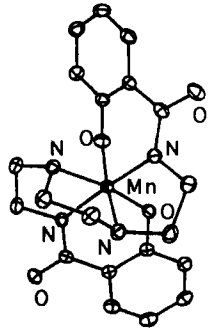

FIG. 35. [Mn^{IV}(1,10-bis(salicylamido)hexamethylenetetraamine)]. [Reproduced with permission from (*247*). Copyright 1992 the American Chemical Society.]

sphere and the triply deprotonated ligand 1,4,7-tris(*o*-aminobenzyl)-1,4,7-triazacyclononane (Fig. 36) (*250*).

4. Mn(V)

Structurally characterized Mn^{V} complexes are rarer still. The new examples of mononuclear manganese complexes in this oxidation

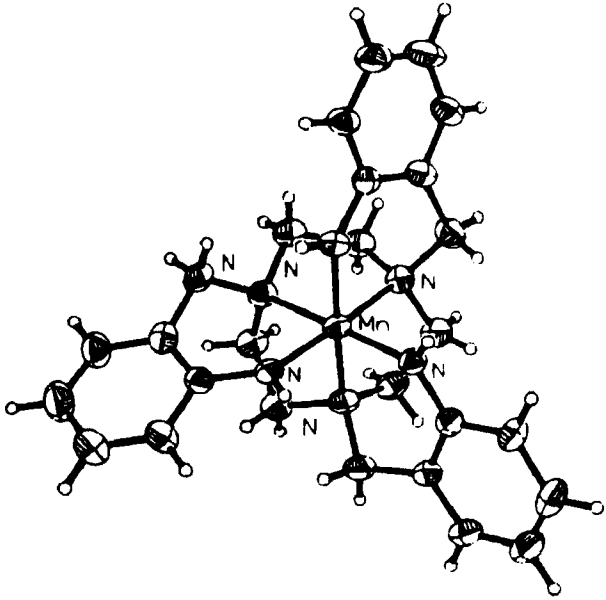

FIG. 36. [Mn^{IV}(1,4,7-tris(*o*-aminobenzyl)-1,4,7-triazacyclononane)]$^{+}$. [Reproduced with permission from (*250*). Copyright 1995 the American Chemical Society.]

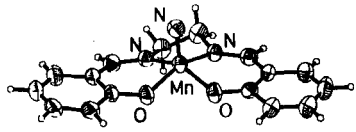

FIG. 37. [Mn^{V}(*N,N'*-bis(salicylideneimino)-2,4-dimethyl-2,4-butanediamine)(N)]. [Reproduced with permission from (*251*). Copyright 1996 the American Chemical Society.]

state have been of nitrodo, N^{3-}, and Mn–oxo derivatives. Most of these adopt a square pyramidal geometry with the organic ligand occupying the axial plane while the oxo or nitrido group occupies an axial site (*251–253*). A manganese–nitrido complex with this orientation appeared with the ligand $salen^{2-}$ and the same ligand with all of the ethylene backbone's protons replaced by methyl groups, $saltmen^{2-}$ (Fig. 37) (*251*). Both the Mn^{V} =O group and the Mn^{V}≡N groups were first characterized in porphyrin systems, but only the Mn^{V}≡N has been structurally characterized (Fig. 38) (*254*). More recently, two Mn^{V}=O complexes have been crystallographically characterized (*255–257*), for example the complex shown in Fig. 39. A unique feature of all of these Mn^{V} complexes is the short Mn–nitrido and Mn–O bonds. The Mn–N bonds are on the order of 1.50–1.54 Å, and the Mn–oxo bonds have been determined to be about 1.54–1.55 Å. Most of these complexes are square pyramidal, but some variation is now known. A recent report of a reputed trigonal bipyramidal Mn^{V}–nitrido complex composed of two bidentate ligands has appeared (*253*), and a six-coordinate Mn^{V} complex was produced by Wieghardt and co-workers in 1996 (*258*) (Fig. 40) that employs a trimethyl tacn ligand, one acetylacetonate ligand, and a terminal nitrido. The Mn–N (nitrido) distance in this complex is 1.518 Å. One nitrogen donor atom from the tacn ligand occupies the axial position opposite to the nitrido at

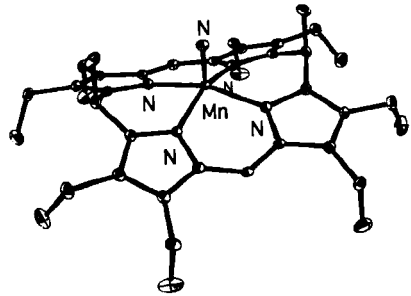

FIG. 38. [Mn^{V}(OEP)(N)]. [Reproduced with permission from (*254*). Copyright 1983 the American Chemical Society.]

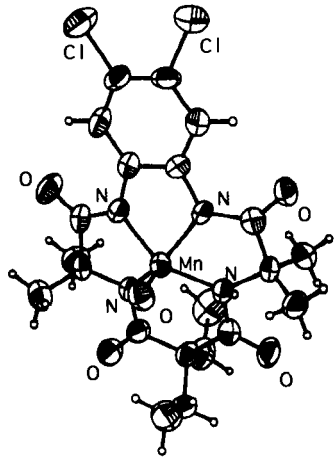

FIG. 39. $[Mn^{V}(L)(O)]^{-}$. [Reproduced with permission from (*256*). Copyright 1990 the American Chemical Society.]

an elongated distance of 2.301 Å compared to the other two N donors from this ligand at 2.055 Å and 2.073 Å. The structures of both of these types of Mn^{V} complexes, $Mn^{V}=O$ and $Mn^{V}\equiv N$, are important structural models for epoxidation and aziridination reagents, and for the OEC with respect to the possible formation of a $Mn^{V}=O$ during turnover.

B. BINUCLEAR

The majority of model compounds synthesized for studying the biomimetic chemistry of manganese are binuclear complexes, due to the

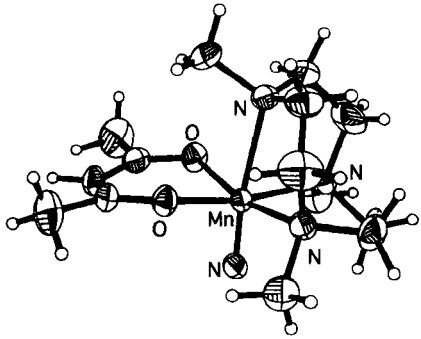

FIG. 40. $[Mn^{V}(Me_3tacn)(acac)N]$. [Reproduced with permission from (*258*). Copyright 1996 the American Chemical Society.]

relative ease and reproducibility of their preparation when compared with complexes of higher nuclearity. There are a number of binuclear manganese enzymes for which binuclear complexes can function as direct structural models (discussed earlier). Furthermore, higher nuclearity clusters in model chemistry and biological chemistry can often be described as assemblies of well-characterized binuclear units. Within the myriad of binuclear manganese complexes synthesized to date, a few core structural motifs appear with regularity. Each core is distinguished by a characteristic Mn–Mn distance that is relatively invariant with changes in the supporting ligands. As such, the Mn–Mn distance, where it is known, is often used as evidence of a particular core structure when a full crystal structure is not available. This is often the case in the biological systems themselves, which have been studied by X-ray absorption spectroscopy and from which Mn–Mn distances are determined even in cases where no crystal structure is available. Table II lists the binuclear manganese complexes whose cores have been structurally characterized along with their respective Mn–Mn separations. Although a multitude of dimanganese complexes have been prepared within each core structure, we will restrict the discussion in this section to those that have been structurally characterized by X-ray crystallography or X-ray absorption spectroscopy.

TABLE II

GENERAL TRENDS IN MN–MN DISTANCES OF SOME COMMON BRIDGING MOTIFS

Bridging motif	Oxidation state	Mn–Mn Distance (Å)
$Mn_2(\mu\text{-}O)_2$	III/III	2.8
	III/IV	2.6–2.7
	IV/IV	2.6–2.7
$Mn_2(\mu\text{-}OR)_2$	II/II	3.2–3.3
	II/III	3.1–3.4
	III/III	3.1–3.2
	III/IV	3.25
$Mn_2(\mu_{1,3}\text{-}OAc)(\mu\text{-}OR)$	II/II	3.6
	III/III	3.3
$Mn_2(\mu\text{-}O)(\mu_{1,3}\text{-}OAc)_2$	II, III, IV	3.1–3.6
$Mn_2(\mu\text{-}O)_2(\mu_{1,3}\text{-}OAc)$	III/IV	2.6
$Mn_2(\mu\text{-}OR)(\mu_{1,3}\text{-}OAc)$	II/III	3.4–3.5
	III/III	3.5–3.6

[a] References are given in text or are in (*280*).

The simplest binuclear structure possesses two manganese ions bridged by a single oxo or hydroxo ligand. Because dioxo- and dihydroxo-bridged manganese dimers tend to be thermodynamically stable, the mono-oxo and monohydroxo complexes are isolated and characterized only with sterically demanding ligands that do not provide two labile manganese coordination sites in a *cis* orientation. Only three complexes with biologically relevant ligands have been structurally characterized, these have two manganese bridged by a single hydroxide. The only nonporphyrin manganese dimer bridged by a single hydroxo linkage is the binuclear complex of the macrocyclic ligand tpictn (Fig. 41) (*259*). The Mn–Mn separation in this highly supported structure is 3.6 Å, with a Mn–O–Mn angle of 126.8°. Mn_2(tpictn)(μ-OH) is a special case, however, in that the $Mn_2(\mu$-OH) core is supported by a macrocyclic ligand that spans both Mn^{II} ions. The only unsupported complexes having a single hydroxide bridge are the Mn^{III} porphyrin complexes $[Mn^{III}(OEP)]_2(\mu$-OH) (*260*) and $[Mn^{III}(TPP)]_2$ (μ-OH) (*261*) (Fig. 42). These complexes exhibit Mn–O–Mn angles of 152.7° and 160.4°, respectively, consistent with the bridging hydroxo group. The more linear geometry of the TPP derivative is probably due to steric demands of the pendant phenyl groups, resulting in a longer Mn–Mn distance, 3.993 Å, for this complex than for the OEP derivative. $[Mn^{III}(5\text{-}NO_2saldien)]_2(\mu$-O) (*262*) has a single oxide ligand bridging two Mn^{III} ions and has a Mn–Mn distance of 3.490 Å (Fig.

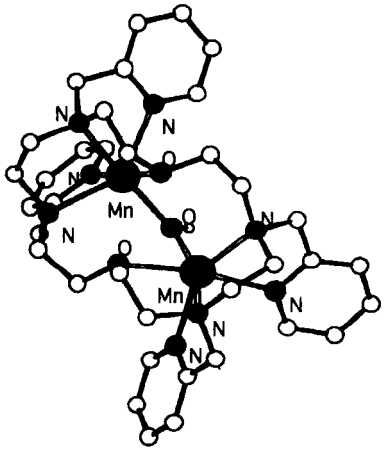

FIG. 41. $[Mn^{II}_2$(tpictn)(μ-OH)]. [Reproduced with permission from (*259*). Copyright 1995 the Royal Society of Chemistry.]

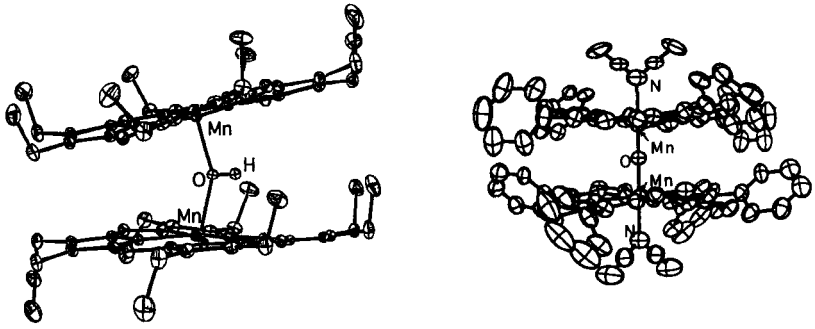

FIG. 42. $[Mn^{III}(OEP)]_2(\mu\text{-}OH)^+$ (left) and $[Mn^{IV}(TPP)N_3]_2(\mu\text{-}O)$ (right). [Reproduced with permission from (*261*) and (*265*). Copyright 1996 the American Chemical Society and copyright 1981 the Royal Society of Chemistry, respectively.]

43). The hydrotris[(3,5-diisopropyl)pyrazolyl]borate derivative $[Mn^{III}(HB(3,5\text{-}iPr_2pz)_2(3\text{-}iPrO\text{-}5\text{-}iPrpz))]_2(\mu\text{-}O)$ (*263*) (Fig. 43), has a similar Mn–Mn distance, 3.53 Å, and a more linear Mn–O–Mn geometry explained by steric demands of the hindered $HB(3,5\text{-}iPr_2pz)_2(3\text{-}iPrO\text{-}5\text{-}iPrpz)$ ligand. The Mn^{IV} complex with tetraphenyl porphyrin forms an oxo-bridged complex, $[Mn^{IV}(TPP)N_3]_2(\mu\text{-}O)$, with a nearly linear Mn–O–Mn angle (*264*, *265*) (Fig. 42).

Analogs of μ-OH-bridged complexes having a single μ-alkoxo ligand are known as well. In fact, when analogous μ-OH and μ-OR bridged complexes are structurally characterized, the structural parameters are often quite similar. At this time the only structurally characterized complexes having a single μ-OR ligand involve the highly supported 2-OHsalpn ligand motif (*266–268*) For example, $[Mn^{III}$(2-OH-

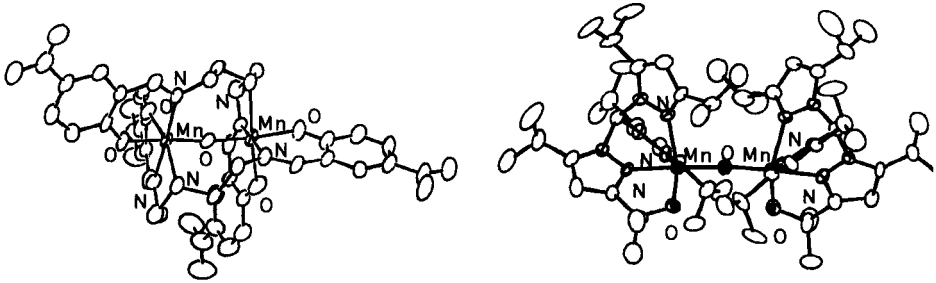

FIG. 43. $[Mn^{III}(5\text{-}NO_2saldien)]_2(\mu\text{-}O)$ and $[Mn^{III}(HB(3,5\text{-}iPr_2pz)_2(3\text{-}iPrO\text{-}5\text{-}iPrpz))]_2$ $(\mu\text{-}O)$. [Reproduced with permission from (*262*) and (*271*). Copyright 1990 and 1991 the American Chemical Society, respectively.]

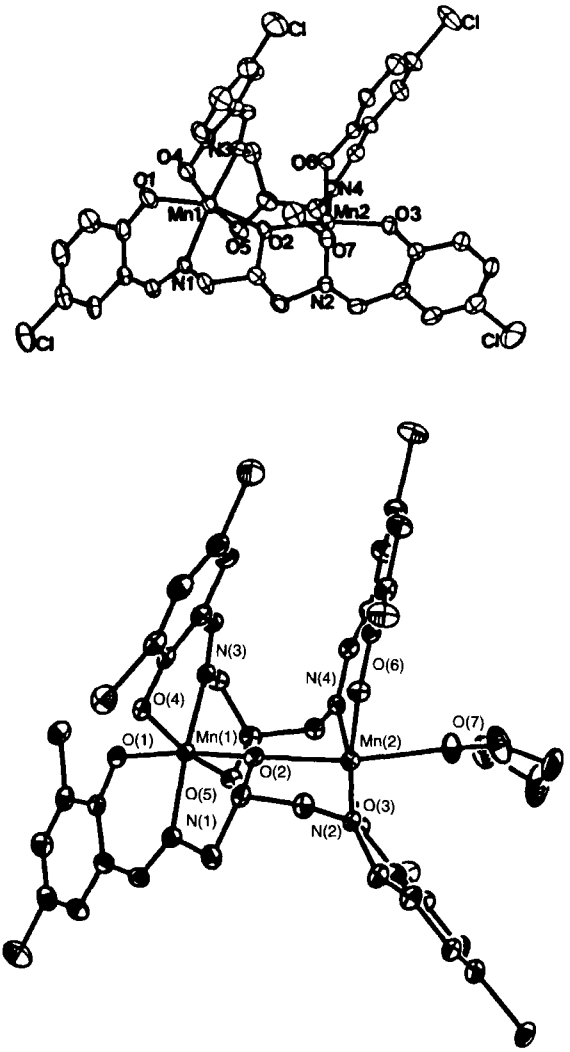

FIG. 44. $[Mn^{III}(2\text{-OH-}(5\text{-Clsal})pn)]_2(CH_3OH)$ and $[Mn^{III}Mn^{IV}(2\text{-OH-}(3,5\text{-}(Cl)_2sal)pn)_2(THF)]^+$. [Reproduced with permission from (*270*). Copyright 1992 the American Chemical Society.]

(5-Clsal)pn)]$_2$(CH_3OH) (Fig. 44) has a Mn–Mn distance of 3.808° and a Mn–O–Mn angle of 129° (*269*), within the range expected for $Mn^{III}_2(\mu\text{-OH})$ complexes (discussed earlier). The analogous mixed-valent $[Mn^{III}Mn^{IV}$ (2-OH-(3,5-$(Cl)_2$sal)pn)$_2$(THF)]$^+$ complex also has a

single alkoxide bridge (*270*) but with a shorter Mn–Mn distance of 3.65 Å and a Mn–O–Mn angle of 126.7° (Fig. 44).

Bis-μ-oxo dimanganese complexes are the most prevalent structurally characterized dimanganese motif in the literature. A smaller number of bis-μ-hydroxo- and bis-μ-alkoxo-bridged analogs are also known. Because of the prevalence of similar structures differing only in the supporting ligands, binuclear manganese bis-μ-oxo, bis-μ-hydroxo, and bis-μ-alkoxo complexes are most conveniently considered as discrete manganese cores in which the supporting ligands play a stabilizing role. This view is supported by the remarkable similarity in core structure among complexes having very different ligands. We will begin by discussing lower valent states and continue with increasing oxidation state of the manganese in the binuclear cluster. $[Mn^{II}_2(HB(3,5\text{-}iPr_2pz)_3)]_2(OH)_2$, with a Mn–Mn distance of 3.314 Å, is to date the only crystallographically characterized binuclear manganese complex with two hydroxo bridges (*271*) (Fig. 45). When this complex is oxidized by MnO_4^- or O_2, the bis-μ-oxo complex $[Mn^{III}(HB(3,5\text{-}iPr_2pz)_3)]_2(O)_2$ is formed (Fig. 45). This oxidized complex has a much shorter Mn–Mn distance of 2.696 Å between two five-coordinate manganese^{III} ions. The six-coordinate complex [Mn^{III}(bispic-

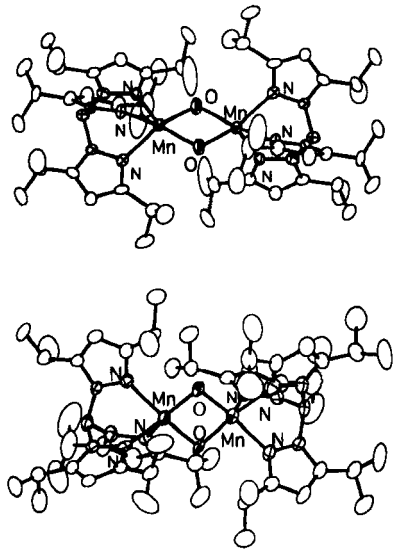

FIG. 45. $[Mn^{II}_2(HB(3,5\text{-}iPr_2pz)_3)]_2(OH)_2$ (top) and $[Mn^{III}(HB(3,5\text{-}iPr_2pz)_3)]_2(O)_2$ (bottom). [Reproduced with permission from (*271*). Copyright 1991 the American Chemical Society.]

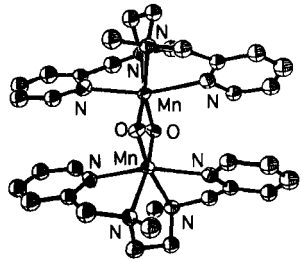

FIG. 46. [Mn^{III}(bispicMe$_2$en)]$_2$(μ-O). [Reproduced with permission from (*272*). Copyright 1994 the American Chemical Society.]

Me$_2$en)]$_2$(μ-O) (Fig. 46), has nearly the same Mn–Mn distance, 2.699 Å, because the Jahn–Teller elongation axis common in Mn^{III} ions does not include a bridging ligand (*272*). No bis-μ-hydroxo dimanganese(III) cores have been structurally characterized, but the analogous bis-μ-methoxo dimanganese(III) complex [Mn^{III}(salpn)]$_2$ (μ-OCH_3)$_2$ (Fig. 47) has been prepared and exhibits a 3.192 Å Mn–Mn distance (*244*). The longer Mn–Mn distance for the alkoxide-bridged complex reflects the Jahn–Teller elongation axis on each of the symmetry-related manganese ions, which includes a bridging alkoxide ligand. The supported [Mn^{III}(2-OHsalpn)]$_2$ (Fig. 48) has two alkoxide bridges as well, but with slightly longer Mn–Mn separation due to the highly supported ligand structure (*273*, *274*).

Mixed-valent dimanganese(III,IV) complexes with the $Mn^{III}Mn^{IV}$ (μ-O)$_2$ core have structural parameters very similar to the corresponding Mn_2^{IV}(μ-O)$_2$ complexes, with Mn–Mn distances in the 2.7-Å range. In spite of the similarity to homovalent cores, the prototypical [Mn^{III} Mn^{IV}(bpy)$_4$(μ-O)$_2$]$^{3+}$ (*275*) and [$Mn^{III}Mn^{IV}$(phen)$_4$(μ-O)$_2$]$^{3+}$ (*276*) com-

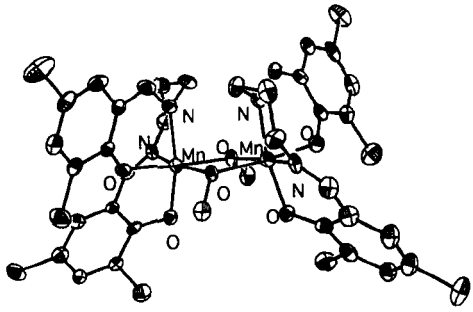

FIG. 47. [Mn^{III}(3,5-diCl-salpn)(μ-OCH_3)]$_2$. [Reproduced with permission from (*244*). Copyright 1991 American Chemical Society.]

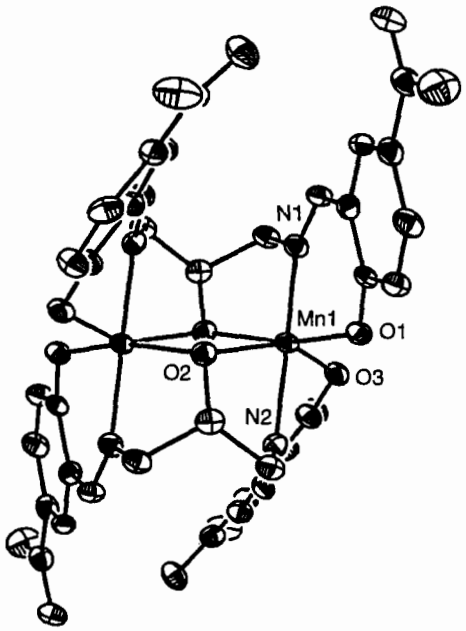

FIG. 48. $[Mn^{III}(2\text{-}OH(5\text{-}NO_2)salpn)]_2$. [Reproduced with permission from (*273*). Copyright 1993 the American Chemical Society.]

plexes are valence localized in the solid state, with one manganese exhibiting the axial elongation associated with isolated Mn^{III} centers and the other having more octahedral geometry consistent with Mn^{IV} (Fig. 49). Other $Mn^{III}Mn^{IV}(\mu\text{-}O)_2$ complexes exhibit valence localization as well (*272*, *277*, *278*). The only example of a mixed-valent $Mn^{III}Mn^{IV}$ bis-μ-alkoxo-bridged complex is $[Mn^{III}Mn^{IV}(2\text{-}OHsalpn)_2]^+$ (*279*), which

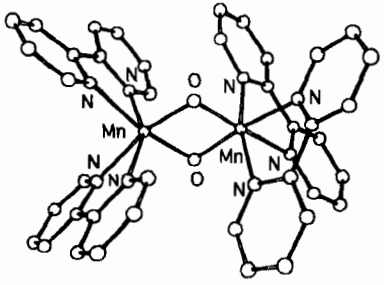

FIG. 49. $[Mn^{III}Mn^{IV}(bpy)_4(\mu\text{-}O)_2]^{3+}$. [Reproduced with permission from (*275*). Copyright 1995 the American Chemical Society.]

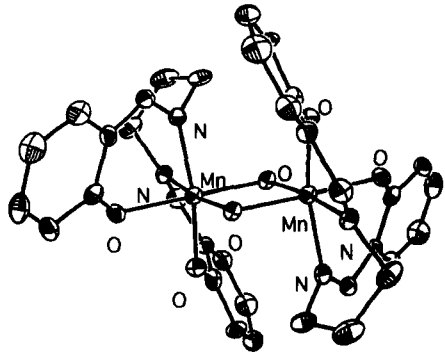

FIG. 50. $[Mn^{IV}(salpn)]_2(\mu\text{-}O)_2$. [Reproduced with permission from (*244*). Copyright 1991 the American Chemical Society.]

has a Mn–Mn separation of 3.3 Å, substantially longer than for bis-μ-oxo complexes in the same oxidation state.

The higher valent $Mn_2^{IV}(\mu\text{-}O)_2$ complexes have been prepared with many supporting ligands, but all show the characteristic Mn–Mn distance of 2.7 Å (*34*). The prototypical complex $[Mn^{IV}(salpn)]_2(\mu\text{-}O)_2$ is shown in Fig. 50 (*280*, *281*). Each successive protonation of $[Mn(salpn)]_2(\mu\text{-}O)_2$ to give $[Mn^{IV}(salpn)]_2(\mu\text{-}O)(\mu\text{-}OH)^+$ and $[Mn^{IV}(salpn)]_2(\mu\text{-}OH)_2^{2+}$ was shown by X-ray absorption spectroscopy to result in an increase in the Mn–Mn distance of 0.10 Å (*282*, *283*). The structural effect of protonation on the $Mn_2^{IV}(\mu\text{-}O)_2$ core is considerably less pronounced than alkylation of the corresponding $Mn_2^{III}(\mu\text{-}O)_2$ complexes due to rearrangement of the Jahn–Teller axis in the Mn^{III} case. A new structure type for $Mn_2^{IV}(\mu\text{-}O)_2$ Schiff-base complexes was reported for the complex $[Mn^{IV}(salen)]_2(\mu\text{-}O)_2$ ligand (*234*, *284*, *285*). In these complexes (Fig. 51), the salen ligand bridges the two manganese ions.

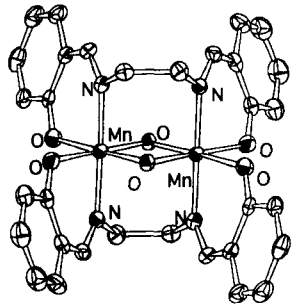

FIG. 51. $[Mn^{IV}(salen)]_2(\mu\text{-}O)_2$. [Reproduced with permission from (*284*). Copyright 1998 Elsevier Science.]

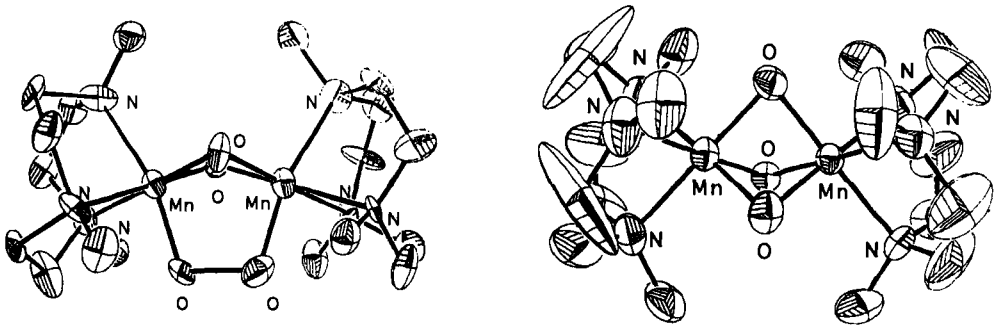

FIG. 52. {[Mn^{IV}(tacn)]$_2$(μ-O)$_2$(μ-O_2)} (left) and [Mn^{IV}(tacn)]$_2$(μ-O)$_3$ (right). [Reproduced with permission from (*286*) and (*287*). Copyright 1988 and 1990 the American Chemical Society, respectively.]

There are two unique examples of triply bridged Mn_2^{IV} dimers that deserve comment at this point. The first is the [Mn^{IV}(tacn)]$_2$(μ-O)$_3$ complex with three bridging oxo ligands and a Mn–Mn distance of 2.3 Å (Fig. 52) the shortest Mn–Mn distance of any binuclear complex to date (*286*). The second is {[Mn^{IV}(tacn)]$_2$(μ-O)$_2$(μ-O_2)} (Fig. 52), which is the only example of a binuclear Mn complex having a μ-1,2 bridging peroxide ligand and a Mn–Mn distance of 2.531 Å (*287*). These two complexes may be considered as Mn_2^{IV}(μ-O)$_2$ cores with either an additional μ-oxo or the μ-1,2-peroxo added as a third ligand. Because of the additional ligand, the Mn_2^{IV}(μ-O)$_2$ core is puckered in contrast to simple Mn_2^{IV}(μ-O)$_2$ cores. The importance of the latter structure is that it may be the best model to date for the initial manganese–oxygen species formed immediately upon O–O bond formation in the critical S_4–S_0 transition in photosynthetic oxygen evolution.

There is a large and important class of binuclear manganese complexes having at least one μ-carboxylate bridge in conjunction with one or two μ-oxo bridges. This class of μ-oxo–μ-carboxylato complexes is important not just in the context of binuclear manganese enzymes such as catalase [which has recently been shown to contain such a core (*125*)], but as analogs for iron oxo–carboxylato complexes, which are very important in the chemistry of nonheme iron redox enzymes. The simplest example in this class of manganese compounds is represented by the μ-oxo–μ-carboxylato system [Mn^{III}(bispicen)]$_2$(μ-O)($\mu_{1,3}$-OAc) with a Mn–Mn separation of 3.28 Å (*288*) (Fig. 53). This core motif has been structurally characterized only in the dimanganese(III) oxidation state (*289*). Although no examples of crystallographically characterized Mn_2^{III}(μ-OH)(OAc) cores exist, the topologically similar Mn_2^{III}(salampn)(OAc) complex (*290*) has a Mn_2^{III}(μ-OR)

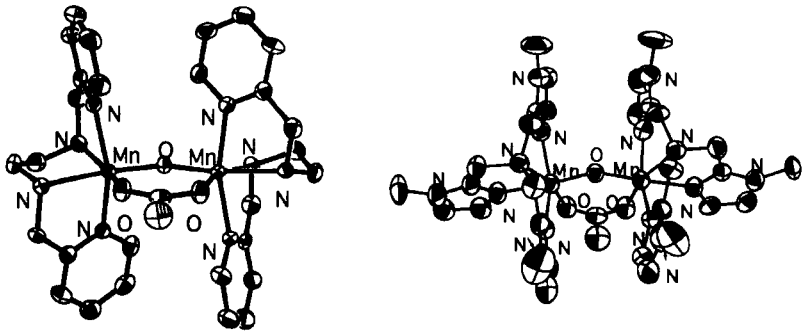

FIG. 53. $[Mn^{III}(bispicen)]_2(\mu\text{-}O)(\mu_{1,3}\text{-}OAc)$ (left) and $[Mn^{III}(tmima)]_2(\mu\text{-}O)(\mu_{1,3}\text{-}OAc)$ (right). [Reproduced with permission from (*288*) and (*289*). Copyright 1994 and 1993 the American Chemical Society, respectively.]

(OAc) core with a Mn–Mn separation of 3.55 Å. The catalase mimic Mn^{II}_2(2-OHbenzimpn)(OAc) (Fig. 54), has the same core in the lower oxidation state (*291*) with a nearly identical Mn–Mn separation, 3.54 Å.

The more common members of the class of μ-oxo–μ-carboxylato complexes have three bridging ligands instead of two. The $Mn_2(\mu\text{-}O)_2(\mu\text{-}RCO_2)$ core may be considered as a $Mn_2(\mu\text{-}O)_2$ core with a carboxylate spanning the Mn–Mn vector (*292–294*). However, the presence of the additional carboxylate bridge induces the $Mn_2(\mu\text{-}O)_2$ unit to be bent. For example, $[Mn^{IV}(bpy)(H_2O)]_2(\mu\text{-}O)_2(\mu_{1,3}\text{-}OAc)^{3+}$ (Fig. 55) has a dihedral angle between $Mn^{IV}(\mu\text{-}O)_2$ planes of 162° and a Mn–Mn distance of 2.64 Å (*295*), which is somewhat shorter than Mn–Mn separations in typical $Mn^{IV}_2(\mu\text{-}O)_2$ cores. Reduced derivatives containing the $Mn^{III}Mn^{IV}(\mu\text{-}O)_2(\mu_{1,3}\text{-}OAc)$ core have similar structural parameters

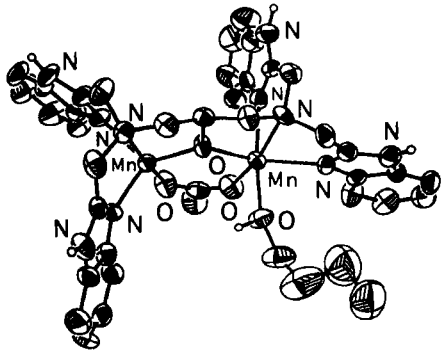

FIG. 54. Mn^{II}_2(2-OHbenzimpn)(OAc). [Reproduced with permission from (*291*). Copyright 1994 the American Chemical Society.]

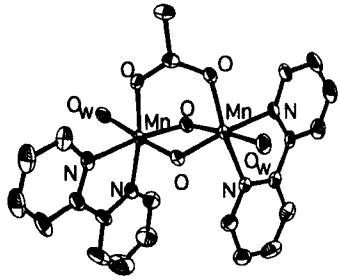

FIG. 55. $[Mn^{IV}(bpy)(H_2O)]_2(\mu\text{-}O)_2(\mu_{1,3}\text{-}OAc)^{3+}$. [Reproduced with permission from (*295*). Copyright 1994 the American Chemical Society.]

(*296*). No bis-μ-hydroxo–μ-carboxylato cores have been isolated. However, several examples of $Mn_2^{III}(\mu\text{-}OR)_2(\mu_{1,3}\text{-}OAc)$ complexes have been prepared and characterized (*266*). Mn_2^{III}(2-OHsalpn)$(MeOH)_2(\mu\text{-}OMe)(\mu_{1,3}\text{-}OAc)$ is typical, with a Mn–Mn separation of 2.9 Å (*266*).

The μ-oxo–bis-μ-carboxylato structure type, $Mn_2(\mu\text{-}O)(\mu\text{-}OAc)$, with two *syn-syn* carboxylate groups and a single μ-oxo ligand has been structurally characterized with a number of supporting ligands, but only in the dimanganese^{III} oxidation state. The Mn–Mn distance in these compounds is in the range of 3.1–3.2 Å, as would be expected for the single oxo bridge. This core topology is particularly interesting because it is the only μ-oxo–μ-carboxylato motif to have been isolated in three different protonation states: $Mn_2^{III}(\mu\text{-}O)(\mu\text{-}OAc)_2$, $Mn^{II}Mn^{III}(\mu\text{-}OH)(\mu\text{-}OAc)_2$, and $Mn_2^{II}(\mu\text{-}OH_2)(\mu\text{-}OAc)_2$ (*297–299*). Representative members of this series are illustrated in Fig. 56. It is noteworthy that each protonation is accompanied by a decrease in oxidation state and a consistent increase in Mn–Mn separation from 3.1 to 3.4 to 3.6–3.8 Å. This is consistent with the decreased donor ability of the single-atom bridge with each successive protonation, which promotes longer bond lengths as well as stabilizing the lower dimer oxidation states.

Dimanganese model complexes having only carboxylate bridges are known primarily in the lower manganese oxidation states, and complexes supported by only a single μ-carboxylate unit are particularly rare (*300–302*). However, there are examples of dimanganese(II) complexes bridged by a single carboxylate. $Mn_2^{II}(RCO_2)$ core has the bridging carboxylate in a *syn-anti* configuration with a long Mn–Mn distance of 5.6 Å, Scheme 14, and complexes in which the carboxylate bridge is in the *anti-anti* configuration have exceptionally long 5.9- to 6.0-Å Mn separations. Bis-μ-carboxylato complexes, $Mn^{II}(\mu\text{-}RCO_2)_2$,

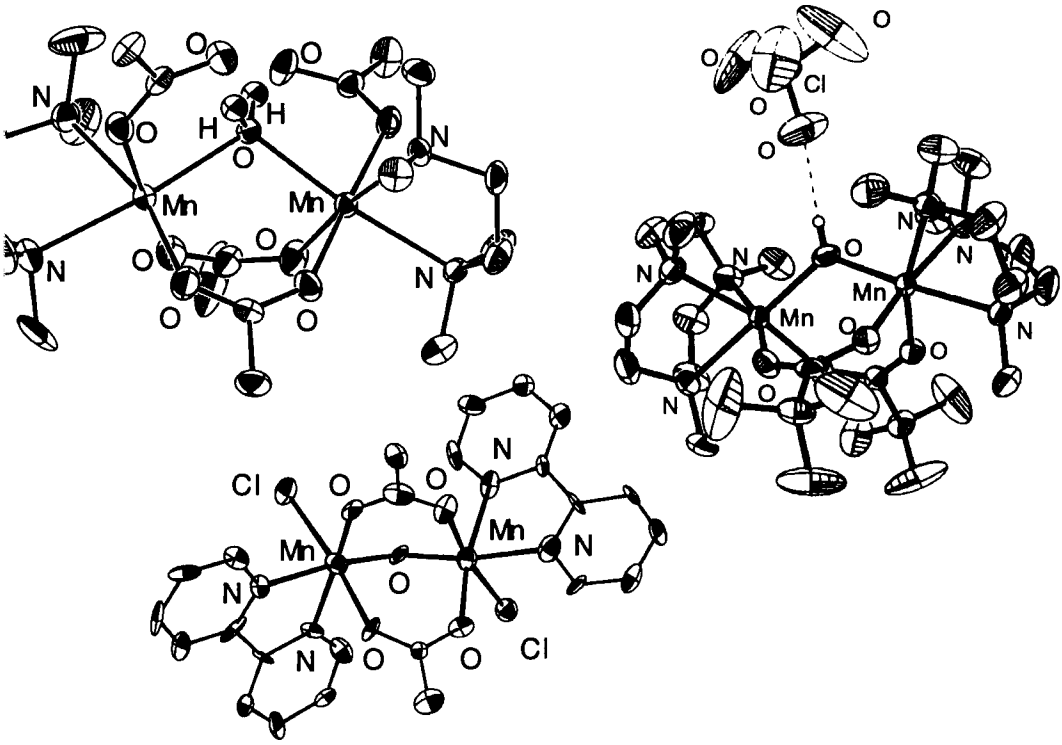

FIG. 56. Examples of $Mn_2(\mu\text{-}O)(\mu\text{-}RCO_2)_2$ cores with varying protonation of the "μ-O" bridge. Upper left: $[Mn^{II}(N,N,N',N'\text{-tetramethyl(ethylenediamine)})]_2(OAc)_2(\mu\text{-}OAc)_2(\mu\text{-}OH_2)$. Right: $\{[Mn^{II}Mn^{III}(Me_3tacn)_2](\mu\text{-}(CH_3)_3COO)_2(\mu\text{-}OH)\}^{+2}$. Lower left: $[Mn^{III}(bipy)Cl_2]_2(\mu\text{-}OAc)_2(\mu\text{-}O)$. [Reproduced with permission from (*472*), (*298*), and (*473*), respectively. Copyright 1992 American Chemical Society, copyright 1996 WILEY-VCH Verlag, and copyright 1993 American Chemical Society, respectively.]

have much shorter 4.3-Å Mn–Mn separations with a *syn-syn* configuration for both μ-carboxylate groups. Addition of a third carboxylate group, $Mn^{II}(\mu\text{-}RCO_2)_3$, yields a Mn–Mn distance of 3.6–4.0 Å (*303*).

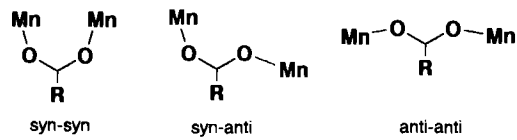

SCHEME 14.

Other unsupported $Mn_2^{III}(\mu\text{-}OR)_2$ cores have Mn–Mn separations of 3.0–3.2 Å. Complexes having one supported μ-alkoxo and one unsup-

ported μ-methoxo ligand can have Mn–Mn distances of 3.0 Å or lower (*266*, *267*).

Alkoxo–μ-carboxylato complexes are topologically similar to their bis-μ-oxo analogs, however, the Mn–Mn distances tend to be considerably longer in the μ-alkoxo complexes than in corresponding μ-oxo derivatives. For example, μ-alkoxo–μ-carboxylato complexes, $Mn_2^{III}(\mu\text{-OR})(\mu\text{-RCO}_2)$, have typical Mn–Mn separations of about 3.5 Å. This is considerably longer than the 3.3-Å separation observed for $Mn_2^{III}(\mu\text{-O})(\mu\text{-RCO}_2)$. $Mn_2(\mu\text{-OR})_2(\mu\text{-RCO}_2)$ complexes have Mn–Mn distances ranging from 2.9 to 3.0 Å, which is about 0.40 Å longer than the oxo–carboxylato-bridged analog. Carboxylato–bis-μ-alkoxo complexes having the $Mn_2^{II}(\mu\text{-OR})(\mu\text{-RCO}_2)_2$ core have even longer 3.3- to 3.4-Å separations (*304*) which extend to as much as 3.5 Å upon oxidation to the $Mn^{II}Mn^{III}(\mu\text{-OR})(\mu\text{-RCO}_2)_2$ oxidation level (*305*, *306*). This compares favorably with 3.4 Å for the $Mn_2^{II}(\mu\text{-OH})(\mu\text{-RCO}_2)$ (*297*, *298*) complex recently prepared, demonstrating that alkylation of μ-oxo-bridged dimanganese cores is a good structural analog for protonation.

μ-Phenoxide-bridged dimanganese clusters are structurally similar to their alkoxide-bridged counterparts (*304–306*). However, an additional factor not present in alkoxo-bridged complexes is the possibility of rotation about the Ar–O bond in phenoxo complexes (*238*, *307*, *308*). Because the donor ability of the phenoxide ligand is dependent on the orientation of the metal ion with respect to the aromatic plane, we might expect that this would be manifested in structural changes upon Ar–O rotation in μ-phenoxide-bridged manganese dimers. In fact, when $Mn_2^{II}(\mu\text{-ArO})_2$ dimers are examined, it is observed that as the dihedral angle between the Mn_2O_2 plane is increased from nearly zero to nearly 90°, the Mn–Mn distance increases from 3.26 Å (*304*) to 3.42 Å (*307*). This is consistent with the phenolate oxygen being a weaker donor when the metal ion acceptor is oriented perpendicularly to the aromatic plane.

There are a limited number of N-bridged or imidazole-bridged dimanganese complexes with biologically relevant supporting ligands (*309*), consisting of azide-bridged complexes. Azide ligation is often used as a model for peroxide ligation to manganese complexes due to the greater stability of azide complexes, which facilitates structural characterization. Azide may bridge either in a μ-1,1 fashion, yielding Mn–Mn separations of 3.4–3.5 Å, or as an μ-1,3 bridge to give a 3.5-Å separation (*310*, *311*). With respect to imidazole-bridged complexes, a complex with the ligand DCBI, 4,5-dicarboxyimidazole, was recently reported, $[Mn^{IV}(3,5\text{-di-}t\text{-butylsalpn})]_2(DCBI)$, with a Mn–Mn separation of 6.18 Å (Fig. 57) (*312*).

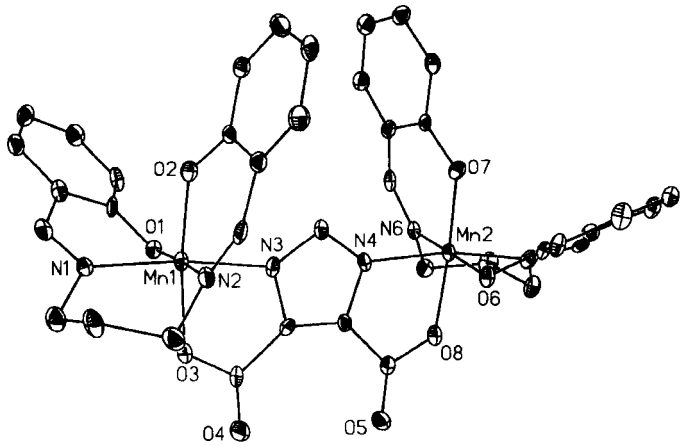

FIG. 57. $[Mn^{IV}(3,5\text{-di-}t\text{-busalpn})]_2DCBI$. [Reproduced with permission from (*312*). Copyright 1997 the American Chemical Society.]

C. TRINUCLEAR

Trimanganese clusters (and clusters of higher nuclearity) can usually be considered as assemblies consisting of the binuclear units discussed in the previous section. There are no known trimanganese enzymes. However, it has been proposed in the past that the four-manganese active site in the OEC may actually be composed of a trinuclear and mononuclear manganese site (discussed earlier). The only trimanganese complexes having only μ-oxo bridges between the manganese ions are those of the $Mn_3(\mu\text{-}O)_4$ class (*292*, *313*, *314*). These consist of a $Mn_2(\mu\text{-}O)_2$ core that is spanned by a $Mn(\mu\text{-}O)_2$ unit (Fig. 58). The topology of these complexes is reminiscent of the Mn_2

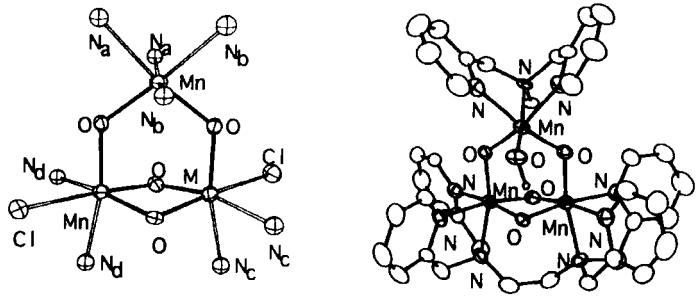

FIG. 58. Two examples of trimeric structures with MnO_2-bridged $Mn_2(\mu\text{-}O)_2$ cores. [Reproduced with permission from (*292*) and (*313*). Copyright 1992 and 1990 the American Chemical Society, respectively.]

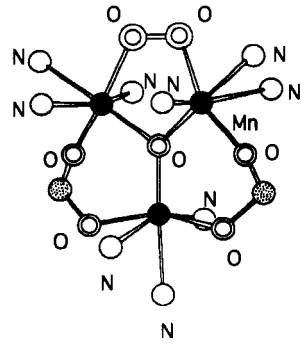

FIG. 59. The trimeric (μ_3-O)(μ-peroxo complex). The other ligands are acetates and diethylenetriamine. [Reproduced with permission from (*317*). Copyright 1988 the American Chemical Society.]

(μ-O)$_2$(μ-RCO$_2$) core, with the Mn(μ-O)$_2$ unit replacing the RCO$_2$ unit of the latter.

There are several reported structures of the Mn$_3$(μ_3-O) unit supported by additional μ-carboxylate bridges (*315*, *316*). The Mn$_3^{III}$(μ_3-O)(MeCO$_2$)$_6$ complex has each manganese ion bridged by two carboxylate and one μ_3-oxo group structurally analogous to the Mn$_2$(μ-O)(μ-RCO$_2$)$_2$ complexes. The Mn–Mn separation in Mn$_3^{III}$(μ_3-O)(MeCO$_2$)$_6$, 3.35 Å, is longer than in Mn$_2$(μ-O)(RCO$_2$)$_2$ and is more reminiscent of the distance in the Mn$_2$(μ-OH)(μ-RCO$_2$)$_2$ complexes. A unique member of this class of μ_3-oxo trimanganese complexes has a single $\mu_{1,2}$-peroxo ligand bridging two of the manganese ions (*317*) (Fig. 59). Another has been produced with a μ_3-OH and a bridging catecholate (*318*).

Trinuclear manganese motifs are common among carboxylate complexes. The Mn$_2^{III}$Mn^{II}(μ-OR)$_2$(μ-RCO$_2$)$_4$ core has found been with various Schiff-base-containing supporting ligands (*269*, *319*, *469*). These cores are characterized by two terminal Mn^{II} ions, which "encapsulate" a central Mn^{III} ion with Mn–Mn neighboring distances of 3.5 Å, which is consistent with the Mn^{II}Mn^{III}(μ-OR)(μ-RCO$_2$)$_2$ dimanganese cores having an identical bridging motif. The μ-hydroxo-bridged analog, Mn$_2^{III}$Mn^{II}(μ-OH)$_2$(μ-RCO$_2$)$_4$, has a similar structure with a somewhat shorter 3.4-Å Mn–Mn separation (Fig. 60) (*320*). Univalent Mn$_3^{II}$ trimers having only bridging carboxylate units, Mn$_3^{II}$(μ-RCO$_2$)$_6$, exhibit a Mn–Mn bridging motif in which one of the three bridging carboxylate undergoes a carboxylate shift in which one of the carboxylate oxygens bridges two Mn^{II} ions (Fig. 61) (*321*). Therefore, these core units are more precisely defined as Mn$_3^{II}$($\mu_{1,3}$-RCO$_2$)$_4$($\mu_{1,1}$-RCO$_2$)$_2$

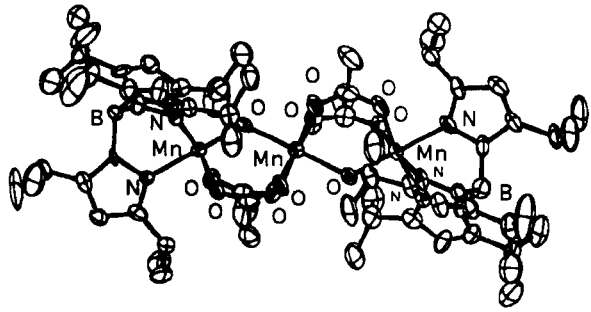

FIG. 60. A $Mn^{III}/Mn^{II}/Mn^{III}$ trimer with a $Mn_2^{III}Mn^{II}(\mu\text{-}OH)_2(RCO_2)_4$ motif. [Reproduced with permission from (*320*). Copyright 1994 the American Chemical Society.]

with a characteristic Mn–Mn separation of 3.5–3.6 Å. The μ-phenolato-bridged trimanganese(II) complexes exhibit a similar carboxylate shift, giving the $Mn_3^{II}(ArO)_2(\mu_{1,3}\text{-}RCO_2)_2(\mu_{1,1}\text{-}RCO_2)_2$ core with intermanganese separations of 3.27 Å (Fig. 62) (*322*).

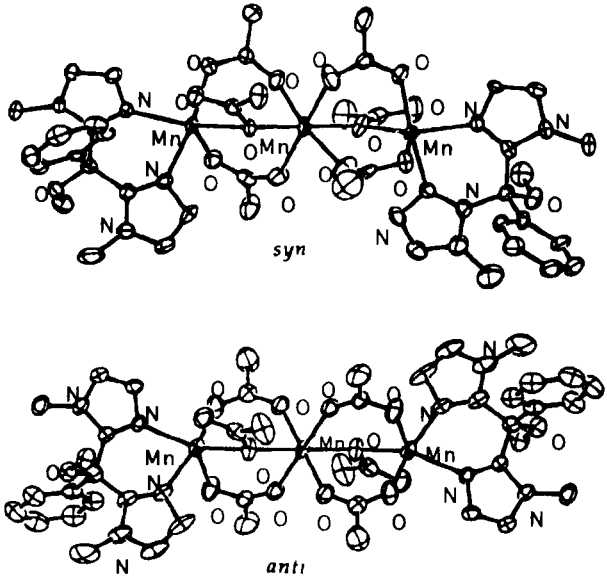

FIG. 61. Mn^{II} trimer with a $Mn_3^{II}(RCO_2)_6$ bridging motif that includes bridging $\mu_{1,3}$-carboxylates and $\mu_{1,1}$-carboxylates. [Reproduced with permission from (*321*). Copyright 1990 Wiley-VCH Verlag.]

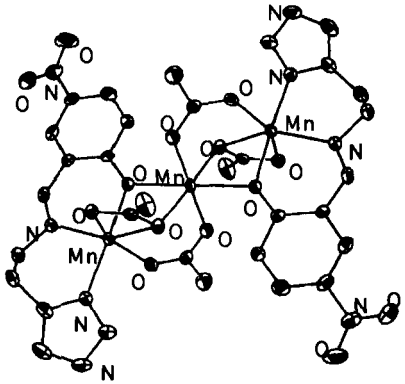

FIG. 62. $Mn^{II}_3(ArO)_2(\mu_{1,3}\text{-}RCO_2)_2(\mu_{1,1}\text{-}RCO_2)_2$ core. $[Mn^{II}_3(5\text{-}NO_2salim)_2(OAc)_4]$. [Reproduced with permission from (*322*). Copyright 1995 the American Chemical Society.]

D. TETRANUCLEAR

As with binuclear manganese complexes, several recurring tetramanganese core structures have been synthesized with different supporting ligand sets (*44*, *323*, *324*). The simplest tetranuclear manganese cluster is the cubane core, Mn_4O_4, which has tetrahedral symmetry in the absence of distortion. A generalized scheme of a cubane core is shown in Scheme 15. This core is arranged in such a way that two oxo bridges exist between any two manganese ions so that all of the manganese ions are equivalent. A number of mixed-valent distorted cubane core structures are known in which the manganese distances are not all equivalent (*325*, *326*). This core was proposed in the past as a model for the manganese cofactor in photosynthetic oxygen evolution, so it has been synthesized with a number of supporting ligand architectures. One of the oxo groups in the cubane core can be replaced with a carboxylate donor to form the asymmetric $Mn_4O_3(PhCO_2)$ complex, in which the four manganese are no longer equivalent and Mn–Mn distances of 2.8 and 3.3 Å are observed. This complex is unique among tetramanganese cores in exhibiting $\mu_{1,1}$ and $\mu_{1,3}$ bridging by a single carboxylate group. An oxo group may also be replaced by a μ_3-chloride ligand to yield the distorted cubane, $Mn_4(O)_3Cl$ (Fig. 63) (*327*, *328*). In this mixed-valent $Mn^{III}_3Mn^{IV}$ complex the three $Mn^{III}Mn^{IV}O_2$ faces have Mn–Mn separations of 2.8 Å, as expected for bis-μ-oxo-bridged $Mn^{III}Mn^{IV}$ complexes. However, the Mn^{III}_2(O)(Cl) faces have an average Mn–Mn distance of 3.3 Å. Alkoxide-containing cubane analogs (*329*), $Mn_4(OR)_4$, have also been prepared and shown to be topologically similar to the conventional oxide-containing cores with somewhat longer Mn separations.

$Mn_4O_nX_m$ Core Structures

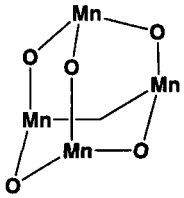

Adamantane

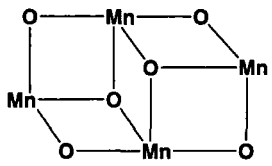

"Fused-Open" Cubane

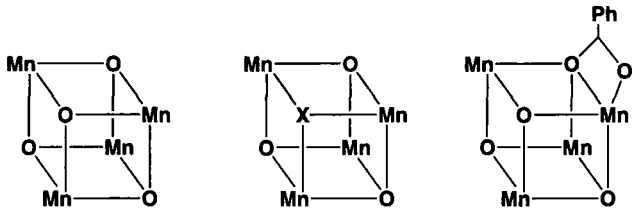

A Selection of Cubane Core Structural Types

"Butterfly" Type Cores

SCHEME 15.

Addition of two oxide donors yields the adamantane complexes, Mn_4O_6, which also have oxo bridges separating all of the manganese (Scheme 15) (*330*). The difference between the cubane and adamantane core is the presence of two oxygen atoms, leading to the proposition that an adamantane-to-cubane conversion in the OEC may lead to oxygen evolution (*31*, *199*, *200*). Another Mn_4O_6 cluster tetranuclear cluster is the "fused open cubane," in which a Mn_4O_6 cluster is formed that is the equivalent of two face-sharing Mn_3O_4 cubanes, with one manganese site vacant (*329*) (Scheme 15). Loss of two oxide bridges from a cubane core yields the Mn_4O_2 core complexes, commonly called butterfly clusters, which have an Mn_2O_2 core as their foundation and two μ_3-oxo groups connecting to the two pendant Mn ions lying above the Mn_2O_2 plane (Scheme 15) (*331*, *332*). A centrosymmetric Mn_4O_2 core has also been observed as well. In these complexes, two μ_3-oxo groups from Mn_2O_2 bridge to two additional manga-

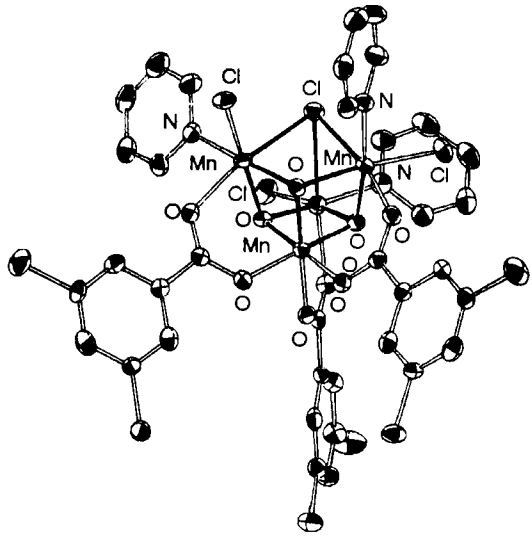

FIG. 63. A manganese cubane cluster with a corner oxygen atom replaced by a chloride. [Reproduced with permission from (*327*). Copyright 1993 the American Chemical Society.]

nese ions, but they are now disposed on opposite faces of the Mn_2O_2 plane.

There are a number of tetramanganese clusters that cannot be considered as merely distorted members of the basic classes, but that may also be relevant in biological manganese chemistry. For example, a highly symmetric tetramanganese complex is formed with the ligand 2-OHpicpn (*333*). This complex, an efficient catalyst for the catalase-like disproportionation of hydrogen peroxide, is an Mn_4L_4 structure in which each pair of manganese ions is bridged by a single alkoxide bridge covalently attached to the picpn unit (Fig. 64). Each manganese is separated from its neighbor by 3.7 Å. In this complex all of the Mn–Mn linkages are identical, so it is not precisely a dimer-of-dimers model. However, the complex $Mn_4O_4(tphpn)^{4+}$ contains two Mn_2O_2 cores cofacially oriented and linked by two alkoxide bridges covalently bound to the tphpn ligand (*334*) (Fig. 64). In this case, two different Mn–Mn linkages support the cluster, and this is accurately considered as a dimer-of-dimers structure. A variation on this theme is the dimer-of-dimers complex $[Mn_2O_2(tmdp)]_2^{4+}$, which also has two Mn_2O_2 dimers, but in this case linked by methylene spacers of the tmdp ligand. This complex has a rather short 2.6-Å Mn–Mn distance across the dioxo core, but a long 5.9-Å Mn–Mn distance across the methylene spacer connecting the two dimers (*335*) (Fig. 65).

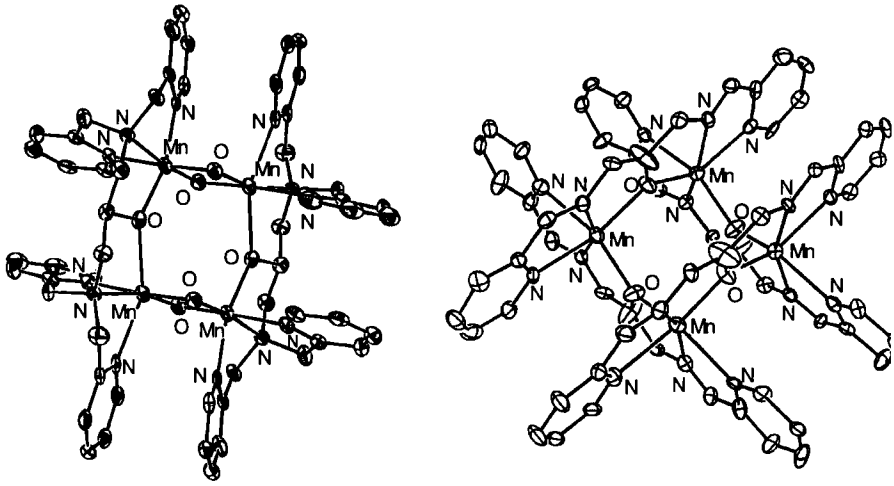

FIG. 64. Two tetramers. Left, is the $[Mn_4O_4(tphpn)_2]^{4+}$ tetramer. Right, $[Mn_4^{II}$(2-OH picpn)$_2$] tphpn = *N,N,N',N*,-tetrakis(pyridylmethyl)-1,3-diaminopropan-2-ol. 2OHpicpn is the Schiff-base condensation product of pyridine-2-carboxaldehyde with 1,3-diaminopropan-2-ol. [Reproduced with permission from (*334*) and (*333*), respectively. Copyright 1991 and 1996 the American Chemical Society, respectively.]

A number of chainlike tetramanganese complexes may also be relevant to biological manganese chemistry. The $Mn_4O_6(bpy)_6^{4+}$ complex (*336*) has the same core stoichiometry as the adamantane complexes (Fig. 66). However, this complex contains four Mn^{IV} ions in a linear configuration in which each pair of neighboring manganese ions is bridged by two oxo bridges with a Mn–Mn distance of 2.7 Å. Longer Mn–Mn distances of 4.9 and 6.4 Å are observed between the 1,3 and 1,4 manganese ions. A topologically similar complex, Mn_4(2-OHPh Phen)$_6$, was prepared having six phenoxide instead of oxide bridges (*337*). The Mn-1–Mn-2 distance here is 3.4 Å, characteristic of dimanganese diphenoxide complexes, in which the Ar dihedral angle with the Mn_2O_2 plane is nearly 90°. $Mn_4O_2(tphpn)_2(H_2O)_2(CF_3SO_3)_2^{3+}$ has a $Mn_4(O)_2(RO)_2$ core with two manganese linked to a Mn_2O_2 core through alkoxo bridges (Fig. 67) (*338*).

IV. Physical Properties

Hydrated manganese in acidic aqueous solution exists in two oxidation states, Mn^{II} and Mn^{III}, with a potential of +1.51 volts separating them (*339*). Therefore, Mn^{III} in solution is a strong oxidant. This

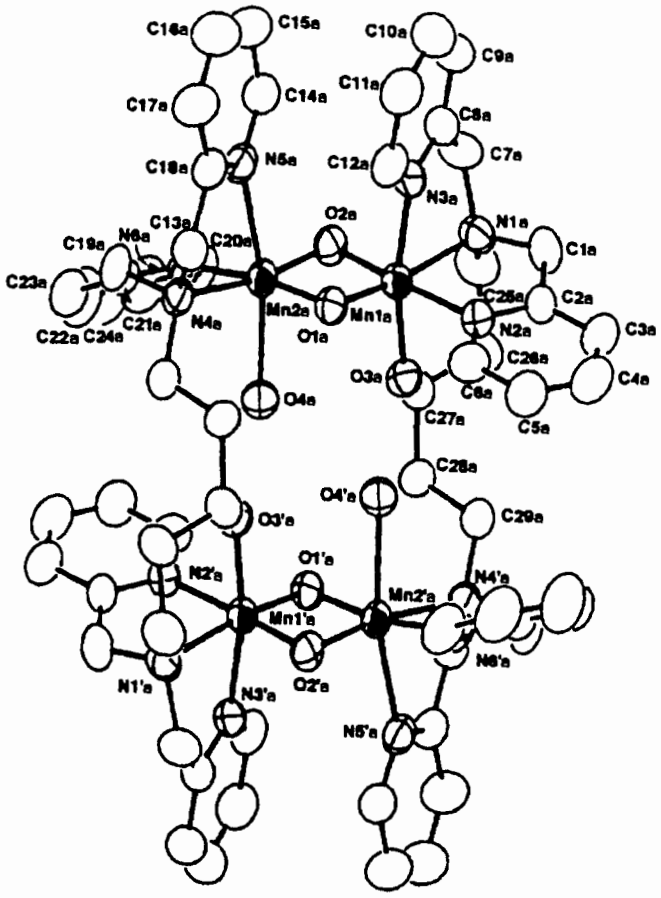

FIG. 65. A dimer of dimers. Two $(\mu\text{-}O^{2-})_2$ bridged $Mn^{III}Mn^{IV}$ dimers are bridged to one another via the ligand. Water molecules are also bound to the manganese of this complex. [Reproduced with permission from (*335*). Copyright 1994 the Chemical Society of Japan.]

arises from the strong driving force to form the stable half-filled d^5 subshell of Mn^{II} from the d^4 Mn^{III} ion. The Mn^{IV} state, which is a d^3 ion, exists as the dioxide MnO_2 or as oligomeric forms thereof. Permanganate ion, having a d^0 Mn^{VII} center, is diamagnetic.

Mononuclear metal–ligand complexes with the Mn^{II}–Mn^{V} oxidation states are all known provided suitable chelating ligands are provided, and polynuclear complexes with Mn^{II}–Mn^{IV} are known as well. Consequently, to understand the spectroscopy of polynuclear complexes, it is necessary to begin by examination of the electronic properties of

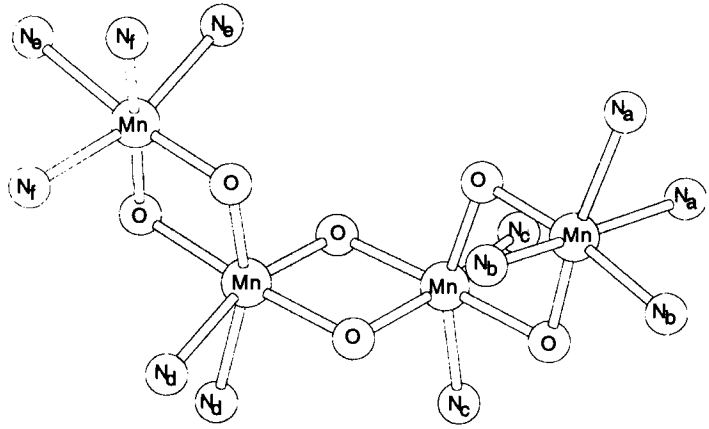

FIG. 66. The first coordination sphere of the complex $Mn_4O_6(bpy)_6^{4+}$ showing the core structure. Matching subscripts on the nitrogens designate that they originated from the same bipy molecule. [Reproduced with permission from (*336*). Copyright 1994 the American Chemical Society.]

manganese ions in these oxidation states. Mn^{II} in an octahedral ligand field has a $^6A_1$ ground state that has spin $S = 5/2$ but is an orbital singlet. Therefore, no spin-orbit coupling arises from the ground state of Mn^{II}, and S is a good quantum number for describing

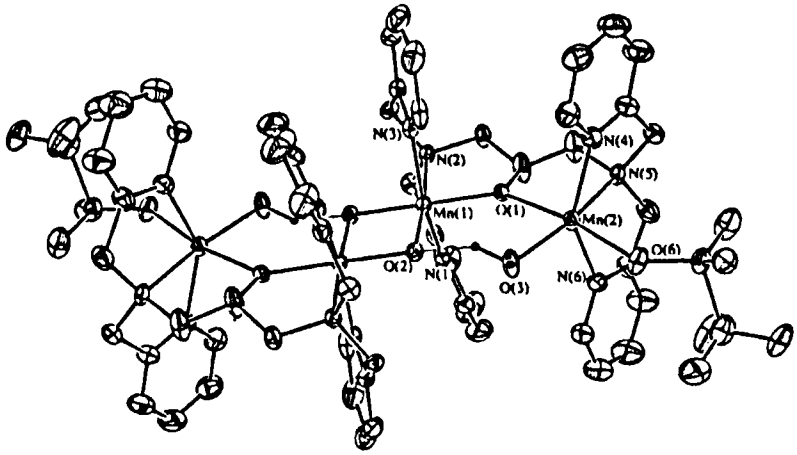

FIG. 67. The linear chain structure with the tphpn ligand. The two inner manganese are involved in Mn_2O_2 core and are then bridged to the outer two manganese ions by ligand alkoxides. [Reproduced with permission from (*338*). Copyright 1990 the American Chemical Society.]

the spin levels of this ion. The same is true for the d^3 Mn^{IV} ion, which has an orbital singlet $^4A_2$ ground state in an octahedral field. However, the ground state of the octahedral d^4 Mn^{III} ion is the orbital doublet ^5E, which gives rise to substantial spin-orbit coupling, $L \cdot S$. Therefore, S is not a good quantum number for describing Mn^{III} electronic properties, and the value $L + S$ is used. The Mn^V complexes thus far isolated are square pyramidal and diamagnetic. This suggests a very strong axial splitting in the t_{2g} orbital set leading to a singlet ^1A ground state in these complexes.

A. Electronic Spectroscopy

Because the most intense bands in the visible spectroscopy of manganese compounds are charge-transfer bands involving the bound ligands (i.e., metal-to-ligand or ligand-to-metal charge transfer), the visible spectra of polynuclear complexes tend to be very similar to those of mononuclear complexes with the same ligands. Consequently, little information on the structure of polynuclear complexes is contained in their electronic spectra. Exceptions to this rule are certain localized mixed-valence complexes that exhibit intervalence charge transfer bands (ITs) formally involving electron transfer between nonequivalent metal sites in the complex. Because this can only occur in polynuclear complexes that are valence localized in the ground state, valence-delocalized complexes cannot exhibit IT bands. An example of an IT transition at 1170 nm (ε = 270 $M^{-1} \cdot cm^{-1}$) is found in the $[Mn^{II}Mn^{III}salamp_2]^-$ complex, whose structure is shown in Fig. 68,

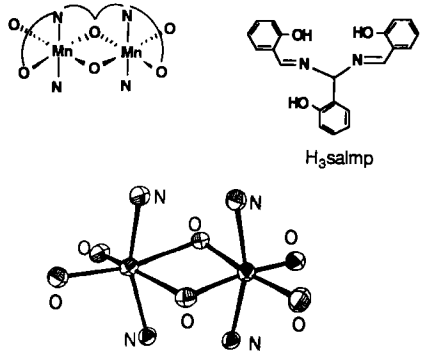

FIG. 68. Core structure of $[Mn^{II}Mn^{III}(salmp)_2]^-$, a diagram of the ligand and the binding motif for one ligand to the manganese are shown above the core structure. [Reproduced with permission from (*308*). Copyright 1991 the American Chemical Society.]

along with a representation of the ligand (*308*). The appearance of IT bands is rationalized based on Marcus theory. Electron transfer between two coupled metal centers, M_A and M_B, is rapid compared to molecular vibrations, resulting in a low-lying excited state in which an electron formerly residing in an orbital of predominantly M_A character has been promoted to an orbital of predominantly M_B character. This excited state may relax via a nonradiative mechanism wherein the ligand environment adjusts along a vibrational normal mode to return to the ground state configuration. Therefore, the energy and lifetime of IT excited states can be strongly influenced by the vibrational structure of the polynuclear complex.

UV-vis spectroscopy proved particularly enlightening with respect to the catalase system (*23*, *30*, *132*). The spectra of model complexes bridged by carboxylate and oxo bridges were quite similar to those observed for the catalase. This led researchers to the proposal that such a motif might also be present, a hypothesis that has been borne out by the crystal structure of the catalase (*125*).

B. Magnetism

Temperature-dependent magnetic susceptibility is often used in the study of polynuclear metal complexes to determine the magnitude of spin exchange energetics between two metal centers in the same molecule (*340*, *341*). This magnitude is called J and is a measure of the energy difference between successively higher molecular spin states when a molecule is placed in a magnetic field. The temperature dependence of the molar magnetic susceptibility χ_m arises from two sources. The first is zero-field splitting, which is measured by D and is observed in mononuclear complexes as well as polynuclear complexes. The primary factor contributing to D in manganese complexes is coupling of the orbital angular momentum and spin angular momentum vectors, and is defined by $L \cdot S$. Octahedral Mn^{II} has a $t_{2g}^3e_g^2$ configuration with a $^6A_1$ ground state, and Mn^{IV} has a $t_{2g}^3e_g^0$ configuration with a $^4A_2$ ground state. Because both of these ground states are orbitally singlet and have no net orbital angular momentum, D will typically be on the order of 0.10 cm^{-1} or less in complexes of these ions (*339*). Therefore, in polynuclear complexes of these ions, S is a good quantum number and the magnetic exchange interaction between the ions can be described by using a spin-only Hamiltonian. However, Mn^{III} has a $t_{2g}^3e_g^1$ configuration with a ^5E ground state, which is an orbital doublet that will have a substantial contribution to the overall magnetic moment arising from the net orbital angular mo-

mentum. As a result, Mn^{III} systems may have D on the order of a few cm^{-1}. For such a system, S is not a good quantum number to describe the energy of the state, and a spin-only description of the magnetic exchange may not apply. The low-temperature susceptibility of Mn^{III} complexes are often dominated by the thermal depopulation of the higher spin states giving a diamagnetic ground state at low temperature.

The second source for the temperature dependence of χ_m is spin–spin ($S_1 \cdot S_2$) coupling or spin exchange, which is unique to polynuclear complexes. $S_1 \cdot S_2$ coupling arises when the spins on two metal centers, M_1 and M_2, are correlated. The two spins may be coupled antiferromagnetically so that the ground spin state S for the system is $S = S_1 - S_2$. On the other hand, the spins may be coupled ferromagnetically to give a ground spin state $S = S_1 + S_2$. We will discuss $S_1 \cdot S_2$ coupling in the context of binuclear systems with the understanding that the general principles applied in the binuclear case also apply to higher polynuclear complexes.

Characterized Mn_2^{II} systems are typically weakly coupled, with J values on the order of 10 cm^{-1} or less (*30*). The orbitally single $^6A_1$ ion is therefore a good example of a system whose temperature-dependent magnetic susceptibility is well treated by the spin-only formalism due to the lack of $L \cdot S$ coupling from the Mn^{II} ground state. The spin-only Hamiltonian is given by $H = S_1 J S_2$ where J is the spin-coupling constant with units of energy and S_1 and S_2 are the spin operators. The eigenvalues E for the system $H\Psi = E\Psi$ are given by $E = J[S(S + 1) - S_1(S_1 + 1) - S_2(S_2 + 1)]$ and the spin energy levels are given by 0, $2J$, $6J$, $12J$, $20J$, and $30J$. The temperature-dependent magnetic susceptibility is then a result of the depopulation of higher spin states as the temperature is decreased, according to the Boltzmann distribution of states, i.e., $P_n = A_n \exp(E_n/kT)/\Sigma A_n \exp(E_n/kT)$, where E_n and A_n are the energy and degeneracy of state n and P_n is its relative population. For an antiferromagnetically coupled system, the ground state is diamagnetic and the magnetic moment should approach zero as the temperature is lowered. Ferromagnetic coupling gives rise to a paramagnetic $S = 5$ ground state so that the low-temperature magnetic moment will approach 11 BM per binuclear complex. Binuclear Mn^{IV} complexes may also be treated by a spin-only Hamiltonian with eigenvalues $E = 0$, $2J$, $6J$, and $12J$. The ground state is also a spin singlet in this case, but the high-temperature moment should approach 5.4 BM/binuclear complex due to equivalent population of all of the spin states.

The Mn^{III} ion has an ^5E ground state that is orbitally nondegenerate. Even so, the spin-only contribution to the temperature-dependent magnetic susceptibility in strongly coupled $Mn^{II}Mn^{III}$, Mn_2^{III}, and $Mn^{III}Mn^{IV}$ complexes may be treated in the same way as for the Mn_2^{II} case discussed earlier. For cases in which $J \gg D$, D can be considered as a perturbation on the spin-only energy levels and the spin-only formalism is usually adequate to explain the magnetic data and to calculate J. For systems with extremely weak coupling (i.e., $J \ll D$, J may be considered as a perturbation on the D-split levels, and the magnetism will be dominated by D. However, when J and D effects are of the same order of magnitude, treatment of the temperature-dependent susceptibility is complicated by the fact that neither S nor L is a good quantum number for describing the spin exchange. A full treatment of magnetic exchange involving both spin and orbital contributions is quite involved and beyond the scope of this discussion (*340*, *341*). Great care must be exercised in the treatment of data on weakly coupled systems containing Mn^{III} in order to accurately assign which effect is responsible for the observed temperature-dependent magnetic data. In many cases, one cannot uniquely fit the magnetic data to a single set of J, D, and g values.

C. EPR Spectroscopy

Electron paramagnetic resonance spectroscopy is one of the primary tools in studying the electronic structure of polynuclear complexes (*341*). Whereas magnetic susceptibility studies are capable of detecting electronic interactions as small as a wavenumber (discussed earlier), the EPR spectrum of a polynuclear complex may be sensitive to intramolecular exchange couplings as small as 0.001 cm^{-1} even at room temperature. Additionally, the ^{55}Mn nucleus has a nuclear spin (I) of 5/2. For a mononuclear system, six hyperfine lines are predicted. However, for a multinuclear system containing n Mn ions, as many as 6^n lines may be observed. This gives rise to a rich EPR spectroscopy among polynuclear manganese complexes, which has been used extensively in the study of biological manganese systems and model complexes.

Mononuclear Mn^{II} and Mn^{IV} complexes exhibit characteristic EPR spectra that are, for the most part, insensitive to the ligand environment around the metal. However, the EPR spectra of polynuclear complexes are strongly dependent on the metal ligation environment, the nature of bridging ligands, and the degree to which the metal

ions are coupled. We will examine some of the relevant binuclear and polynuclear cases in more detail.

1. Binuclear Complexes

Mononuclear Mn^{II} complexes almost always exhibit a single derivative signal with a crossover at $g = 2$ and often having a well-defined six-line Mn hyperfine splitting superimposed on it, as expected from an $S = 5/2$ spin system with only slight spin-orbit coupling. However, two antiferromagnetically coupled Mn^{II} ions coupled antiferromagnetically would be expected to be EPR silent at low temperature owing to the ground-state spin singlet. Binuclear Mn_2^{II} complexes often do exhibit an EPR spectrum due to thermal population of the $S = 1$ through $S = 5$ spin states. Although these are non-Kramer's systems with integer spin, which often do not show X-band EPR spectra in mononuclear complexes due to zero-field effects, such effects are minimal in Mn^{II} due to the $^6A_1$ ground state, and there are a number of examples of EPR spectra of Mn^{II} dimers (*279, 438, 439, 474, 476*).

Binuclear mixed-valent $Mn^{II}Mn^{III}$ complexes nearly always exhibit an EPR signal because the ground state and all thermal excited spin states are Kramer's spin systems. The form of the spectrum depends strongly on the magnitude of J and on the zero-field splitting imparted by the Mn^{III} ion. Strongly coupled systems typically exhibit a signal at $g = 2$ with a multiline hyperfine splitting from two Mn ions; more weakly coupled systems show signals with $g > 2$ due to transitions involving zero-field split levels (*305, 475*).

Unlike Mn_2^{II} dimeric systems, Mn_2^{III} complexes almost never show EPR spectra in the X-band region due to zero-field splitting that puts allowed transitions out of range of X-band energy (9.5 GHz). However, strongly-coupled ($J = 100$ cm^{-1}) mixed-valence $Mn^{III}Mn^{IV}$ systems show very characteristic EPR spectra at $g = 2$, consisting of between 12 and 19 well-resolved Mn hyperfine lines, consistent with an $S = 1/2$ ground state. A typical such spectrum, for $M^{III}Mn^{IV}$ $(\mu\text{-}O)_2L_2$, is shown in Fig. 69. Although 36 lines are theoretically possible for two coupled manganese ions, between 12 and 19 lines are usually observed in practice due to overlap of some of the hyperfine lines. The $g = 2$ signal is the only one typically observed for strongly coupled $Mn^{III}Mn^{IV}$ systems such as the $Mn^{III}Mn^{IV}$ $(\mu\text{-}O)_2$ complexes (*140*), but more weakly coupled $Mn^{III}Mn^{IV}$ systems ($J = 10$ cm^{-1}) may also exhibit a lower-field signal at higher temperatures that is associated with thermal population of a zero-field split $S = 3/2$ excited state (*202*), a feature also often observed in the EPR spectra of mononuclear Mn^{IV} complexes, which are also $S = 3/2$ ions (*140*).

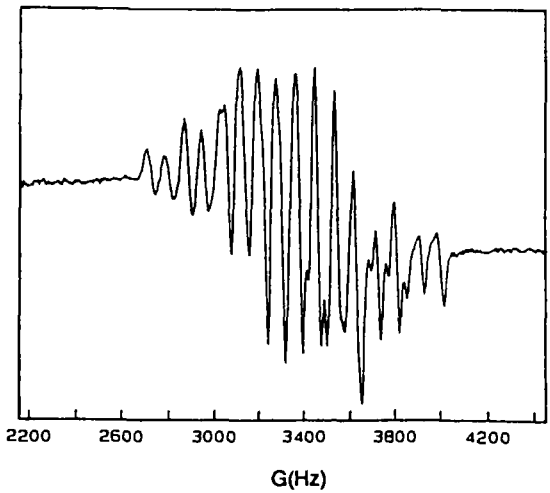

FIG. 69. A $Mn^{III}Mn^{IV}$ exchange coupled EPR spectrum, from $[Mn^{III}Mn^{IV}(bpza)_2(\mu\text{-}O)_2]^{3+}$. bpza = 2-(2′-pyridyl)benzimidazole. [Reproduced with permission from (*465*). Copyright 1994 Elsevier Science.]

Strongly coupled binuclear Mn_2^{IV} complexes have never been shown to exhibit X-band EPR spectra due to the low-energy singlet ground state. Because stabilization of the high-valent Mn^{IV} requires very strong oxyanionic ligands, nearly all such Mn_2^{IV} complexes have at least one bridging oxo or hydroxo ligand, and they may contain additional bridges such as carboxylate ions, all of which contribute to a generally strong coupling in such systems. Consequently, there are few examples of weakly coupled Mn_2^{IV} systems to make generalizations about the presence or lack of EPR spectroscopy in these systems. However, we might expect that because ground-state spin-orbit contributions to zero-field splitting are absent in Mn^{IV} ions, higher spin triplet and quintet states might be EPR active here just as they sometimes are in the Mn_2^{II} complexes. A recent example of an EPR signal arising from a weakly coupled ($J = -2.3$ cm^{-1}) Mn_2^{IV} dimer was observed for the complex $[Mn^{IV}(\text{di-}t\text{-butylsalpn})]_2$DCBI (Fig. 70) (*312*).

2. *Polynuclear Complexes*

Several factors unique to polynuclear systems make the interpretation of their spectra more complicated than for the binuclear cases. One such factor is that a given manganese ion may couple to two or more other ions with *different* exchange magnitudes, J_1 and J_2. The interpretation of such spectra is often simplified by assuming that J_2

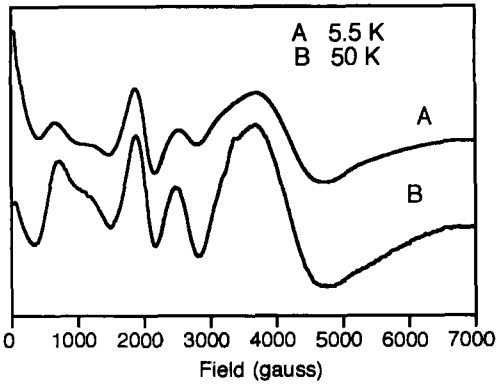

FIG. 70. X-band EPR spectra of the weakly coupled $[Mn^{IV}(3,5\text{-di-}t\text{-busalpn})]_2DCBI$ complex. [Reproduced with permission from (*312*). Copyright 1997 the American Chemical Society.]

is much smaller than J_1 and can either be neglected or treated as a perturbation on the spin splitting by J_1. On the other hand, J_1 may be exactly equal to J_2 (in a highly symmetric trinuclear species for example), thus reducing the spin exchange problem to a simple manifold of states treatment as for binuclear species. However, when J_1 is of the same order of magnitude as J_2, then the spin splitting is complex and cannot be treated by a simple manifold of states.

A second factor complicating the EPR spectroscopy of polynuclear species is the fact that the possible number of Mn hyperfine splittings increases as 6^n where n is the number of manganese ions contributing to the hyperfine interaction. Furthermore, the hyperfine splitting constant A decreases as $1/n$. Therefore, EPR spectra of polynuclear complexes may exhibit broadened signals due to a large number of unresolved hyperfine splittings, which may not be distinguishable from broadening from other sources such as slow tumbling or anisotropy.

3. *EPR of Biological Manganese Complexes*

EPR is one of the most useful techniques brought to bear in the study of polynuclear manganese centers in biology. For example, it was the hyperfine splitting in the CW EPR spectrum of spinach thylakoid membranes that first showed conclusively that the oxygen evolving complex in PS II consisted of a multinuclear cluster of *coupled* manganese ions (*160*, *161*). The EPR from the S_2 oxidation state of active PS II centers has also been the primary signal for tracking the redox cycling of the OEC during oxygen evolution by PS II (*33*, *42*, *46*). There have also been numerous attempts to establish the nuclear

and oxidation levels of the manganese cluster. Brudvig, for example, used variable-temperature EPR data to support a tetranuclear cluster (*342*, *343*). Several other groups have variously assigned these EPR spectra to two dimers (*344*), dimers of dimers, and tetramers (*345*). More recently, Dismukes has argued that the S_2 spectra result from a tetranuclear cluster composed of 3 Mn^{III} and 1 Mn^{IV} ions (*346*). To obtain a good fit of the data, the Mn^{III} ions are predicted to be five coordinate with an inverted order for the *d*-orbital energies. The S_2 signal has also yielded information on the ligand environment (*187*, *347*) through ^{15}N labeling and observation of the ^{15}N hyperfine splitting with ENDOR spectroscopy, and on the binding of substrate and inhibitors (*348*) to the OEC and model complexes (*203*, *349*). Very recently, two new EPR signals have been observed. The S_0 signal was shown to be multiline in the presence of methanol (*170–172*). Using parallel-mode EPR spectroscopy, Britt has shown a beautiful multiline signal for the S_1 oxidation level (*174*). Interpretations of these new signals hold great promise for understanding this enigmatic cluster's structure.

Enzymes containing binuclear Mn sites are especially amenable to structural elucidation using EPR spectroscopy. The EPR spectra of various oxidation levels in the binuclear manganese catalase were used to assign the low-valent active form as a weakly coupled Mn_2^{II} center and the "superoxidized" inactive form as a strongly coupled $Mn^{III}Mn^{IV}$ centers (*7*, *23*, *136*, *138–140*, *350*, *351*). These assignments were based in part on a comparison with the EPR spectra of crystallographically characterized model compounds. The arginase active site was shown to be a binuclear Mn^{II} center by the shape of the spectra and the number and spacing of Mn hyperfine couplings (*7*). The structures proposed for both the manganese-containing catalase and arginase from these studies were essentially confirmed by subsequent X-ray crystal structure analysis (*8*).

D. X-Ray Absorption Spectroscopy

Although it is an unconventional spectroscopic technique, X-ray absorption spectroscopy (XAS) has been the primary tool in the elucidation of the structural features of biological multinuclear Mn centers for which high-resolution crystallographic data are not yet available (*23*, *24*, *134*). This is typically done by comparing features observed in the XAS of the biological complex with similar features found in the spectra of crystallographically characterized Mn model complexes. We defer an extended discussion of the theory and principles of XAS

to several reviews on the subject of XAS in biological and model manganese complexes (*24*, *134*). However, a few basics will suffice to understand the information that is contained in XAS of polynuclear complexes.

Unlike UV and visible electronic spectroscopy, which involve promotion of outer-shell valence electrons, X-ray absorption involves the promotion of *core* electrons to higher energy using X-ray frequencies (*24*, *134*). As such, X-ray absorption is a high-energy technique. There are really two techniques that come under the heading of X-ray absorption. *X*-ray *A*bsorption *N*ear *E*dge *S*tructure, XANES, involves promotion of a 1*s* electron to the 3*d* level in the case of manganese. (This is for the K shell; L edges with core electrons from the $n = 2$ shell are now being examined for models and enzyme.) This gives rise to an absorption "edge" whose energy is very characteristic of the oxidation state of the manganese. As a general rule, manganese in higher oxidation states exhibits absorption edges at higher energies, as might be expected from the tighter binding of core electrons in higher oxidation states. In fact, the edge energy seems to correlate best to the average number and bond lengths of ligands bound to the metal. In polynuclear complexes, shifts in the edge energy are correlated with changes in the *average oxidation* state of the manganese ions. This complicates the use of XANES in higher nuclearity complexes because one-electron oxidation results in a smaller change in the average oxidation state as complex nuclearity increases. Even so, this technique has been used extensively in tracking the oxidation states of the manganese cluster in PS II upon S-state advancements. The progressive edge shift upon increasing oxidation state for polynuclear manganese complexes is nicely illustrated by the XANES spectra of the isostructural series $Mn_2(2\text{-OHsalpn})_n^2$ ($n = -2$ to $+1$) in four successive oxidation states (Fig. 71) (*467*).

As the X-ray energy is increased beyond that required for promotion of the core electron, ejection of core electrons into the continuum occurs. This ejected electron propagates from the Mn center until it encounters another atom from which it can be back-scattered. The interference of back-scattered waves with propagating waves leads to an interference pattern that is manifested as an oscillation in the X-ray absorption pattern. Fourier transformation of this oscillating spectrum from the frequency domain to the distance domain gives a new spectrum whose abscissa contains information on the distance between the target atom (i.e., the Mn center) and the back-scattering atoms. This second technique is called *E*xtended *X*-ray *A*bsorption *F*ine *S*tructure, EXAFS, and has been the only spectroscopic tech-

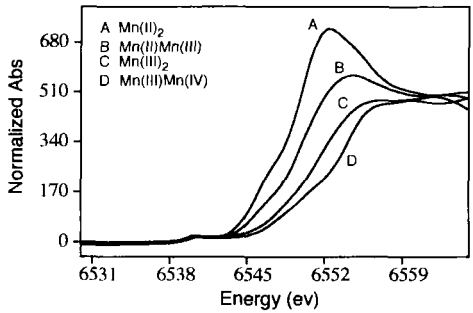

FIG. 71. XANES spectra of the family of complexes $[Mn(2OHsalpn)]^n$ ($n = -2, -1, 0, +1$), and the oxidation states on the manganese go from $Mn^{II}Mn^{II}$ to $Mn^{III}Mn^{IV}$. Noticeable changes occur in the edge energy with each increase in the oxidation state of the manganese. [Reproduced with permission of the author, from (*467*).]

nique to yield direct direct structural information about the manganese cluster in PS II.

The XANES of the Mn catalase provided the first definitive proof that this enzyme cycles between the Mn_2^{II} and Mn_2^{III} oxidation levels (*137*, *352*) The extent of catalase activity correlated with the proportion of Mn_2^{II} or Mn_2^{III} enzyme; however, samples with Mn^{IV} quantitatively showed reduced activity. The EXAFS of the Mn catalases have been less informative because of the Mn–Mn separations in the reduced, active enzymes (*135*). Nevertheless, EXAFS of the "superoxidized" enzyme demonstrated that the $Mn^{III}Mn^{IV}$ enzyme has a Mn–Mn separation of $\approx$2.7 Å, which is consistent with a di-μ_2-oxo core (*135*). Subsequent spectroscopic analysis confirmed that a "diamond core" with a bridging *syn,syn* acetate formed the enzyme active site (*9*).

While interpretation of the XAS for the Mn catalase has been relatively straightforward, the application of XANES and EXAFS to the OEC has led to several significant disagreements among workers in this field (*24*, *28*, *33*, *46*, *48*, *134*, *154*). Klein and Sauer first collected XAS data on the OEC and provided the first detailed structural and oxidation-state information about the Mn cluster (*353*, *354*). The XANES indicated that the S_1 and S_2 enzyme forms contained significant amounts of Mn^{III} and Mn^{IV}. At the same time, both S states could be examined by EXAFS and exhibited short Mn–Mn vectors of 2.7 Å (*154–159*), which is consistent with a high-valent di-μ_2-oxo core, for example the structure in Figs. 49 and 50. Because the S_2 state contains a Kramer's spin ladder (i.e., nonintegral spin system) as shown by EPR spectroscopy, the S_1 state was assigned as $Mn_2^{III}Mn_2^{IV}$ and the

S_2 state was assigned as $Mn^{III}Mn_3^{IV}$. All of the groups using XAS have agreed upon these oxidation levels and general structural details (*24*, *33*, *154*, *156*, *158*, *159*). However, there are members of the EPR community that suggest that the oxidation levels should be adjusted downward by two oxidation states (*346*). The justification for this is that low-coordination-number Mn^{III} ions may have aberrantly high edge energies. If this is true, fits of the EPR spectra would be consistent with XAS data. However, investigations of many model compounds have not supported the idea that XANES edges are this sensitive to coordination number changes (*24*, *33*, *134*).

One area of significant controversy is whether the Mn center is oxidized upon each S-state transition (*24*, *33*) Klein and Sauer argued that upon forming S_3, the edge energy did not increase sufficiently to support manganese oxidation (*355*). However, the S_2-state EPR spectrum disappears upon additional oxidation to S_3, which indicates that the oxidizing equivalent must be in close proximity to the manganese cluster (*46*). These observations have led some investigators to suggest that the substrate (water) is partially oxidized or that a protein residue near the active center is oxidized. Significant excitement was generated when Boussac and Rutherford formed a new EPR signal in EGTA (Ca-depleted) samples (this signal was later shown to occur with acetate addition) (*176*, *356*). The broad radical signal was assigned to histidine radical. However, Britt has shown recently that this signal originates from tyrosine Y_Z, which is the intermediate oxidized charge carrier of the enzyme (*177*, *178*) Subsequent investigation has placed this tyrosine at <5 Å from the manganese cluster. Thus, there is no longer additional evidence suggesting a nonmanganese site of oxidation. In fact, groups have suggested that the Klein and Sauer analysis is flawed based on the experimental conditions or by the fitting of the edge energies (*24*). Unfortunately, there still is no definitive resolution to this issue. At present, our bias is to assign oxidation to manganese at each S-state transition; however, it is possible that our views will evolve with new data.

Another area of significant controversy has been the interpretation of the higher scattering in the EXAFS. Klein and Sauer originally reported a Mn–X scatterer at $\approx$3.3 Å (*357*). This feature was irreproducible (*355*), and only when better sample preparation and detectors became available did this scatterer appear reproducibly (*24*, *33*, *156*, *158*, *358*). Some of the contribution to this peak comes from Mn–C scattering; however, this interaction alone cannot explain the intensity of this feature (*24*). For this reason, the 3.3-Å peak is attributed to Mn–Mn or Mn–Ca scattering. There has been great discussion as

to the identity of the scatterer, and definitive proof of the presence of calcium has not been published (*477*). However, there are recent reports at scientific meetings suggesting that Mn can be seen at 3.4 Å in Sr^{2+}-treated samples. If these withstand further scrutiny, they would provide strong evidence support for the close proximity of Ca to Mn clusters.

The other cofactor often neglected in discussions of the OEC is chloride. Again, EXAFS data have been obtained to address whether or not chloride is bound to the manganese cluster (*33*, *358*, *359*). These experiments are technically very difficult. There is the possibility that chloride (or bromide in bromide-substituted samples) may be observed in the EXAFS spectrum. However, we believe that it is unlikely that one can resolve this issue, because the signal-to-noise ratio may not be sufficient (*156*) to observe only one chloride per four manganese ions. Very recently, chloride EXAFS of manganese model complexes has been reported (*360*). This new application of EXAFS may be able to resolve this issue.

XAS studies of the S_0 state have also been obtained by several groups (*24*, *33*). These are also technically demanding experiments because the S_1 state is the dark stable-oxidation-state level of the OEC. Chemical reductants are used to generate S_0, often with light flashes required for reoxidation. Therefore, it is difficult to know precisely the amount of S_0 that is formed and also whether any of the reaction centers have lost manganese by treatment with reductants. Given these caveats, it appears that the S_0 state in some preparations may contain Mn^{II} (*24*, *33*, *361*). This would suggest a total oxidation assignment of $Mn^{II}Mn^{III}Mn_2^{IV}$. An alternative interpretation is that there is only Mn^{III} and Mn^{IV} present in S_0, giving a cluster assignment of $Mn_3^{III}Mn^{IV}$ (*24*, *362*). It may also be possible that different methods of generating S_0 may give different relative oxidation states for the manganese in the cluster. Perhaps evaluation of the S_0 EPR spectrum will allow definitive interpretation of the XANES spectra.

V. Reactivity

The structures and properties of manganese complexes have provided much useful information on the possible structures and metal–metal or metal–ligand interactions of manganese ions in biological systems. How enzymes carry out their respective transformations is another integral aspect for understanding the overall whole of manganese-containing redox enzymes. Model complexes have been probed

over the years to ascertain how they mimic the reactivity of manganese-containing enzymes, with much of this work focused on the redox-active manganese enzymes, catalase, MnSOD, and the OEC. Further delving into such chemistry often unearths unexpected results and may lead to beneficial new chemistries.

The following segment on the reactivity of manganese complexes will be broken into two sections. The first will cover some of the areas that compose research into the reactivity of manganese-based systems as applied to a specific synthetic organic transformation. The second segment will concentrate on systems designed specifically to model the reactivity of particular enzyme systems.

A. Organic Transformations

Manganese has a rich history within the field of organic synthesis (*363*, *364*). For example, the permanganate anion has long been used as an oxidant to produce a variety of products (*363*). Manganese^{III} acetate also has been extensive explored over the years for the initiation of free radical reactions that lead to carbon–carbon bond formation. These topics have been reviewed and will not be presented further here (*363*, *364*). Manganese chemistry, however, has made an impact in other areas as well, notably the asymmetric epoxidation of alkenes.

1. Epoxidation

a. Salen-Based Systems (Kochi–Jacobsen–Katsuki epoxidation chemistry) One prime example of the application of manganese complexes to organic synthesis is the burgeoning field of transition metal-epoxidation catalysts based on the salen^{2-}ligand (*235*, *365–367*). Recent work in this area has emphasized the stereospecific generation of enantiomeric epoxides, in good yields and with high enantiomeric excesses. Such chemistry is of interest in light of the exquisite control exhibited by nature in producing such stereocenter-bearing oxidation products. Thus, one goal in exploring biomimetic oxidations is to achieve the same level of regio- and stereoselectivity as can be achieved through enzymological transformations. Furthermore, stereoselective epoxidation catalysis promises the ability to produce chiral products that are intermediates in or final products in stereospecific syntheses of use in fields such as medicinal chemistry. Since the early 1990s, manganese salen-based systems have been designed that have shown promise for the preparation of asymmetric epoxides. As is the style in organic chemistry, this important transformation has been named after key researchers in its development, and will hereaf-

ter be referred to as Kochi–Jacobsen–Katsuki epoxidation chemistry. In general, previously described chemistry does not produce epoxidized products in enantiomerically pure form (*235*, *365–367*), especially if the epoxidized olefin's structure does not promote the formation of one enantiomer over another. Thus, many enantiomeric epoxides are often prepared as racemic mixtures. Therefore, it was necessary to design a system that would facilitate stereocontrol by orienting the substrate with respect to the oxygen atom to be transferred from the epoxidizing reagent to the substrate. Preferably, this oxo transfer would occur with large enantiomeric excesses. This goal has been achieved in part by the Mn–salen-based systems (*235*, *365–367*).

Epoxidation chemistry with a variety of metal complexes has been explored over the years. Historically, the Mn–salen catalysts grew out of research focused on understanding the reactivity of cytochrome P_{450} (*368*, *369*). This cytochrome is employed in many enzymes that catalyze a variety of oxidations of organic substrates, including the epoxidation of alkenes (*370*). Usually these reactions are accomplished with complete stereochemical control. Interest in modeling this reactivity has led to a rich literature on biomimetic oxidations (*365*, *367–369*, *371–375*). Because cytochrome P_{450} is a heme enzyme, the initial studies were conducted with iron porphyrin model complexes. Groves showed that one could carry out epoxidations with these model complexes in the presence of an added oxidant, iodosylbenzene (*368*, *376–378*). Further studies showed that manganese porphyrin systems were even more efficient epoxidation catalysts (*375*, *378*). Studies on these systems also contributed to the development of the oxygen rebound mechanism for oxygen atom transfer from high-valent metal–oxo porphyrins to substrate. Since the early catalysis work, a variety of Mn^{III}porphyrin systems have been prepared with various modifications designed to improve the stereochemical control of the catalysts (discussed earlier). Due to the syntheses required to obtain such complexes, simpler, more easily prepared compounds would be desirable (*235*). The related Mn^{III}(salen)X family of complexes, where X is frequently a chloride anion, satisfies these requirements. A crystallographically characterized example of this type of complex is shown in Fig. 29.

In 1986, Kochi and co-workers (*379*) reported on the epoxidation capabilities of a series of Mn^{III}(salen)Cl complexes prepared from ring-substituted salicylaldehyde derivatives and ethylenediamine. Their work established that these complexes were effective catalysts for the epoxidation of alkenes. Kochi was unable to crystallographically char-

acterize the active oxygen atom transfer species, but based on the product evidence and analogy to the porphyrin systems, a $Mn^{V}=O$ intermediate was invoked as the oxygen transfer agent. Comparison to other metal–oxo compounds capable of epoxidizing alkenes also lent support to this proposal. Earlier, Kochi's group had explored other $M^{n+}=O$ complexes, such as (salen)$Cr^{V}=O$ (*380*, *381*). This complex could be crystallographically characterized and was shown to catalytically epoxidize some alkenes (*380*, *381*). The Mn–salen systems showed behavior similar to that of the chromium system, in particular with the appearance of a new UV-vis band at ~530 nm in the presence of the oxidant iodosylbenzene. In the chromium system, iodosylbenzene produces the $Cr^{V}=O$ product with the concomitant change in the UV-vis spectrum. Although the recently structurally characterized $Mn^{V}=O$ complexes (*255*, *256*) (Fig. 39) are not competent with respect to epoxidation chemistry, they do lend additional support to the existence of the $Mn^{V}=O$ intermediate during epoxidation.

Kochi's group used spectroscopy, kinetics, and isotope labeling to explore these epoxidations and proposed a mechanism for the reaction (*379*). Studies of the new UV-vis spectrum suggested that it was not the catalytically active compound and that it resulted from the initial oxidized manganese product (salen)$Mn^{V}=O$ condensing with a $[Mn^{III}(salen)]^{+}$ to give a (salen)$Mn^{IV}-O-Mn^{IV}$(salen) complex. This new complex slowly disproportionates to reform $[Mn^{III}(salen)]^{+}$ and (salen)$Mn^{V}=O$. This behavior is consistent with observations made earlier for porphyrin chemistry. A recent article by Feichtinger and Plattner (*382*) provides additional proof for the existence of $Mn^{V}=O$ intermediates in these systems via mass spectrometry, in which they observe mass peaks that are most consistent with the presence of $Mn^{V}=O$ moieties. With regard to actual epoxidation, Kochi proposed the formation of an $Mn-O-C-C\cdot-R$ intermediate, wherein a radical is positioned on the carbon β from the manganese, as shown in Scheme 16. This intermediate is still invoked for the function of these

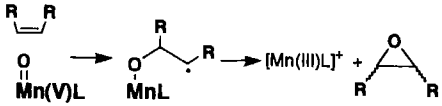

SCHEME 16.

catalysts (discussed later) and is supported by the correlation of the nature of the substituent on the 5-position of the ligand's phenyl rings with the reaction rates. The more electron-withdrawing groups tended to reduce the selectivity of the complex so that it reacted at

nearly equivalent rates with a variety of substrates. Furthermore, complexes with the more electron-withdrawing groups were capable of oxidizing cyclohexane, which also suggested that a "radical-like" intermediate forms. The presence of more electron-withdrawing groups at this position also led to higher epoxide yields. This initial report also included isotopic labeling studies designed to ascertain the source of the transferred oxygen atom. When run in dry solvent with ^{18}O-labeled iodosylbenzene (75% label), the norbornylene oxide product was labeled (75% label) with ^{18}O. In a reaction with ^{18}O-iodosylbenzene and 3.5 molar equivalents of added $H_2{}^{16}O$-enriched water, the amount of ^{18}O in the product was reduced by 32%. When the labels are reversed, ^{16}O-labeled iodosylbenzene, and 3.5 equivalents of $H_2{}^{18}O$ are added, then 26% of the product shows ^{18}O incorporation. If the amount of $H_2{}^{18}O$ is increased to 10 equivalents, then 74% of the product shows ^{18}O incorporation. In addition, under these conditions, the oxygen of the iodosylbenzene should not be able to exchange with the water present. These results suggest, that in the normal system run in the presence of water, the oxo of the $Mn^{V}{=}O$ may be exchanged. Such exchange behavior was reported by Kochi for the Cr systems (*381*). Exchange of the oxygen atom in a $Mn^{V}{=}O$ complex in $H_2{}^{18}O$ has been more recently reported (*256*).

Other groups have since picked up on this theme and have begun to explore the potential of these complexes to catalyze the asymmetric epoxidation of alkenes (*374*). Notable among these are the Jacobsen (*383–385*) and Katsuki research groups (*386–388*). Thus, there now exist a wide variety of complexes based on the Mn^{III}(salen)X paradigm from numerous research groups that have been reported to be competent epoxidation catalysts. These have been predominantly applied to epoxidizing *cis*-alkene substrates (*235*, *365–367*). The logic behind this choice is based on unfavorable steric effects with the manganese complex. More recently, however, some *trans* and tetrasubstituted alkenes have been successfully epoxidized, with good enantiomeric excesses observed (*367*). The broad range of complexes has yielded a broad range of results as well, with overall yields that range from a few percent of desired products to well over 90%, with enantiomeric excesses that cover a comparable range (*235*, *365–367*). Thus, with the right catalyst, a chemist may easily control the stereochemistry of a desired alkene and do so in high yield as well. A more recent report from Jacobsen's laboratories relates the ability of cobalt–salen catalysts to produce enantiomerically pure epoxides in aqueous systems with excellent stereocontrol (*389*). Due to the obvious breadth of this field, with its burgeoning number of catalysts and the varied applicability based on substrate, we will not attempt to assess the

effectiveness of the numerous catalysts that have been reported. Instead, we will narrow our focus to an overview of this type of reactivity. For coverage in more depth, the reader is directed to the various reviews that have been published over the past few years (*235*, *365–367*).

To conduct epoxidation chemistry, the precursor Mn^{III}(salen)X complex must be oxidized to the Mn^{V}=O state. This can be accomplished by a variety of reagents (*235*, *365–367*). Much of the initial work in this field utilized iodosylbenzene; however, the drawbacks of this reagent have spurred intense efforts to identify more soluble and cleaner oxygen atom donors. NaOCl has emerged as the oxidant of choice in several studies, in which the reactions are often run in a two-phase format, with the substrate and Mn^{III} catalyst in an organic layer (often CH_2Cl_2) and with an aqueous layer bearing the sodium hypochlorite. Hydrogen peroxide, in large excesses, has seen limited use, whereas *m*-CPBA (*m*-chloroperbenzoic acid) has also been utilized at low temperatures in purely organic phase reactions. The results in systems using hydrogen peroxide are often enhanced by the addition of an *N*-alkylimidazole. Some newer work has employed atmospheric dioxygen as the oxidant, which is an appealing reagent for any process that might be considered for industrial scale applications.

In general, the work in this field supports the notion that Mn^{V}=O is the active reagent for the epoxidation of alkenes, with the substrate presumably approaching in a side-on manner to the Mn^{V}=O moiety (*235*, *365–367*). By what mechanism, however, does the actual oxygen atom transfer occur? The side-on approach was initially proposed to account for the observed reactivity of unfunctionalized *cis* alkenes over *trans* alkenes with porphyrins (*376*, *377*). In the case of the salen systems, this route of approach has been lent support by the addition of steric bulk to these complexes and the suggested similarity to the porphyrin systems (*235*, *365–367*). The functionalization of the 3- and 5-positions of the phenyl rings of the ligand has further refined the proposed approach of the alkene as occurring across the catalyst's ligand backbone. The exact mechanism of the transfer of the oxygen atom, however, has not been fully worked out (367, *390*). At least two proposals have been put forward for the mechanism involved for these reactions. Arguments for both of these mechanistic positions appeared back-to-back in *Angewandte Chemie* articles in 1997 (*391*, *392*).

The first mechanistic proposal involves the side-on approach of the alkene to the catalyst. The radical intermediate, the Mn−O−C−C·−R (discussed earlier) then forms (Scheme 16). This β-carbon radical then combines with the oxygen atom, presumably leading to con-

comitant product release and reduction of the manganese to the Mn^{III} oxidation state. Some earlier work by Jacobsen has been taken to support the potential for a concerted process in some cases, based on the epoxidation of trans-2-phenyl-1-vinylcyclopropane (*393*). The cyclopropane ring of this substrate should be sensitive to a radical intermediate, to give ring-opened products. Such products were not observed. Otherwise, the epoxidation product distributions generally support the notion of the radical intermediate proposed by Kochi (*379*). Furthermore, the epoxidation product distributions are most consistent with there having been the potential for free rotation about a previously existing alkene C–C axis before closure of the epoxide ring. Oxygen atom transfer via a concerted addition across the alkene bond would not be expected to yield products consistent with rotation about the previous alkene bond (*379*). A supporting experiment by Kochi *et al.* showed that epoxides, for example (*Z*)-β-methylstyrene oxide, added to an active epoxidation system in the presence of another alkene substrate are not themselves isomerized (*379*). This result indicates that the observed isomerizations occurred during the oxygen transfer steps, and not after the epoxide ring had formed.

An alternative viewpoint is based on the earlier work of Sharpless and co-workers from their research on oxygen transfer reactions with metal–oxo catalysts (*394*), for which the existence of metallaoxetane rings forming during oxygen transfer was proposed. In 1995, a proposal, based on calculations using Macromodel/MM3 (*395*), suggested that such a mechanism might function in the Mn^{III}(salen) systems, as well. This mechanistic proposal (*392*, *395*) holds that the olefin approaches the $LMn^{V}=O$ complex, followed by formation of the four-membered metallaoxetane ring. One donor atom of the salen ligand is displaced, presumably a phenolate donor, into the site *trans* to the former oxo oxygen (Scheme 17). This ring then opens into a radical M–O–C–C·–R intermediate identical to that invoked for the radical mechanism and closes to release epoxide and the $[Mn^{III}L]$

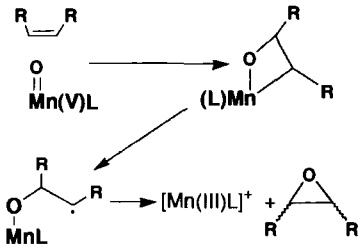

SCHEME 17.

precursor complex. Again, bond rotation would be feasible for the M−O−C−C·−R intermediate, leading to the observed mixture of products. The common factor in both of these proposals is the transient existence of M−O−C−C·−R.

Finally, exploration of nonporphyrin manganese-containing systems that are competent in epoxidizing alkenes are not limited to salen-based systems (*396*). Tris(acetylacetonato)Mn(III) in the presence of pivaldehyde and dioxygen was observed to enantioselectively epoxidize *cis*-alkenes. The dioxygen/pivaldehyde system has also been tested with Mn^{III}(salen), but appears to be less efficient overall than systems utilizing sodium hypochlorite (*396*). An interesting system (*249*) based on a $[Mn^{IV}(Me_3tacn)(OMe)](PF_6)$ complex has also been reported. Water-soluble alkene-bearing substrates were readily epoxidized by this system, in which the Mn^{IV} complex is proposed to activate hydrogen peroxide at room temperature in the aqueous solution; however, this complex is not reported to do this in an enantioselective manner.

b. Porphyrins The preparation of manganese-containing porphyrin systems for use as epoxidation catalysts has been intensively studied (*372*, *373*, *375*, *397*). Research in Mn^{III}-porphyrin epoxidation chemistry predated the current generation of the salen systems (discussed earlier). The Mn^{III}–porphyrin systems do not appear to exhibit the same degree of broad applicability as the Mn^{III}(salen)X systems. For porphyrin complexes to function well with respect to generating an enantiomeric excess of one product, they often require that modifications be made to the porphyrin ligand to create pockets or other structures that lead to the enantioselective epoxidation of a substrate (*372*, *373*, *375*, *397*). Often these modifications require extensive syntheses to produce an elaborate chiral porphyrin. This is one drawback to the porphyrin systems compared with the relatively more easily synthesized salen ligands. A second drawback is that these complexes may not be as robust as the salen-based system and have been reported to decompose due to oxidation of the porphyrin (*235*, *365–367*). To combat this latter problem, olefin epoxidations with Mn–porphyrin catalysts are often run with a large excess of substrate (*235*, *365*). This is less efficient and potentially quite costly when expensive substrates are to be epoxidized. Overall, the porphyrin systems give results with test substrates, for example styrene, that are on a par with the results reported for the Mn(salen) systems. They have also been shown to be functional with reagents other than iodosylbenzene such as sodium hypochlorite and dioxygen (*365*, *372*, *373*, *375*, *397*). An

example of a crystallized Mn^{III}–porphyrin system is shown in Fig. 72 (*398*). This actual complex as shown has been utilized in aziridination reactions (discussed later), which it proved effective and catalytic. This same porphyin with a Mn^{III}–Cl core, instead of $Mn^{III}(OH)(CH_3OH)$, has been applied to epoxidation catalysis and has been shown to be one of the more efficient porphyrin epoxidation catalysts (*399*).

The mechanisms proposed for manganese–porphyrin-catalyzed epoxidation of olefins are similar in several respects to that proposed for salen systems (*365*, *400*), and this was utilized initially to provide insight into the Mn–salen systems. In the case of porphyrins, a $Mn^{V}=O$ moiety is also formed by reaction with the secondary oxidant, for example iodosyl benzene, and the olefin is then believed to approach in a side-on manner. Various intermediates have been proposed for the epoxidation of the olefin, including ones in which the alkene is polarized to give "positive" and "radical" ends, and those shown earlier for the salen systems. The concept of the metallaoxetane (*371*, *372*) was employed to explain isomerization of some of the olefinic substrates during conversion to the epoxide products, but now

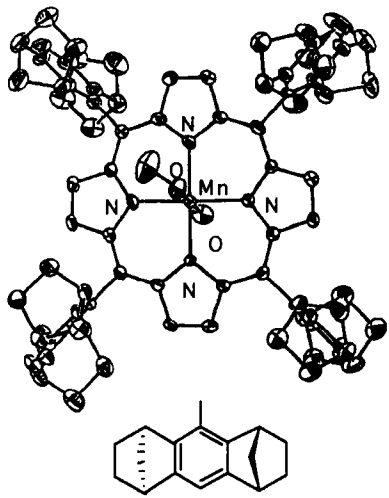

FIG. 72. Structure of the $Mn^{III}(P)(OH)(CH_3OH)$. P = [5,10,15,20-tetrakis (1,2,3,4,5,6,7,8-octahydro-1,4:5,8-dimethanoanthracen-9-yl)porphyrin]$^{2-}$. This complex has been tested as a catalytic aziridination catalyst (*398*). This same porphyrin ligand in an $Mn^{III}PCl$ complex has been tested as an epoxidation catalyst. It is one of the more efficient porphyrin epoxidation catalysts (*399*). [Reproduced with permission from (*398*). Copyright 1997 the Royal Society of Chemistry.]

is regarded as unlikely (*400*). Thus, the reaction mechanism for the porphyrin systems also remains quite controversial.

Porphyrin chemistry is not limited to epoxidation chemistry. There has been considerable recent interest in the toxicology of peroxynitrite, $ONOO^-$ (*71*, *73*, *74*, *401*). This dangerous compound is known to nitrate aromatic amino acids and has been implicated in processes and disease states as far ranging as amyotrophic lateral sclerosis (ALS) (*402*), Parkinson's disease (*71*, *72*), and cell apoptosis. Presumably peroxynitrite is formed by the rapid condensation of superoxide with nitric oxide. It is now known that peroxynitrite can be efficiently destroyed by amphiphilic manganese porphyrins in liposomal assemblies (*403*). The process is believed to proceed by the reaction of Mn^{III}(porphyrin) and $ONOO^-$ to give Mn^{V}=O(porphyrin) and nitrite, NO_2^-. The nitrite can then react rapidly to give a Mn^{III}(porphyrin) and NO_2°. Subsequent electron transfer to biological reductants destroys the NO_2°, and regenerates the catalyst (*403*, *404*).

2. *Nitrido Group Transfer/Aziridination*

A new entrant on the high-valent manganese reagent scene are the manganese–nitrido complexes (*251–253*). Only a handful of these have been structurally characterized to date, but their potential as a nitrogen-transfer reagents is being explored. The initial work in this field again resulted from experiments with porphyrin-based systems. In 1983, Groves and co-workers generated a Mn^{V}–nitrido compound and showed that in the presence of trifluoroacetic acid anhydride, this compound could transfer a nitrogen to produce an aziridine on cyclooctene (*405*), the nitrogen analog of an epoxide. The nitrogen atom of this ring bears a trifluoroacetyl moiety. One promising recent example of a catalytic porphyrin based aziridination system was reported in 1997 (Fig. 72) (*398*). This compound produced aziridination products from alkene precursors, for example styrene, with the aziridine nitrogen bearing a tosyl group from the co-oxidant (tosyliminoiodo)benzene, PhINTs. Up to 480 turnovers were reported, with reported yields ranging from 44–76% and enantiomeric excesses between 44–66%. The newer nonporphyrin Mn–nitrido systems react in a stoichiometric manner and are not catalytic like the Mn^{V}=O systems. Catalytic systems are now a focus of research with the newer systems (*253*). Despite the current lack of catalytic turnover, Mn^{V}–nitrido systems promise to yield new, useful and easier pathways to a number of amine or aziridine products. Applications of these complexes to the amination of carbohydrates may allow these compounds

to be more readily synthesized in reactions that employ milder reagents than might otherwise be utilized (*253*).

Initial studies have shown that the transfer of the nitrido nitrogen atom moiety to an organic substrate from a nonporphyrin Mn^{V}–nitrido complex is feasible (*251*). Both the complex with the underivatized $salen^{2-}$-ligand complex, as well as the $tetramethylsalen^{2-}$, $saltmen^{2-}$, with four methyl groups appended to the two backbone carbons of the ligand, were prepared. Figure 37 shows the crystal structure of this complex. The latter was employed in nitrogen-transfer reactions due to its greater solubility in organic solvents and was found to be a competent nitrogen-transfer agent to a variety of silylated enol substrates in the presence of trifluoroacetic acid anhydride. This reaction produced α-aminoketone products, with the product amine acetylated with a trifluoroacetyl group. Studies on these systems continue, with the ultimate goal being the production of a complex that is competent for asymmetric nitrogen transfer, presumably in a manner similar to the Kochi–Jacobsen–Katsuki epoxidation format.

Another interesting result in this field is the report that the nitrogen of a (salen)$Mn^{V}{\equiv}N$ to another Mn^{III}(5-MeOsalchxn)Cl complex, where chxn represents 1,2-diaminocyclohexane (*406*). This process was shown to be reversible by the addition of the Mn^{III}(salen)Cl to a solution of (5-MeOsalcxhn)$Mn^{V}{\equiv}N$, wherupon the N^{3-} could be transferred "back" to regenerate the "original" (salen)$Mn^{V}{\equiv}N$ complex. Related work has shown that a nitrido can be transferred from a Mn^{V} nitrido(porphyrin) complex to a Cr^{III}(porphyrin) complex to yield $[Mn^{III}(porphyrin)]^{+}$ and Cr^{V}nitrido(porphyrin) (*407*).

A note on the synthesis of Mn^{V}–nitrido complexes seems warranted at this point. There now exist several reports of first-row transition-element nitrido complexes (*408*), of which a growing number are manganese complexes. There are also a broad range of syntheses available. Manganese–nitrido complexes have been reported via the irradiation of manganese–azido precursors in several cases, although the yields vary (*258*, *405*, *409*). Other techniques employ ammonia or ammonium in the presence of a chemical oxidant (*251–253*). The work of Carierra *et al.* (*251*) with Mn^{III}(salen) derivatives employed ammonium hydroxide and sodium hypochlorite to generate the nitrido complex. In newer complexes with bidentate ligands that expand this class of compounds, the nitrido complex is prepared via a synthesis that utilizes *N*-bromosuccinamide as the oxidant with the addition of gaseous ammonia to the Mn-complex/*N*-bromosuccinamide solution at low temperature (*253*).

3. *Chlorination*

Many routes for the chlorination of alkenes exist, and one new entry in recent years has been manganese-based chlorinating reagents. Many of these systems have been prepared by Bellesia and co-workers (*410–414*). These systems in general produce *trans*-chlorinated alkenes. In only one system has the proposed halogenating complex been structurally characterized (*245*).

Most of the systems explored for the chlorination of alkenes with manganese have involved high-valent manganese compounds or the known oxidant Mn^{III} acetate. The systems reported by Bellesia *et al.* (*410–412*) have been tested against a substantial body of alkene-containing substrates. One system that these researchers devised was based on a mixture of $Mn^{III}O_2$ and Me_3SiCl in THF (*410*, *411*), and a later system was devised that employed $Mn^{IV}O_2$, $Mn^{II}Cl_2$, and acetyl chloride in DMF (*412*). This group proposed that a transient "$Mn^{IV}Cl_4$" or "$Mn^{III}Cl_3$" acts as the reactive halogenating reagent in some of their systems. They also showed that such a Mn-based system could chlorinate ketones in the α-position (*415*) under milder conditions than earlier work (*416*). Two other similar systems have also been reported, the first based on Mn^{III}acetate, $CaCl_2$ and acetyl chloride (*417*) and the other on $KMnO_4$ and oxalyl chloride (*418*, *419*).

A variety of mechanisms may be functioning for these different systems. In the systems of Bellesia and the Mn^{III} acetate system of Donnelly *et al.*, it was proposed that these reactions occurred via a non-chain radical mechanism (*411*, *417*). The product distributions observed are most consistent with chlorination by a radical pathway and not by an ionic pathway. This is best demonstrated by norbornylene (*420–422*). The products of chlorination for these systems were *trans*-2,3-dichloronorbornane and a much smaller amount of *cis*-2,3-dichloronorbornane, and no other products were observed. The latter compounds would result from the generation of a nonclassical carbocation during chlorination. The lack of such products speaks against an ionic intermediate, and the observed products are consistent with chlorination having occurred via a radical-based halogenation. A mechanism involving radical character in this system is given credence by the known chemistry of Mn^{III} acetate, which is known to initiate radical-based chemistry (*363*, *364*).

In 1997, Markó and co-workers (*423*) followed up on their initial report of the $KMnO_4$ and oxalyl chloride system. This new system consists of $KMnO_4$, Me_3SiCl, benzytriethylammonium chloride with dichloromethane as the solvent. It gives good yields of dichlorinated alkenes. The permanganate anion is brought into solution by the ben-

zyltriethylammonium chloride, and the addition of four molar equivalents of Me_3SiCl produces the halogenating reagent, which they propose to be a dichlorobis(trimethylsilol)manganese complex.

None of these systems presents an initial, structurally characterized halogenating agent. Recently we reported that the Mn^{IV}(salpn)Cl_2 complex (*245*), which had been crystallographically characterized previously (Fig. 33), acted as a new reagent capable of halogenating alkenes in a *trans* manner. In this case a stoichiometry of two dichloro complexes to one alkene was required, and the final manganese product has been identified as Mn^{III}(salpn)Cl. The products formed with this reagent are consistent with a nonchain radical mechanism.

B. Enzyme Model Systems

1. Manganese Peroxidase

The reactivity of the manganese peroxidase (MnP) system has been explored with model compounds. The chemistry of MnP is the one-electron oxidation of the lignin substrate that initiates decomposition of the lignin structure. Some of the initial functional modeling chemistry in this field established the ability of Mn^{III} complexes to initiate the decomposition of lignin analogs, for example, the decomposition of dimeric lignin models in the presence of Mn^{III} and α-hydroxy acids (*95*, *103*). The products from these experiments involving Mn^{III} lactate and a variety of other α-hydroxy acids showed that Mn^{III} was indeed capable of initiating the one-electron oxidation of lignin. Another study with the lignin analog, and test substrate for LiP and MnP, vanillylacetone also showed that these systems were capable of such oxidations (*424*). Furthermore, the lactate was proposed to stabilize the Mn^{III} to prevent generation of Mn oxides before the manganese ion could act on the lignin, yet would not produce a complex so stable as to prevent the Mn^{III} lactate complex from oxidizing lignin. More recent work has shown that lignin-degrading fungi produce oxalate, which is required for the enzyme to function. Based on these model studies and data, it has been proposed that oxalate may stabilize the Mn^{III} to prevent loss of Mn^{III} by disproportion to Mn^{II} and $Mn^{IV}O_2$.

In these studies, the manganese complex was generated *in situ* from added manganese and ligand. In 1991, Saadeh *et al.* reported the preparation and isolation of complexes with α-hydroxy acids, for example lactic acid, 2-hydroxyisobutyric acid (HIB) and 2-hydroxy-2-ethylbutyric acid (HEB) (*425*). The latter two ligands led to Mn^{IV} complexes with O_6 first coordination spheres, whereas Mn^{III} complexes were prepared and characterized with lactic acid. The crystal structure of the complex with HIB shows it to be two $Mn^{IV}L_2$ units that are

bound to a single sodium through the facial array of hydroxy oxygens in the complex. The monomer is shown in Fig. 34. Among the other complexes prepared were Mn^{III} dimers with chelated and bridging lactates or malonates (*425*).

These isolated and well-characterized complexes were then utilized to explore the ability of such α-hydroxy acid–manganese complexes to oxidize the lignin analog vanillylacetone. A scheme representing the Mn^{III} system is shown in Scheme 18 (*425*). It was found that the Mn^{IV}

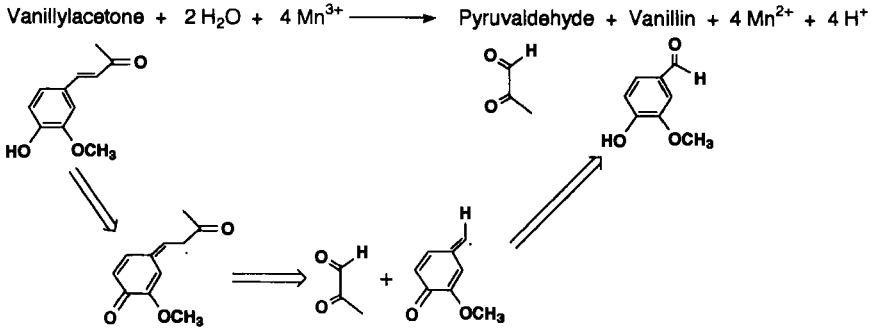

SCHEME 18.

complex with HIB and the Mn^{III}–lactate complexes were both capable of oxidizing this organic substrate. The oxidation product, pyruvaldehyde, is consistent with the oxidation of the substrate via successive one-electron oxidations by manganese (*425*). The reaction is proposed to begin via the generation of a phenoxy radical, which then rearranges to form a ketone from the phenol alcohol and places a radical alpha to the ketone. Two successive Mn^{III}-initiated oxidations lead to the formation of pyruvaldehyde. A final oxidation of the remaining substrate radical, followed by incorporation of the second molecule of water and a rearrangement, yields vanillin. Furthermore, Mn^{II} was identified by EPR spectroscopy in these reaction mixtures. This lends additional strong support to the one-electron oxidant role for manganese in MnP.

A second area of MnP model chemistry has dealt with Mn^{II} oxidation by Fe-porphyrin systems. An early example suggested that Mn^{II} in the presence of excess pyrophosphate could be catalytically oxidized to Mn^{III} by an Fe-porphyrin system. In these experiments, sulfonated porphyrins were utilized, and the co-oxidant was potassium monopersulfate. Co-substrates, such as veratryl alcohol, were reported to enhance the rate of Mn^{II} oxidation (*468*).

Another interesting reactivity-related system is the recent report of an iron-containing porphyrin that has been functionalized with propi-

onate arms, patterned from the crystallographic data for MnP (*426*). This system was designed to study electron transfer from the iron/porphyrin to the manganese ion. The porphyrin bears pentafluorophenyl groups on three of its meso positions, and the fourth meso position is modified by the addition of an alkyl arm that terminates in a 6-(methylamino)-2,2′-bipyridine functional group that is intended to be the site of manganese binding. Among other characterization data, EPR spectra confirm the presence of Fe^{III} and Mn^{II} in the final product, and the apparent lack of magnetic interactions between the two ions suggests that they are not coupled to one another. In the presence of the oxidant pentafluoroiodosylbenzene, the Mn^{II} EPR signal was observed to slowly disappear. The addition of 2,6-dimethylphenol, a standard test substrate for MnP, led to the formation of the oxidation product 2,2′,6,6′-tetramethyldiphenoquinone and the reappearance of the Mn^{II} EPR signal. This appears to be fully reversible and was shown to function in a catalytic manner. In control experiments, neither Mn^{II} bound to the iron-free modified porphyrin nor $Mn^{II}(bipy)_2Cl_2$ were oxidized by pentafluoroiodosylbenzene. In the presence of a (chloro)[tetrakis(pentafluorophenyl)porphyrin] iron complex and pentafluoroiodosylbenzene, $Mn^{II}(bipy)_2Cl_2$ was observed to be oxidized. These results are consistent with the petafluoroiodosylbenzene oxidation of the iron/porphyrin portion of the complex with ensuing electron transfer to oxidize the bound Mn^{II}. The Mn^{III} thus produced would then oxidize the substrate.

2. Manganese Superoxide Dismutase

The various complexes that have been tested for their ability to mimic MnSOD form another set of systems that have been the focus of reactivity studies. One emphasis of research in this area has been the potential for the development of pharmaceutical agents that are good SOD mimics. This research is driven by the proposal that much of the damage following a shortage of oxygen due to a stroke or heart attack may be the result of a build-up of superoxide and its hazardous by-products (discussed earlier). The goal, therefore, is to design agents to scavenge superoxide and to thereby prevent an appreciable build-up of this molecule. Much of this work has centered on manganese, because this element is less likely to be able to catalyze other side reactions, such as Fenton-like chemistry (*221*, *222*, *427*).

The manganese complexes that have been prepared to date cover a range of structural types and ligands. Due to the self-dismutation of superoxide ($2.0–3.2 \times 10^5\ M^{-1} \cdot s^{-1}$) (*52*, *63*), these complexes need to be quite efficient to qualify as catalysts of superoxide dismutation. Several complexes have proven to be competent MnSOD mimics. Un-

fortunately, one of the main techniques once utilized to establish SOD activity suffers from potential interference, so early examples of catalytic MnSOD mimics may not actually be catalytic in nature. Thus, from all that has been published, it is clear that there are roughly two classes of compounds: those that are efficient and catalytic mimics for MnSOD, and those that interact with superoxide but are not necessarily catalytic in their interaction.

In 1993 Weiss, Riley, and co-workers reported a study on purported SOD mimics by stopped-flow UV-vis spectroscopy (*428*) in which they assessed reactivity by following the decay of the superoxide absorption at 245 nm. Two of the earlier techniques that had been used to assess SOD activity included observation by UV-vis spectroscopy of the oxidation of nitroblue tetrazolium (NBT) (*68*) or the oxidation of a cytochrome *c* by superoxide (*52*). Both systems used superoxide from an *in situ* generator, frequently xanthine oxidase, wherein the complex being analyzed was compared to a calibrated oxidation of the chromophore alone and in the presence of MnSOD. The direct observation of the decrease in the superoxide signal with time by UV-vis is also possible, and superoxide may be introduced as a solution (*428*) or generated, in some cases, by pulsed radiolysis (*79*, *80*). In these direct observation experiments, the rate of decay of superoxide in the presence of the complex is compared to the rates of decay of superoxide alone and in the presence of one unit of activity of MnSOD. In all cases, the systems are usually referenced, or calibrated, against the same set of conditions with MnSOD. Due to interactions with cytochrome *c* with components of assay mixtures other than superoxide, false readings of activity were often observed for some early SOD mimics. The NBT, stopped-flow, or pulsed radiolysis techniques have tended to provide the more accurate answers on the ability of reputed MnSOD mimics. To be considered active in any manner with respect to the decay of superoxide in the stopped-flow analyses, Weiss *et al.* stated that compounds based on their analyses needed to exhibit k_{cat} values in excess of $10^{5.5}$ $M^{-1} \cdot s^{-1}$ (*428*).

The complex of manganese with desferrioxamine B (*429–432*), reported to be a MnSOD mimic in 1987, illustrates this point. In the initial studies, the cytochrome *c* assay was applied, and this compound was reported to be a catalytic MnSOD mimic. Follow-up studies by Riley and co-workers by stopped-flow techniques showed that this complex interacts at best on a stoichiometric level with superoxide, but it could not be considered to be a catalyst and was termed "inactive" (*428*). This occurred due to interactions with cytochrome *c* wherein the manganese complex interfered with the reduction of cytochrome *c*, leading in effect to a false positive. Thus, although some

systems may no longer be considered to be catalytic, many of these still may exhibit interactions with superoxide.

Despite earlier systems that eventually proved not to be catalytic, catalytic MnSOD mimics have been successfully prepared with several examples appearing since 1990. One of the first appeared in 1993 by Kitajima and co-workers (*208*) and is based on the ligand hydrotris(3,5-diisopropylpyrazol-1-yl)borate, HB-*i*-Pr. The two five-coordinate MnSOD mimics that were prepared in this report are the Mn^{II} complex with one HB-*i*-Pr ligand and one bidentate benzoate, and another Mn^{II} complex composed of one HB-*i*-Pr, one unidentate benzoate, and one equivalent of 3,5-diisopropylpyrazole. The crystal structure of the latter is shown in Fig. 13. These complexes yielded IC_{50} values of 0.75 and 0.80 $\mu mol \cdot dm^{-3}$, respectively. These values were determined by observing the inhibition of the reduction of nitroblue tetrazolium by superoxide in a calibrated system using xanthine/xanthine oxidase as a superoxide generator. The IC_{50} value implies that a concentration of that particular reagent exhibits activity equivalent to 50% of that observed for one unit of actual MnSOD enzyme under the specific conditions of the experiment in question. For comparison, an iron complex tested by Weiss *et al.* (*428*) that was shown to be "active" in the presence of superoxide exhibited a k_{cat} value of $2.15 \times 10^6\ M^{-1} \cdot s^{-1}$, and an IC_{50} value of 2.1 $\mu mol \cdot dm^{-3}$.

Riley, Weiss, and co-workers have prepared a series of MnSOD mimics using macrocyclic ligands (*221*, *222*, *427*). The first report with several simple macrocycles indicated that the seven-coordinate Mn^{II} complexes with the 15- and 16-member pentaaza macrocycles and axial chlorides were efficient catalysts for the dismutation of superoxide (Fig. 20) (*221*). At pH 8.1, the pentaaza and hexaaza complexes exhibited k_{cat} values of $2.2 \times 10^7\ M^{-1} \cdot s^{-1}$ and $1 \times 10^6\ M^{-1} \cdot s^{-1}$, respectively. At a physiological pH, pH = 7.4, only the complex with the 15-member ring was active. The complex with the 16-member ring proved to be quite pH sensitive. At pH 7.4, the efficiency of the functional complex increased to a k_{cat} value of $4.1 \times 10^7\ M^{-1} \cdot s^{-1}$. This initial work was followed up by modification of the periphery of the macrocyclic ligand to create a family of new MnSOD mimics (*222*). These complexes were then screened by stopped-flow UV-vis spectroscopy. All of the complexes tested catalytically decomposed superoxide, with k_{cat} values ranging from 1.4 to $9.1 \times 10^7\ M^{-1} \cdot s^{-1}$ at pH 7.4. The best of these was dichloro(*trans*-2,3-cyclohexano-1,4,7,10,13-pentaazacyclopentadecane)manganese(II).

A third system is based on Mn^{III}–Schiff-base complexes. There are two reports of reactivity of such systems with superoxide. The first, by Matsushita and Shono, appeared in 1981 (*433*). In this study, the

authors observed that in the presence of superoxide, $Mn^{III}LCl$ complexes, where L is a Schiff-base ligand such as $salen^{2-}$, and in KO_2/complex ratios <2–3, oxygenated products were observed for complexes with Mn(III/II) reduction potentials of about −0.19 V or lower vs. a Hg pool (approximately 0.21 V vs. SCE). Complexes with more positive reduction potentials, ranging from −0.18 to 0.00 V vs. the Hg pool, were reduced, but oxygenated products were not observed. In 1993, Baudry *et al.* examined Mn^{III}(salen)-based systems with ligands that had been designed for the Mn^{III}(salen)Cl epoxidation systems (*434*). The activity of these complexes considerably varied, from rates that were nearly undetectable to rates indicative of fairly efficient MnSOD mimics. One of these Mn^{III}(salen)Cl complexes, with the salen ligand comprised of a 1,2-diaminocyclohexane backbone and 2-hydroxy-3-*tert*-butyl-5-methoxy-benzaldehyde, gave an IC_{50} value of 0.32 $\mu mol \cdot dm^{-3}$, or 3200 U/mM. The activity in this system was measured against the reduction of the nitroblue tetrazolium absorption. In 1997 it was reported that underivatized Mn^{III}(salen)Cl, referred to as EUK-8, was also a competent superoxide scavenger (*435*).

A Mn^{II} complex with an all-nitrogen first-coordination sphere was reported in 1996 to be a competent MnSOD mimic (*436*). In this case the complex is composed of two meridonally binding 2,6-bis(benzimidazol-2-yl)-pyridine ligands. When tested against the NBT system, this complex was reported to exhibit an LC_{50} value of 0.72 $\mu mol \cdot dm^{-3}$. This level of activity is comparable to that observed for the other systems tested by the nitroblue tetrazolium system.

Most manganese complexes that have been reported to react with superoxide, however, do not react catalytically. Several have been reported by various groups in attempts to generate catalytic systems, but these only show stoichiometric interactions with superoxide. Examples of this group of complexes includes the recently reported seven-coordinate Mn^{II} complex, with the same ligand and a structure similar to the complex shown in Fig. 25 (*229*).

In conclusion, systems have been generated that do interact catalytically with superoxide and function as MnSOD mimics. The potential for errant readings of activity with the indirect assays of SOD mimics shows the need for careful control experiments, and perhaps the wider application of direct techniques for the determination of MnSOD mimicry to prevent false positives and to provide readily compared k_{cat} values.

3. *Catalase*

Work on the catalase frontier has focused on the synthesis of binuclear manganese complexes that are capable of catalyzing the dispro-

portionation of hydrogen peroxide. This field has grown considerably over the past few years, and a large number of catalase mimics are now known. Catalase and catalase model systems have been reviewed previously (*3*, *5*, *23*, *25*, *26*, *29*, *30*, *436*). In general, two types of catalase chemistry may be mimicked by manganese model complexes. The first is the reactivity of the catalase itself. The second is the catalase-like reaction thought to occur in the OEC between the S_0 and S_2 states of that enzyme (*437*). Several model systems have been prepared, and a selection of these will be described in some detail. A table of rate data, Table III, is presented so that these systems may be more readily compared. A few systems not discussed here are also presented in the table.

One of the earliest functional mimics of catalase was reported by Mathur *et al.* in 1987 (*438*). This system employed the ligand *N*, *N*, *N'*, *N'*-tetrakis-(α-methylenebenzimidazolato)-1,3-diaminopropane-2-ol. The complex formed with this ligand is composed of one ligand, with the alkoxide bridging the two manganese(II) ions, with a proposed bridging chloride and two terminal chlorides, one on each

TABLE III

CATALASE ACTIVITY: ENZYMES AND MODEL SYSTEMS[a]

Enzyme or complex	k_{cat} (s^{-1})	k_{cat}/K_m ($M^{-1} \cdot s^{-1}$)	Reference
Thermus thermophilus catalase	260,000	3.2×10^6	*131, 295, 461, 462*
Lactobacillus plantarum catalase	200,000	5.7×10^5	*23*
Thermoleophilum album catalase	26,000	1.7×10^6	*129*
$[Mn^{IV}(salpn)(\mu\text{-}O)]_2$	250	1×10^3	*446*
$[Mn^{II}(2\text{-}OHpicpn)]_4(ClO_4)_4$	150	70	*333*
$[Mn^{II}(2\text{-}OHsalpn)]_2$	22	350	*440*
$[Mn^{III}Mn^{IV}(\mu\text{-}O)_2(\mu\text{-}OAc)(tacn)(bipy)(MeOH)](ClO_4)_2$	13.2	—	*294*
$[Mn^{III}Mn^{IV}(\mu\text{-}O)_2(\mu\text{-}OAc)(tacn)(OAc)_2](ClO_4)_2$	5.5	—	*294*
$[Mn^{III}$ (anthracenediporphyrin)$]Cl_2$	5.4	—	*443*
$[Mn^{II}_2L^b$ (μ-3,4-NO_2benzoate)$](ClO_4)$	4.4	—	*463*
$[Mn^{II}_2(2OH\text{-}benzimpn)(\mu\text{-}OAc)(n\text{-}BuOH)](ClO_4)_2$	1.2	—	*439*
$(Ba^{2+},Ca^{2+})_2[Mn^{III}_3Mn^{II}(\mu\text{-}O)(\mu\text{-}OH)(\mu\text{-}OAc)_2(tapn)_3]$	1.04	—	*447*
$[Mn^{II}_2L^b(\mu\text{-}C_6H_5CO_2)_2(NCS)]$	0.79	—	*441, 442*
$[Mn^{III}Mn^{IV}(bpg^c)_2(\mu\text{-}O)_2](ClO_4)$	0.26	—	*464*
$[Mn^{III}$(tetraphenylporphyrin)$]^-$	0.013	—	*443*
$[Mn^{II}(H_2O)_6](ClO_4)_2$	0.0063	—	*440*

[a] The rates observed for these systems are for conditions which vary from study to study, whereas the k_{cat} values are presumably maximal rates with saturating hydrogen peroxide.

[b] L = the macrocyclic 2:2 Schiff base condensation of 2,6-diformyl-4-methylphenol with N,N-bis(2-aminomethyl)methylamine.

[c] bpg = bis(*N*,*N*-(2-pyridylmethyl)glycine.

manganese. This proposed structure is similar to that of the related structure shown in Fig. 53. In the absence of crystallographic data, EPR spectroscopy was used to suggest the binuclear structure, with a Mn–Mn distance on the order of 3.3 Å. When reacted in a two-phase system of complex dissolved in butanol and a hydrogen peroxide–bearing water layer, catalytic dioxygen evolution was observed. Over the course of the reaction, a Mn_2^{III} dimer built up, which was proposed to be an oxo-bridged product. This product could be independently prepared for comparison to the product of the catalase-like reaction. As the reaction continued, the pH rose, and the loss of reactivity over time was attributed to this increase in pH, which led to complex decomposition. The proposed mechanism for this catalase mimic involved the initial formation of an oxo-bridged Mn_2^{III} complex from the Mn_2^{II} complex and the formation of one molecule of water. The second step involved the reaction of this new Mn^{III}–O–Mn^{III} compound with hydrogen peroxide to reduce the complex to the Mn_2^{II} state, with the concurrent formation of a second molecule of water and the release of dioxygen. The progress of the reaction was followed by collecting the evolved dioxygen.

In 1994, the chemistry of this system was revisited with an analogous complex (*291*, *439*), one in which the chlorides had been replaced by a bridging acetate and two nonbinding perchlorates. One of the manganese in this structure is five-coordinate, and the other is six coordinate, with a butanol occupying the sixth coordination site. The crystal structure of this complex gives credence to the structure that had been proposed for the catalyst with chlorides (*438*). The exploration of this system led to a new mechanistic proposal. In this case, the lag time for observed catalase activity was reduced by the addition of 2% water to a methanolic solution of the catalyst. They proposed that the water displaces the bridging acetate; thus, a molecule of hydrogen peroxide may more easily displace the terminal waters than the bridging acetate to bridge the two manganese ions itself. The O–O bond of the peroxide was then proposed to be cleaved, producing two Mn^{III}–OH moieties. This intermediate reacts with a second molecule of hydrogen peroxide to release dioxygen and to regenerate the Mn^{II} complex. The terminal hydroxides were protonated during this second step to form two molecules of water, thus completing the disproportionation of hydrogen peroxide (Scheme 19).

In 1992, Wieghardt and co-workers reported two manganese catalase mimics based on triazacyclononane ligands (*294*). These were asymmetric complexes, with one half bearing an *N*,*N*′,*N*″-trimethyl-1,4,7-triazacyclononane molecule bound to a manganese that was bridged via two μ-oxo bridges and one μ-carboxylato bridge to either a manganese bearing a bipyridine ligand and a terminal water or

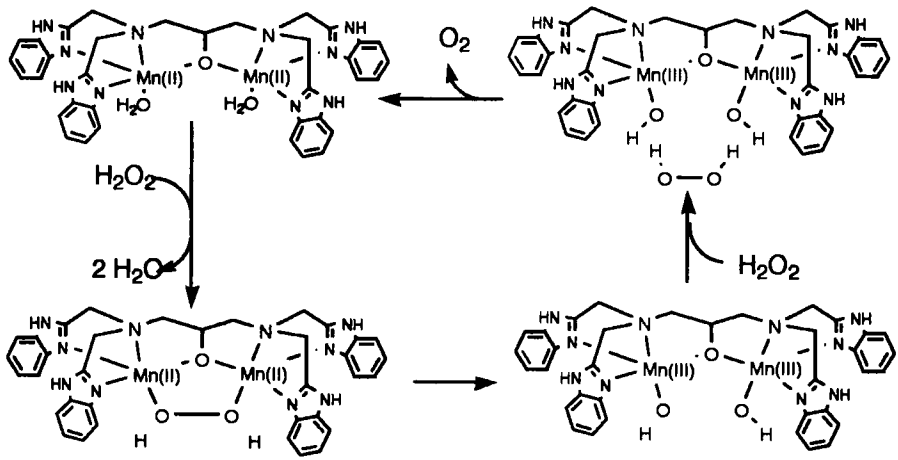

SCHEME 19. Proposed mechanism of hydrogen peroxide disproportionation by $[Mn^{II}(2\text{-OHbenzimpn})(\mu\text{-OAc})]_2^{2+}$. [Reproduced with permission from (*439*). Copyright 1994 the American Chemical Society.]

methanol or one coordinated only by additional acetates. The former complex is shown in Fig. 73. The oxidation state of these systems is $Mn^{III}Mn^{IV}$, and presumably they cycle to $Mn^{II}Mn^{III}$. In sodium acetate–buffered solutions, approximately 1300 turnovers were realized during the first three minutes of these reactions, with rate values of 13.2 and 5.5 s^{-1}, respectively. Overall, both of these catalysts were five orders of magnitude slower than the catalase enzyme.

In 1993, Gelasco and Pecoraro (*273*) reported initial data for a series of complexes based on the 2-OHsalpn ligand, *N*,*N*′-(salicylidenimine)-1,3-diaminopropan-2-ol (Fig. 48). These complexes are effective catalase mimics. With all of the biologically relevant oxidation states of the catalase enzymes, Mn_2^{II}, $Mn^{II}Mn^{III}$, Mn_2^{III}, and $Mn^{III}Mn^{IV}$, having been prepared (*279*). This is the first series of manganese complexes to exhibit this range of oxidation states with the same ligand.

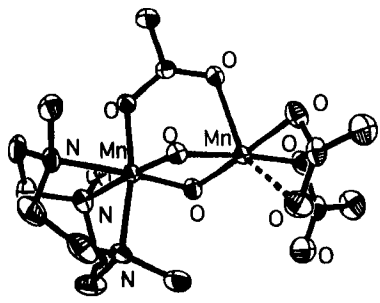

FIG. 73. Structure of $[(Me_3tacn)Mn^{IV}(\mu\text{-}O_2)(\mu\text{-OAc})Mn^{III}(OAc)_2]$. [Reproduced with permission from (*294*). Copyright 1992 the Royal Society of Chemistry.]

Furthermore, this family of complexes exhibited EPR spectra that modeled those observed for the catalase enzymes (*26*, *279*). The $[Mn(2\text{-}OHsalpn)]_2$ complexes disproportionate H_2O_2 by shuttling between the Mn_2^{II} and the Mn_2^{III} oxidation levels. Under appropriate conditions in the presence of hydrogen peroxide, either the Mn_2^{II} or the Mn_2^{III} complex may be produced cleanly. The observed rate for the disproportionation ranged from 4.2 to 21.9 s^{-1}, depending upon the derivatization of the complex's phenolate moieties. The rate-limiting step was determined to be the reduction of the Mn_2^{III} dimer to Mn_2^{II}. Thus, complexes with the more electron-withdrawing ligands proved to be the most efficient catalysts in this system, because this Mn_2^{III} oxidation state was less stabilized. The complexes with the more electron-donating ligands, in contrast, tended to bind peroxide better.

In reactions with hydrogen peroxide (*440*), members of this family of complexes exhibit saturation kinetics. It was observed that the nature of the substituents on the phenolates affected the k_{cat} and K_m values of the complex with respect to hydrogen peroxide disproportionation. It has been proposed (*440*) that this system involves terminal binding of the hydroperoxide anion, HOO^-, to a $[Mn^{III}(2OHsalpn)]_2$ dimer, in a manner similar to that observed in crystal structures of these compounds, with, for example, methanol or THF (Fig. 44). In this case, the hydrogen peroxide is deprotonated by a base equivalent and is bound to the dimer. One of the alkoxide bridges shifts to become a terminal instead of a briding ligand to open a coordination site for HOO^- (Scheme 20). A second base equivalent then deprotonates this hydroperoxide monoanion unit, the dimer is reduced to Mn_2^{II}, and dioxygen forms and is released. A second equivalent of hydrogen peroxide then bridges the Mn_2^{II} dimer, followed by reoxidation of the dimer with the concomitant reduction of this second equivalent of hydrogen peroxide to form two equivalents of hydroxide. These hydroxide molecules are base equivalents as described earlier, so that the two water molecules of hydrogen peroxide disproportionation are formed. Isotope-labeling studies showed that the dioxygen evolved arose from the same molecule of hydrogen peroxide.

Okawa and co-workers have published several papers in recent years on binuclear catalase mimics based on the pentadentate or septadentate binucleating ligands, an example of which is shown in Scheme 21 (*441*, *442*). These ligands have been used to prepare a variety of binuclear Mn_2^{II} complexes. Their ability to catalyze the disporportionation of hydrogen peroxide varies, but is generally low, on the order of 0.79 s^{-1}. A functional scheme for the disproportionation of hydrogen peroxide has been proposed for these complexes that invokes a $Mn^{IV}{=}O$ intermediate (Scheme 21).

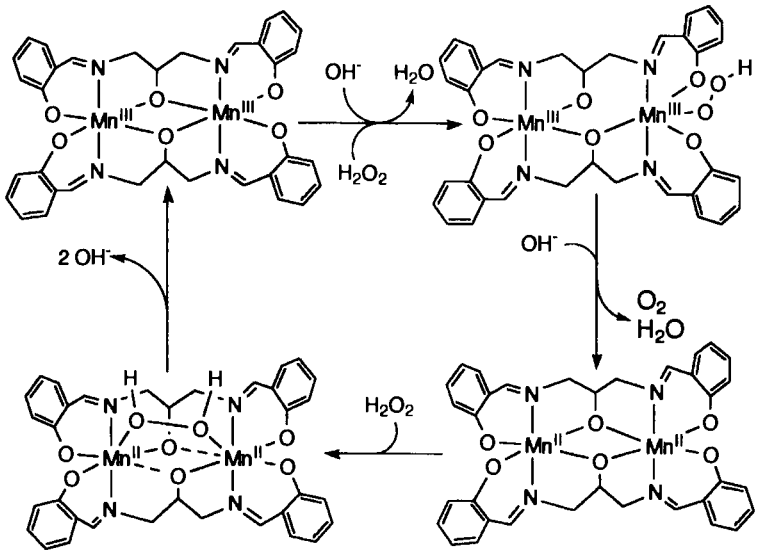

SCHEME 20. Proposed mechanism of hydrogen peroxide disproportionation by the $[Mn(2\text{-}OHsalpn)]_2$ system. [Reproduced with permission from (*440*). Copyright 1998 the American Chemical Society.]

Another unique dimeric system was first reported by Naruta and Maruyama in 1991 (*443–445*). In this system, two Mn^{III}-porphyrin molecules are linked by an anthracene spacer instead of the *o*-phenylene spacer seen in Fig. 75 (discussed later). Their studies showed this

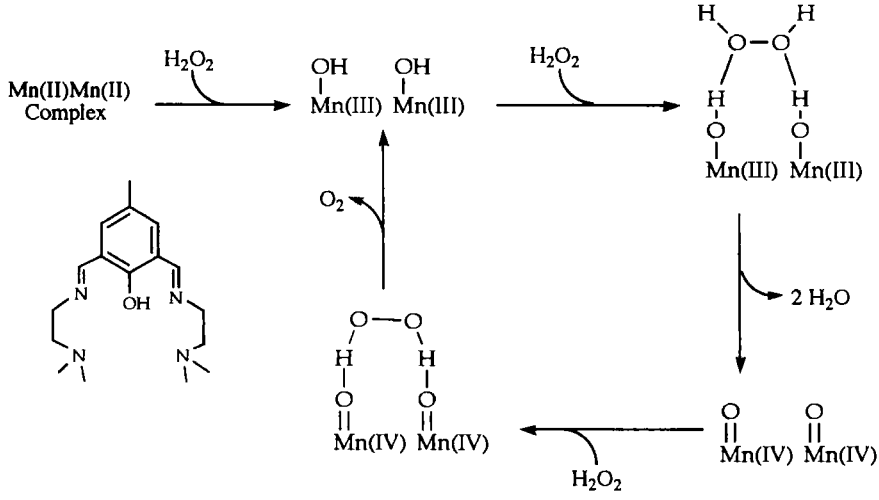

SCHEME 21. A proposed mechanism of hydrogen peroxide disproportionation by Okawa, *et al.*'s system. [Reproduced with permission from (*466*). Copyright 1995 the Royal Chemical Society.]

complex to be a competent catalase mimic, with a rate of 5.4 s^{-1} observed for the disproportionation of hydrogen peroxide. It was proposed that this system functioned by the formation of two Mn^{IV}–OH porphyrin groups or high-valent Mn–oxo porphyrin groups in the presence of H_2O_2 and imidazole, which likely acts as a requisite base. Hydrogen peroxide will then react with this intermediate to yield dioxygen, two molecules of water, and the reduced form of the complex. Isotopic labeling studies showed that isotope mixing was not observed in 1:1 mixtures of ^{16}O and ^{18}O hydrogen peroxide.

This was followed by an article in 1997 (*445*), wherein Naruta *et al.* prepared a dimer with Mn^{IV}porphyrin(OMe)(OMe or OH). The analysis of this system indicated that catalase activity occurred via approach of hydrogen peroxide to the pocket of the dimer, followed by deprotonation and concomitant reduction of the dimer and oxidation of the hydrogen peroxide to dioxygen. Their proposed catalytic cycle is shown in Scheme 22. Similar systems have been used to generate dioxygen from water (discussed later).

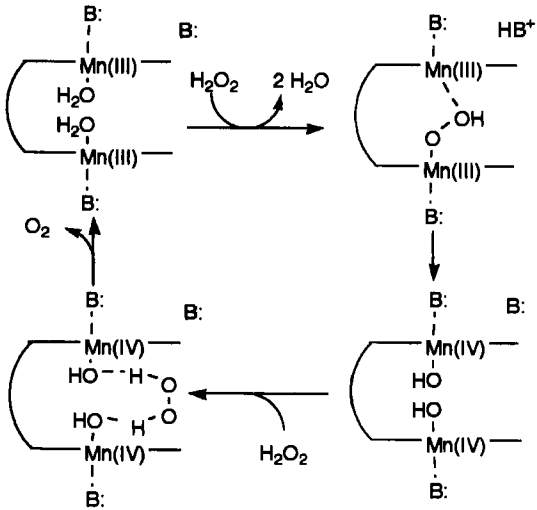

SCHEME 22. A proposed mechanism of hydrogen peroxide disproportionation by Naruta, *et al.*'s system. [Reproduced with permission from (*445*). Copyright 1997 Elsevier Science.]

The most efficient catalase mimic to date is the $[Mn^{IV}salpn(\mu\text{-}O)]_2$ complex (Fig. 50) (*244*, *446*). This complex cycles between Mn_2^{IV} and $Mn^{III}Mn^{III}$. The latter oxidation state is represented by two monomeric units, as exhibited by ligand-scrambling experiments. This was determined in catalase mimicry experiments by utilizing two complexes with differing ligand derivatization. When they were reacted with hy-

drogen peroxide and isolated, mass spectrometry showed that the resulting material contained manganese dimers with both derivatized ligands in one molecule. In experiments without added hydrogen peroxide, no ligand mixing was observed. The ability to form these [Mn^{IV} salpn(μ-O)]$_2$ complexes from [$Mn^{III}L]^+$ precursors also supported this supposition. The dioxygen produced during the reaction with hydrogen peroxide arises from the same molecule of hydrogen peroxide, based upon isotope-labeling studies with labeled hydrogen peroxide. The reoxidation step of this complex's catalytic cycle involves the incorporation of a hydrogen peroxide molecule into the compound in the form of the new oxo bridges. The rate at which this complex is capable of disproportionating hydrogen peroxide is 250 s^{-1}, and saturation kinetics are observed. A proposed catalytic cycle for this system is presented in Scheme 23. Although, this complex shuttles to a higher oxi-

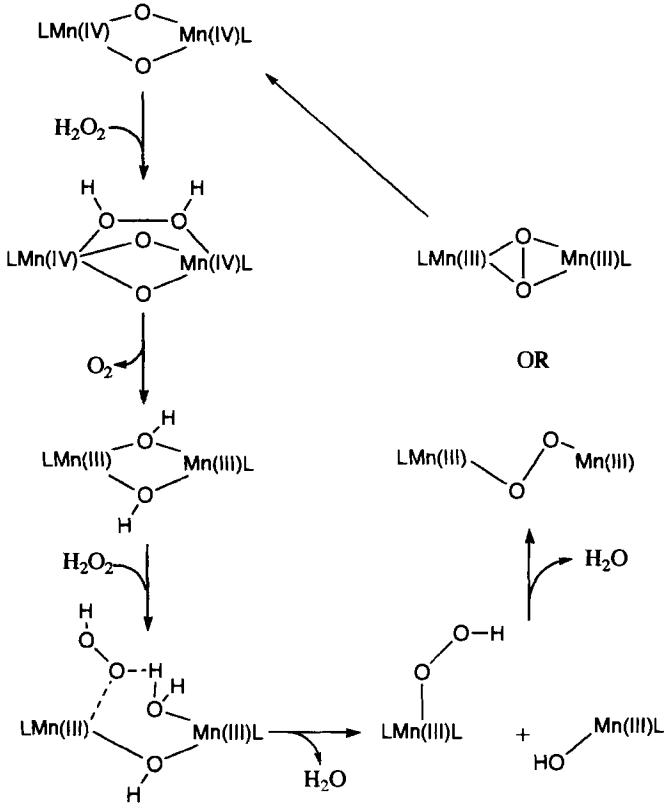

SCHEME 23. A proposed mechanism of hydrogen peroxide disproportionation by [Mn^{IV}(salpn)(μ-O)]$_2$. [Reproduced with permission from (27). Copyright 1992 WILEY-VCH Verlag.]

dation state than is proposed to exist in the catalase, its structural similarities to the OEC make it an excellent model for the catalase-like reaction of the OEC that occurs between the S_0 and S_2 states of that enzyme.

Another class of catalase mimics are comprised of tetranuclear complexes, of which at least two examples are known. The first example was reported in 1990 by Stibrany and Gorun (*447*). In this complex (Fig. 74), two manganese ions are bridged by the alkoxide from the ligand 1,3-diamino-2-hydroxypropane-*N*,*N*,*N*′,*N*′-tetraacetic acid. The tetramer is then formed when these dimeric units are bridged to one another by two acetates and by one oxo and one hydroxo bridge, which hydrogen bond. The overall oxidation state of this compound is $Mn^{II}Mn^{III}_3$. This complex was shown to have a rate of hydrogen peroxide disproportionation on the order of 1.04 s^{-1}. A second tetramer was reported by Gelasco *et al.* in 1995 (*333*). In this complex, four

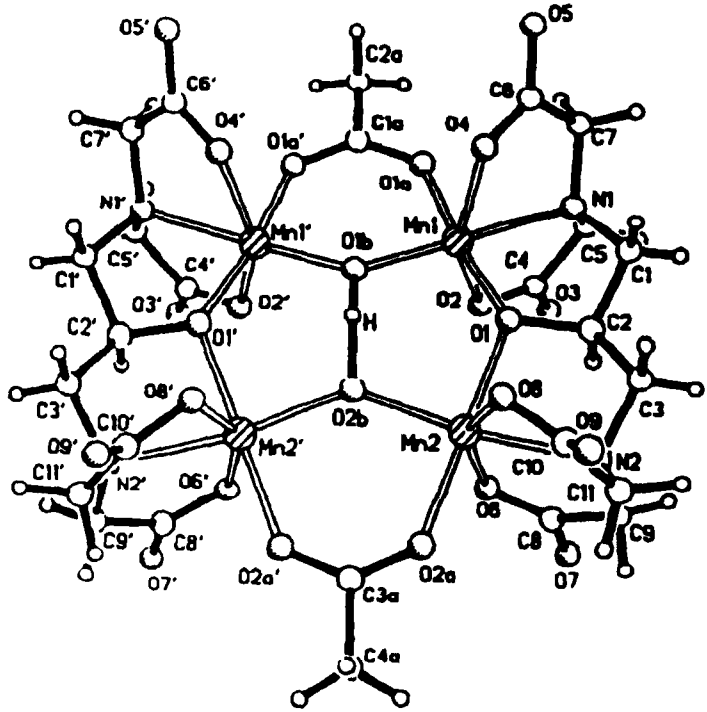

FIG. 74. Structure of $[Mn^{III}_3Mn^{II}(\mu\text{-}O)(\mu\text{-}OH)(\mu\text{-}OAc)_2(L)_3]^{2-}$ anion; L = 1,3-diaminopropan-2-ol-*N*,*N*,*N*′,*N*,-tetraacetic acid. Ca^{2+} or Ba^{2+} were reported as counterions. [Reproduced with permission from (*447*). Copyright 1990 Wiley-VCH Verlag.]

manganese ions are bridged by the ligand *N,N'*-(picolylideneimino)-1,3-di-aminopropan-2-ol, 2-OHpicpn. This complex appears approximately box shaped (Fig. 63), with one ligand lying along each edge of the box. The oxidation state of each manganese in this complex is Mn^{II}. This complex disproportionates hydrogen peroxide at a rate of 150 s^{-1}, making it the second most efficient catalase mimic yet reported. It also exhibits saturation kinetics.

4. Water Oxidation

Dioxygen is at the heart of many biological processes, and without the generation of dioxygen by green plants and algae, the world be a much different place. The need for a catalase or an MnSOD results from an aerobic existence, for example. The overall oxidation of two molecules of water to form dioxygen is a four-electron process. Although the oxidation of the OEC itself occurs by four single-electron events, it has not been determined whether the final oxidation of water to dioxygen is a four-electron process or one that occurs in smaller steps, either by sequential one-electron oxidations or by 2 two-electron processes. One newer and intriguing proposal has suggested that this may occur via hydrogen atom abstraction from water molecules bound to an OEC manganese ion (*182*). That would eventually produce a higher-valent manganese/oxygen moiety such as $Mn^{V}=O$ prior to a final step that forms and releases dioxygen (Schemes 12 and 13). Water oxidation by a variety of inorganic systems (*26*) and considerations, such as thermodynamics, for the oxidation of water to dioxygen by the OEC have been recently reviewed (*37*). Model chemistry related to the viability of hydrogen atom abstraction is discussed in the Section II.G, "The Oxygen-Evolving Complex." We will focus on well-defined manganese model complexes that have been implicated in water oxidation as potential models for the function of the OEC.

Although the OEC's tetranuclear manganese cluster is most likely not light-activated in and of itself, with respect to oxygen evolution, models have been prepared in which manganese complexes oxidize water upon irradiation by light. The classical example is the photochemical decomposition of permanganate, MnO_4^-, a process first reported in 1913 (*448*). Dioxygen could be generated by irradiating either of two ligand–metal charge-transfer bands at 311 nm or 546 nm. The 311-nm band is the more efficient of the two. The release of dioxygen was established to be pH independent in the range from slightly basic to slightly acidic. Isotopic labeling studies with labeled oxygen atoms suggested that the oxygen atoms in the product dioxygen originated on the same permanganate anion. Furthermore, an intermedi-

ate for this decomposition was proposed that will react with oxidizable organic substrates that were stable in the presence of permanganate prior to irradiation of the reaction mixture. In these experiments, dioxygen evolution is curtailed, and the rate of permanganate consumption increases. These data suggested that an intermediate existed during this decomposition process. It was proposed to bear, in part, a Mn^{V}–peroxide moiety. This system is principally of historical interest, in that it served as an early functional model for the OEC. The data for the OEC suggest, however, that such a process does not occur there.

Other manganese-containing molecules have been synthesized since that time that have also been claimed to oxidize water upon irradiation in solution. Two such systems have been prepared by McAuliffe and co-workers (*449–451*). These complexes were prepared with the $salen^{2-}$ ligand, and characterized as $[Mn^{III}L(H_2O)]_2(ClO_4)_2$ compounds wherein the crystal structure shows two planar LMn^{III} moieties bridged by two water molecules. When an aqueous solution of this complex was irradiated, these authors reported that the dioxygen concentration in the solution rose, as measured by an oxygen electrode. Furthermore, they reported this to be a stoichiometric amount of dioxygen. This reaction was conducted in the presence of hydrogen atom accepting quinone molecules, which were reported to be reduced to hydroquinone products. The authors proposed that the dioxygen produced comes from the bridging water molecules, because conducting this reaction in anhydrous ethanol did not appear to noticeably retard the rate of dioxygen production. The productive region of light was found to be the range of 450 to 600 nm, with a maximal rate for dioxygen evolution at 590 nm. The final manganese complex from the process is proposed to be in the form $[(Mn^{III}L)_2O]$. More recently, McAuliffe and co-workers have prepared a system in which two Schiff-base ligands are connected via two naphthyl moieties (*451*). This dimeric product also binds water and has been suggested to oxidize water to dioxygen upon irradiation, too.

Because the tetranuclear cluster of the OEC is most likely not photoactivated in and of itself during turnover, manganese systems that oxidize water without being irradiated first are of interest with respect to understanding the function of this complex enzyme. One system that oxidizes water was prepared and studied by Matsushita and co-workers (*452*, *453*). These complexes are mononuclear $Mn^{IV}L_2Cl_2$ complexes, where L is a bidentate Schiff base comprised of 5-nitrosalicylaldehyde and an alkylmonoamine, with structures that should be similar to $Mn^{IV}(salpn)Cl_2$ (Fig. 33). These researchers showed that

these complexes are capable of oxidizing water to dioxygen in a non-catalytic process. The complexes of this type exhibit high reduction potentials, all near 1.0 V (*454*). Water oxidation was proposed to occur in the manner shown in Scheme 24, wherein two molecules of water

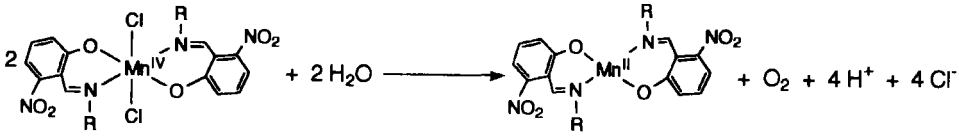

SCHEME 24.

would be oxidized to form dioxygen, and two $Mn^{II}L_2$ compounds would be produced. This evolution of dioxygen from water was confirmed by the observation of ^{18}O-enriched dioxygen following the introduction of isotopically labeled water into a reaction mixture. Titration by $AgNO_3$ indicated that four equivalents of Cl^- were retained in solution, indicating that chloride oxidation had not occurred. The observed pH changes in unbuffered reaction mixtures were consistent with the evolution of four equivalents of proton. The Mn products were confirmed as Mn^{II} complexes; however, no yield was listed. The yield of dioxygen was only half the maximal possible yield, at neutral pH.

Naruta *et al.* published a report of dioxygen evolution from water that was catalyzed by a dimeric-linked manganese–porphyrin dimer complex (*455*), in a system similar to that employed for their catalase mimic (Fig. 75). This complex is composed of two triphenylporphyrins linked via an *o*-phenylene bridge. With this series of complexes, they were able to show oxidation of water to dioxygen. This was accomplished by preparing a solution of the dimeric porphyrin complex in 5% v/v H_2O in acetonitrile in the presence of Bu_4NOH. In dry acetonitrile, reversible electrochemistry was observed, but in the aqueous acetonitrile mixture, an irreversible current discharge was observed at ≥ 1.2 V vs. Ag/Ag^+. Dioxygen evolution was observed over a voltage range of 1.2 to 2.0 V; however, in the absence of the complex, anodic oxidation of the water/acetonitrile mixture did not evolve dioxygen up to +2.3 V. The rate of dioxygen evolution was found to correlate with the concentration of the manganese complex in solution, and up to 9.2 turnovers were achieved. Under the same conditions, the monomeric analogs of these dimeric complexes did not evolve dioxygen. By mass spectrometry, the authors observed that a 1:1 mixture of $H_2{}^{16}O$ and $H_2{}^{18}O$ in the reaction led to a 1:2:1 mixture of $^{16}O_2$, $^{16}O^{18}O$, and $^{18}O_2$, respectively. Finally, they reported that 3.7 electrons were involved

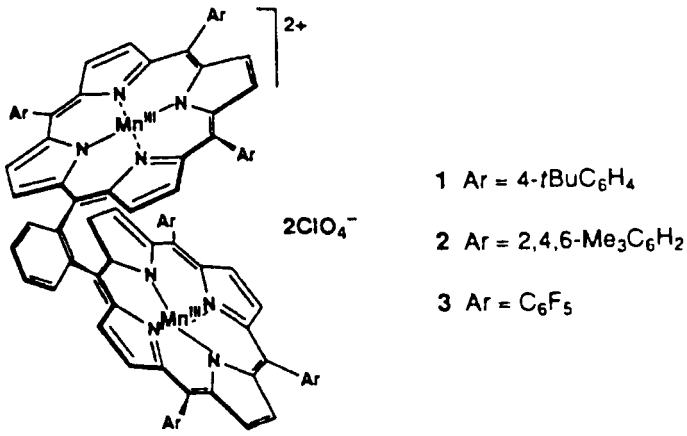

FIG. 75. Representation of the linked porphyrin catalyst utilized for water oxidation. Replacement of the *o*-phenylene linker with an anthracene linker generates the catalase mimic reported in the catalase segment (*443*). The authors have noted that reactivity can be altered by the nature of the linker (*444*). [Reproduced with permission from (*455*). Copyright 1994 Wiley-VCH Verlag.]

in this reaction overall, as determined by a rotating disk electrode and a Levich plot.

Two mechanistic proposals could be made for this dioxygen evolution. The first invokes 2 two-electron processes. Because similar dimers had been shown to disproportionate hydrogen peroxide (*443–445*) (discussed earlier), this proposal would rely on the formation of hydrogen peroxide by a dimer, followed by disproportionation of that hydrogen peroxide by one of the dimers in solution. The second proposal invokes a four-electron process. The authors found no evidence of hydrogen peroxide evolution in their system in the absence of a manganese dimer, either by addition of a dimer to a water/acetonitrile solution after anodic oxidation or by analysis by a hydrogen-peroxide-sensitive electrode. Thus, they proposed that a four-electron process was operative. Their mechanism involves the coordination of two hydroxides to the manganese of the dimer on the inside of the dimer cavity. Oxidation to $Mn^{V}=O$ moieties is then followed by formation of a $Mn^{IV}-O-O-Mn^{IV}$ compound. They proposed that coordination of hydroxide to the manganese could then occur with loss of the $\mu_{1,2}$-peroxo bridge as dioxygen to return the dimer to the initial Mn_2^{III} oxidation state.

A more recent system in which water oxidation has been observed via a manganese complex (*456*) is a manganese system based on the ligand dipicolinate (dpa). When $[Mn^{III}(dpa)_2]^-$ reacts with oxone, po-

tassium peroxymonosulfate, a rather strong oxidant, the generation of dioxygen, and the formation of MnO_4^- was observed. These reactions were carried out in buffered aqueous solutions, over a pH 3–6 range, with an increasing rate of permanganate anion production noted for higher pH levels. The Mn^{III} complex appears to be a precursor to a reactive intermediate, which has been proposed to be a bis(μ-O^{2-})-bridged dimer with a terminal water on each of the manganese, perhaps with a structure similar to that shown in Fig. 55. This green intermediate complex exhibited a $Mn^{III}Mn^{IV}$ 16-line EPR signal and had a distinctive UV-vis spectrum, which converted isosbestically to that of MnO_4^- during the course of the reaction. Below pH 3.5, this system catalytically generated dioxygen. Finally, in control experiments, this system did not appear to generate dioxygen from hydrogen peroxide formed via oxone hydrolysis in the presence of other Lewis acids, such as Ni^{II}/sulfate. This also implied that a redox process involving the manganese complex was producing the observed dioxygen.

To follow up on these observations, some additional ligand systems were screened, including 2,2′-bipyridine (bpy), 1,10-phenanthroline (phen), picolinate (pic), and 2.2′ : 6′,2″-terpyridine (terpy). In the cases with the bidentate ligands, fewer turnovers leading to dioxygen evolution compared to the dpa were observed. In the case of the tridentate terpy, many more turnovers were achieved and no appreciable concentration of MnO_4^- was observed. The authors concluded that the meridionally coordinating tridentate ligands were ideal for promoting the reactivity that they observed, and they attributed the robust nature of the terpy system to a lesser degree of ligand dissociation versus dpa, pic, or bipy (*456*) because the ligand must come off of the manganese ion before it may be converted to a permanganate.

Two mechanistic proposals for this process were suggested. The first requires oxygen atom transfer and the production of an $Mn^V{=}O$ moiety; the second is based on the hydrolysis of a manganese-bound peroxymonosulfate anion to yield a $Mn{-}O{-}O^-$ moiety. In the first case, $Mn^V{=}O$ would combine with either a second equivalent of $Mn^V{=}O$ or an oxone molecule in an overall four-electron process. In the second, a two-electron process leads to the release of dioxygen from the $Mn{-}O{-}O^-$ complex. Neither of these possibilities has yet to be ruled out, and the authors state that they are following up with isotope-labeling studies to ascertain what the reaction mechanism may be. Some preliminary evidence does, however, suggest that oxygen transfer may be involved. By utilizing dimethyldioxirane, a reagent capable of oxygen atom transfer, but not the transfer of a per-

oxo group, in the presence of Mn^{II} and terpy, the authors observed the production of dioxygen.

In conclusion, the reactivity of manganese complexes has proved to be a fertile area for research. It has provided new insights into the function of manganese-containing redox enzymes, and it has provided new synthetic techniques to the field of organic chemistry.

VI. Conclusion

The biological applications of manganese are numerous and quite varied. Although most of these biological roles utilize manganese in structural or hydrolytic systems, some very striking redox systems are also known. The hydrolytic roles are, of course, not to be overlooked with respect to the widespread and critical arginase enzyme, which exhibits a strict requirement for two Mn^{II} ions. The ribonuclease hydrolases of retroviral reverse transcriptase are another key nonredox application—for example, the ribonuclease hydrolase from HIV-1.

The manganese-containing redox enzymes are quite unique. Most of these deal with dioxygen metabolism in one form or another. One key enzyme is the OEC, which generates the dioxygen required by aerobic life forms to exist by catalytically oxidizing water. New evidence now suggests that this enzyme may soon join the ranks of other known metalloenzymes that employ radical protein residues to complete their catalytic cycle. Catalase disproportionates hydrogen peroxide, and the MnSOD catalyzes the dismutation of superoxide. Both are critical for protecting organisms from oxidative damage, one of the hazards of aerobic life. Meanwhile, the newly discovered dioxygenases operate on aromatic-bearing *cis*-diol functionalities and open these rings by catalyzing the incorporation of dioxygen into them. All of these enzymes are driven by the oxophilicity of manganese, which is important in defining the chemistry that occurs. Another interesting feature of several of these enzymes is their iron analogs. MnSOD and Mn–dioxygenase have direct iron enzyme analogs, which in the case of SOD, are known to have nearly identical active sites, and in some cases (but not all) the metal from one may be added to the other with retention of enzyme activity. In addition, MnP bears analogy to the LiP enzymes, which rely solely on heme, although new evidence shows that they, too, may be capable of oxidizing manganese.

However, one notable exception stands out, and that is the OEC. This enzyme is functional only with manganese. With so many man-

ganese enzymes that bear similarities to enzymes that conduct the same or similar reaction with different metals at their active site, why is manganese so strictly required? If the newer proposals for the function of the OEC are correct, then an answer may emerge that suggests that manganese allows the proton-coupled oxidations necessary for water oxidation to occur at a potential at which the oxidizing equivalents may be easily stored. Furthermore, there are sufficient readily available oxidation states available to allow the sequential oxidations to occur, yet despite this stability, once the high-valent $Mn^{V}=O$ is reached, it is not so stable as to prevent the formation of dioxygen.

Finally, with the acknowledged similarities that currently exist between several manganese enzymes and counterparts utilizing other metal ions, it seems quite likely that other redox-active manganese enzymes will be discovered in the future. The discussions of data gathering on enzyme systems and model chemistry, both structural and functional, as presented in this article will provide a foundation for exploring current and as yet undiscovered manganese enzymes.

Acknowledgments

We wish to acknowledge the NIH for funding our research endeavors (GM 39406 to V.L.P.). We also wish to thank Professor G. T. Babcock for providing us with a copy of Scheme 12 and Professor V. V. Barynin for the provision of data on the crystallographic details of the *T. thermophilus* enzyme.

Note Added in Proof

A recent article on the *T. thermophilus* manganese-containing catalase enzyme presents data that indicates that the structure of the active site is affected by pH. The experiments were conducted over the pH range 6.6 to 9.8. The authors propose that at high pH a $Mn^{III}_2(\mu\text{-}O)_2(\mu\text{-}OAc)$ form predominates, while at low pH a $Mn^{III}_2(\mu\text{-}O)(\mu\text{-}OAc)$ form predominates. The latter form has only a single oxo-bridge with a proposed hydroxide and water ligand to fill the remaining coordination sites on the Mn^{III} ions, one site per Mn^{III} (*478*).

References

1. Wedler, F. C. In "Manganese in Health and Disease"; Klimis-Tavantzis, D. J., Ed.; CRC Press, Inc., Ann Arbor, **1994,** 1.
2. Scrutton, M. C. In "Manganese in Metabolism and Enzyme Function"; Schramm, V. L., and Wedler, F. C., Eds.; Academic Press, Inc., New York, **1986,** 147.

3. Dismukes, G. C. *Chem. Rev.* **1996,** *96,* 2909.
4. Wilcox, D. *Chem. Rev.* **1996,** *96,* 2435.
5. Christianson, D. W. *Prog. Biophys. Mol. Biol.* **1997,** *67,* 217.
6. Reczkowski, R. S.; Ash, D. E. *J. Am. Chem. Soc.* **1992,** *114,* 10992.
7. Khangulov, S. V.; Pessiki, P. J.; Barynin, V. V.; Ash, D. E.; Dismukes, G. C. *Biochemistry* **1995,** *34,* 2015.
8. Kanyo, Z. F.; Scolnick, L. R.; Ash, D. E.; Christianson, D. W. *Nature* **1996,** *383,* 554.
9. Stemmler, T. L.; Sossong, Jr., T. M.; Goldstein, J. I.; Ash, D. E.; Elgren, T. E.; Kurtz, Jr., D. M.; Penner-Hahn, J. E. *Biochemistry* **1997,** *36,* 9847.
10. Sossong, Jr., T. M.; Khangulov, S. V.; Cavalli, R. C.; Soprano, D. R.; Dismukes, G. C.; Ash, D. E. *JBIC* **1997,** *2,* 433.
11. Davies, II, J. F.; Hostomska, Z.; Hostomsky, Z.; Jordan, S. R.; Matthews, D. A. *Science* **1991,** *252,* 88.
12. Cowan, J. A. *JBIC* **1997,** *2,* 168.
13. Sträter, N.; Lipscomb, W. N.; Klabunde, T.; Krebs, B. *Angew. Chem., Int. Ed. Engl.* **1996,** *35,* 2024.
14. Hardman, K. D.; Ainsworth, C. F. *Biochemistry* **1972,** *11,* 4910.
15. Hardman, K. D.; Agarwal, R. C.; Freiser, M. J. *J. Mol. Biol.* **1982,** *157,* 69.
16. "The Lectins: Properties, Functions, and Applications in Biology and Medicine"; Liener, I. E., Sharon, N., and Goldstein, I. J., Eds.; Academic Press: New York, 1986.
17. Sharon, N.; Lis, H. "Lectins"; Chapman and Hall: New York, 1989.
18. Naismith, J. H.; Emmerich, C.; Habash, J.; Harrop, S. J.; Helliwell, J. R.; Hunter, W. N.; Raftery, J.; Kalb, A. J.; Yariv, Y. *Acta Cryst.* **1994,** *D50,* 847.
19. Antanaitas, B. C.; Chasteen, N. D.; Freedman, J. H.; Koenig, S. H.; Lilienthal, H. R.; Peisach, J.; Brewer, C. F. *Biochemistry* **1987,** *26,* 7932.
20. Reed, G. H.; Cohn, M. J. *J. Biol. Chem.* **1970,** *245,* 662.
21. Derewenda, Z.; Yariv, J.; Helliwell, J. R.; Kalb (Gilboa), J. R.; Dodson, E. J.; Papiz, M. Z.; Wan, T.; Campell, *EMBO J.* **1989,** *8,* 2189.
22. Deacon, A.; Gleichmann, T.; Kalb (Gilboa), A. J.; Price, H.; Raftery, J.; Bradbrook, G.; Yariv, J.; Helliwell, J. R. *J. Chem. Soc., Faraday Trans.* **1997,** 4305.
23. Penner-Hahn, J. E. In "Manganese Redox Enzymes"; Pecoraro, V. L., Ed.; VCH Publishers, Inc.: New York, **1992,** 29.
24. Penner-Hahn, J. E. In "Structure and Bonding"; Hill, H. A. O., Sadler, P. J., and Thomson, A. J., Eds.; Springer Verlag: Berlin, **1998,** *90,* 1.
25. Pecoraro, V. L.; Gelasco, A.; Baldwin, M. J. In "Mechanistic Bioinorganic Chemistry"; Thorp, H. H., and Pecoraro, V. L., Eds.; ACS Books: Washington, DC, 1995, p. 265.
26. Pecoraro, V. L.; Baldwin, M. J.; Gelasco, A. *Chem. Rev.* **1994,** *94,* 807.
27. Pecoraro, V. L. In "Manganese Redox Enzymes"; Pecoraro, V. L., Ed.; VCH Publishers: New York, **1992,** 197.
28. "Manganese Redox Enzymes"; Pecoraro, V. L., Ed.; VCH Publishers, Inc.: New York, 1992.
29. Vincent, J. B.; Christou, G. In "Advances in Inorganic Chemistry"; Sykes, A. G., Ed.; Academic Press, Inc.: New York, **1989,** *33,* 197.
30. Wieghardt, K. *Angew. Chem., Int. Ed. Engl.* **1989,** *28,* 1153.
31. Wieghardt, K. *Angew. Chem., Int. Ed. Engl.* **1994,** *33,* 725.
32. Yachandra, V. K.; DeRose, V. J.; Latimer, M. J.; Mukerji, I.; Sauer, K.; Klein, M. P. *Science* **1993,** *260,* 675.

33. Yachandra, V. K.; Sauer, K.; Klein, M. P. *Chem. Rev.* **1996,** *96,* 2927.
34. Manchanda, R.; Brudvig, G. W.; Crabtree, R. H. *Coord. Chem. Rev.* **1995,** *144,* 1.
35. Yocum, C. F. In "Manganese Redox Enzymes"; Pecoraro, V. L., Ed.; VCH: New York, **1992,** 71.
36. Thorp, H. H.; Brudvig, G. W. *New J. Chem.* **1991,** *15,* 479.
37. Rüttinger, W. F.; Campana, C.; Dismukes, G. C. *J. Am. Chem. Soc.* **1997,** *119,* 6670.
38. Pecoraro, V. L.; Gelasco, A.; Baldwin, M. J. In "Bioinorganic Chemistry: An Inorganic Perspective of Life"; K. D. P., Ed.; Kluwer Academic Publishers: Amsterdam, **1995,** *459,* 287.
39. Ghanotakis, D. F.; Yocum, C. F. *Annu. Rev. Plant Phys. Plant Mol. Biol.* **1990,** *41,* 255.
40. Pecoraro, V. L. *Photochem. Photobiol.* **1988,** *48,* 249.
41. Diner, B. A.; Babcock, G. T. In "Oxygenic Photosynthesis: The Light Reactions"; Ort, D. R., and Yocum, C. F., Eds.; Kluwer Academic Publishers: Boston, **1996,** 213.
42. Debus, R. J. *Biochim. Biophys. Acta* **1992,** *1102,* 269.
43. de Paula, J. C.; Beck, W. F.; Brudvig, G. W. *New J. Chem.* **1987,** *11,* 103.
44. Christou, G. *Acc. Chem. Res.* **1989,** *22,* 328.
45. Brudvig, G. W.; Crabtree, R. H. In "Progress in Inorganic Chemistry"; Lippard, S. J., Ed.; John Wiley & Sons: New York, **1989,** *37,* 99.
46. Britt, R. D. In "Oxygenic Photosynthesis: The Light Reaction"; Ort, D. R., and Yocum, C. F., Eds.; Kluwer Academic Publishers: Netherlands, **1996,** 137.
47. Babcock, G. T.; Espe, M.; Hoganson, C.; Lydakis-Simantiris, N.; McCracken, J.; Shi, W.; Styring, S.; Tommos, C.; Warncke, K. *Acta Chem. Scand.* **1997,** *51,* 533.
48. "Oxygenic Photosynthesis: The Light Reactions"; Ort, D. R., and Yocum, C. F., Eds.; Kluwer Academic Publishers: Boston, 1996.
49. Hage, R.; Iburg, J. E.; Kerschner, J.; Koek, J. H.; Lempers, E. L. M.; Martens, R. J.; Racherla, U. S.; Russell, S. W.; Swarthoff, T.; van Vliet, M. R. P.; Warnaar, J. B.; van der Wolf, L.; Krijnen, B. *Nature* **1994,** *269,* 637.
50. Armstrong, W. H. In "Manganese Redox Enzymes"; Pecoraro, V. L., Ed.; VCH Publishers: New York, **1992,** 261.
51. "Photosynthesis: From Light to Biosphere"; Mathis, P., Ed.; Kluwer Academic Publishers: Amsterdam, The Netherlands, 1995.
52. Keele, Jr., B. B.; McCord, J. M.; Fridovich, I. *J. Biol. Chem.* **1970,** *245,* 6176.
53. Ludwig, M. L.; Pattridge, K. A.; Stallings, W. C. In "Manganese in Metabolism and Enzyme Function"; Schramm, V. L., and Wedler, F. C., Eds.; Academic Press, Inc.: New York, **1986,** 405.
54. Stallings, W. C.; Pattridge, K. A.; Strong, R. K.; Ludwig, M. L. *J. Biol. Chem.* **1984,** *259,* 10695.
55. Stallings, W. C.; Pattridge, K. A.; Strong, R. K.; Ludwig, M. L. *J. Biol. Chem.* **1985,** *260,* 16424.
56. Stallings, W. C.; Powers, T. B.; Pattridge, K. A.; Fee, J. A.; Ludwig, M. L. *Proc. Natl. Acad. Sci. U.S.A.* **1988,** *80,* 3884.
57. Tierney, D. L.; Fee, J. A.; Ludwig, M. L.; Penner-Hahn, J. E. *Biochemistry* **1995,** *34,* 1661.
58. Lah, M. S.; Dixon, M. M.; Pattridge, K. A.; Stallings, W. C.; Fee, J. A.; Ludwig, M. L. *Biochemistry* **1995,** *34,* 1646.
59. Barra, D.; Schinina, M. E.; Bannister, W. H.; Bannister, J. V.; Bossa, F. *J. Biol. Chem.* **1987,** *262,* 1001.

60. Harris, J. I.; Auffret, A. D.; Northrop, F. D.; Walker, J. E. *Eur. J. Biochem.* **1980,** *106,* 297.
61. Beyer, W. F.; Fridovich, I. *J. Biol. Chem.* **1991,** *263,* 303.
62. McCord, J. M.; Fridovich, I. *J. Biol. Chem.* **1969,** *244,* 6049.
63. Valentine, J. S. In "Bioinorganic Chemistry"; Bertini, I., Gray, H. B., Lippard, S. J., and Valentine, J. S., Eds.; University Science Press: Mill Valley, California, 1994.
64. Youn, H.-D.; Youn, H.; Lee, J.-W.; Yim, Y.-I.; Lee, J. K.; Hah, Y. C.; Kang, S.-O. *Arch. Biochem. Biophys.* **1996,** *334,* 341.
65. Fridovich, I. *J. Biol. Chem.* **1989,** *264,* 7761.
66. McCord, J. M.; Fridovich, I. *J. Biol. Chem.* **1968,** *243,* 5753.
67. Morel, F.; Doussiere, J.; Vignas, P. V. *Eur. J. Biochem.* **1991,** *201,* 523.
68. Beauchamp, C.; Fridovich, I. *Anal. Biochem.* **1971,** *44,* 276.
69. Davies, K. J. A. In "Free Radicals and Oxidative Stress: Environment, Food and Drug Additives"; Rice-Evans, C., Halliwell, B., and Lunt, G. G., Eds.; Portland Press: London, **1994,** *61,* 1.
70. Afanas'ev, I. B. "Superoxide Ion: Chemistry and Biological Implications"; CRC Press, Inc.: Boca Raton, 1989.
71. Darley-Usmar, V.; Wiseman, H.; Halliwell, B. *FEBS Lett.* **1995,** *369,* 131.
72. Jenner, P.; Olanow, C. W. *Neurology* **1996,** *47,* S161.
73. Dawson, V. L.; Dawson, T. M. *J. Chem. Neuroanat.* **1996,** *10,* 179.
74. Beckman, J. S.; Beckman, T. W.; Chen, J.; Marshall, P. M.; Freeman, B. A. *Proc. Natl. Acad Sci. U.S.A.* **1990,** *87,* 1620.
75. Borgstahl, G. E. O.; Parge, H. E.; Hickey, M. J.; Beyer, W. F.; Hallewell, R. A.; Tainer, J. A. *Cell* **1992,** *71,* 107.
76. Ludwig, M. L.; Metzger, A. L.; Pattridge, K. A.; Stallings, W. C. *J. Mol. Biol.* **1991,** *219,* 335.
77. Fee, J. A.; Shapiro, E. R.; Moss, T. H. *J. Biol. Chem.* **1976,** *251,* 6157.
78. Bull, C.; Neiderhoffer, E. C.; Yoshida, T.; Fee, J. A. *J. Am. Chem. Soc.* **1991,** *113,* 4069.
79. McAdam, M. E.; Fox, R. A.; Lavelle, F.; Fielden, E. M. *Biochem. J.* **1977,** *165,* 71.
80. McAdam, M. E.; Fox, R. A.; Lavelle, F.; Fielden, E. M. *Biochem. J.* **1977,** *165,* 81.
81. Osman, R.; Basch, H. *J. Am. Chem. Soc.* **1984,** *106,* 5710.
82. Pick, M.; Rabani, J.; Yost, F.; Fridovich, I. *J. Am. Chem. Soc.* **1974,** *96,* 7329.
83. Valentine, J. S.; Quinn, A. E. *Inorg. Chem.* **1976,** *15,* 1997.
84. Bull, C.; Fee, J. A. *J. Am. Chem. Soc.* **1985,** *107,* 3295.
85. Whiting, A. K.; Boldt, Y. R.; Hendrich, M. P.; Wackett, L. P.; Que, L. *Biochemistry* **1996,** *35,* 160.
86. Que, Jr., L.; Widom, J.; Crawford, R. L. *J. Biol. Chem.* **1981,** *256,* 10941.
87. Que, L. J. In "Iron Carriers and Iron Proteins"; Loehr, T. M., Ed.; VCH Publishers, Inc.: New York, **1989,** *5,* 467.
88. Lipscomb, J. D.; Orville, A. M. In "Metal Ions in Biological Systems"; Sigel, H., and Sigel, A., Eds.; Marcel Dekker, Inc.: New York, **1992,** *28,* 243.
89. Que, Jr., L.; Ryn, H. *Chem. Rev.* **1996,** *96,* 2607.
90. Boldt, Y. R.; Sadowsky, M. J.; Ellis, L. B. M.; Que, Jr., L.; Wackett, L. P. *J. Bacteriol.* **1995,** *177,* 1225.
91. Han, S.; Eltis, L. D.; Timmis. K. N.; Muchmore, S. W.; Bolin, J. T. *Science* **1995,** *270,* 976.
92. Boldt, Y. R.; Whiting, A. K.; Wagner, M. L.; Sadowsky, M. J.; Que, Jr., L.; Wackett, L. P. *Biochemistry* **1997,** *36,* 2147.

93. Shu, L. J.; Chiou, Y. M.; Orville, A. M.; Miller, M. A.; Lipscomb, J. D.; Que, Jr., L. *Biochemistry* **1995,** *34,* 6649.
94. Glenn, J. K.; Gold, M. H. *Arch. Biochem. Biophys.* **1985,** *242,* 329.
95. Glenn, J. K.; Akileswaran, L.; Gold, M. H. *Arch. Biochem. Biophys.* **1986,** *251,* 688.
96. Sundaramoorthy, M.; Kishi, K.; Gold, M. H.; Poulos, T. L. *J. Biol. Chem.* **1994,** *269,* 32759.
97. Sarkanen, K. V.; Ludwig, C. H. "Lignins: Occurrence, Formation, Structure and Reactions"; Wiley-Interscience: New York, 1971.
98. Gold, M. H.; Wariishi, H.; Valli, K. In "Biocatalysis in Agricultural Biotechnology"; Whitaker, J. R., and Sonnet, P. E., Eds.; American Chemical Society: Washington, DC, **1989,** 127.
99. Crawford, R. L. "Lignin Biodegradation and Transformation"; John Wiley & Sons: New York, 1981.
100. Eggert, C.; Temp, U.; Eriksson, K.-E. L. *FEBS Lett.* **1997,** *407,* 89.
101. Youn, H.-D.; Yung, C. H.; Sa-Ouk, K. *FEMS Microbiol. Lett.* **1995,** *132,* 183.
102. Hammel, K. E. In "Degradation of Environmental Pollutants by Microorganisms and Their Metalloenzymes"; Sigel, H., and Sigel, A., Eds.; Marcel Dekker, Inc.: New York, 1992.
103. Wariishi, H.; Valli, K.; Gold, M. H. *Biochemsitry* **1989,** *28,* 6017.
104. Wariishi, H.; Valli, K.; Gold, M. H. *J. Biol. Chem.* **1992,** *267,* 23688.
105. Kuan, I.-C.; Johnson, K. A.; Tien, M. *J. Biol. Chem.* **1993,** *268,* 20064.
106. Kuan, I.-C.; Tien, M. *Proc. Natl. Acad. Sci. U.S.A.* **1993,** *90,* 1242.
107. Khindaria, A.; Barr, D. P.; Aust, S. D. *Biochemistry* **1995,** *34,* 7773.
108. Timofeevski, S. L.; Aust, S. D. *Biochem. Biophys. Res. Commun.* **1997,** *239,* 645.
109. Zapanta, L. S.; Tien, M. *J. Biotech.* **1997,** *53,* 93.
110. Pasczcynski, A.; Huyhn, V.-B.; Crawford, R. L. *Arch. Biochem. Biophys.* **1986,** *244,* 750.
111. Auling, G.; Follman, H. In "Metal Ions in Biological Systems"; Sigel, H., and Sigel, A., Eds.; Marcel Dekker, Inc.: New York, **1994,** *30,* 131.
112. Stubbe, J. *J. Biol. Chem.* **1990,** *265,* 5329.
113. Sjöberg, B.-M. *Structure* **1994,** *2,* 793.
114. Sjöberg, B.-M. In "Structure and Bonding"; Hill, H. A. O., Sadler, P. J., and Thomson, A. J., Eds.; Springer Verlag: Berlin, **1997,** *88,* 139.
115. Mao, S. S.; Holler, T. P.; Yu, G. X.; Bollinger, Jr., J. M.; Booker, S.; Johnston, M. I.; Stubbe, J. *Biochemistry* **1992,** *31,* 9733.
116. Reichard, P. *Science* **1993,** *260,* 1773.
117. Schimpf-Weiland, G.; Follman, H.; Auling, G. *Biochem. Biophys. Res. Commun.* **1981,** *102,* 1276.
118. Willing, A.; Follmann, H.; Auling, G. *Eur. J. Biochem.* **1988,** *170,* 603.
119. Uhlin, U.; Eklund, H. *J. Mol. Biol.* **1996,** *262,* 358.
120. Uhlin, U.; Eklund, H. *Nature* **1994,** *370,* 533.
121. Nordlund, P.; Sjöberg, B.-M.; Eklund, H. *Nature* **1990,** *345,* 593.
122. Nordlund, P.; Eklund, H. *J. Mol. Biol.* **1993,** *232,* 123.
123. Willing, A.; Follmann, H.; Auling, G. *Eur. J. Biochem.* **1988,** *175,* 167.
124. Atta, M.; Nordlund, P.; Aberg, A.; Eklund, H.; Fontecave, M. *J. Biol. Chem.* **1992,** *267,* 20682.
125. Barynin, V. V.; Hempstead, P. D.; Vagin, A. A.; Antonyuk, S. V.; Melik-Adamyn, W. R.; Lamzin, V. S.; Harrison, P. M.; Artymiuk, P. J. *J. Inorg. Biochem.* **1997,** *67,* 196.
126. Griepenburg, U.; Laβmann, G.; Auling, G. *Free Rad. Res.* **1996,** *26,* 473.

127. Beyer, Jr., W. F.; Fridovich, I. *Biochemistry* **1985,** *24,* 6460.
128. Kono, Y.; Fridovich, I. *J. Biol. Chem.* **1983,** *258,* 6015.
129. Algood, G. S.; Perry, J. J. *J. Bacteriol.* **1986,** *168,* 563.
130. Barynin, V. V.; Grebenko, A. I. *Dokl. Akad. Nauk. S.S.S.R* **1986,** *286,* 461.
131. Barynin, V. V.; Vagin, A. A.; Melik-Adamyan, V. R.; Grebenko, A. I.; Khangulov, S. V.; Popov, A. N.; Andrianova, M. E.; Vainshtein, B. K. *Dolk. Akad. Nauk. S.S.S.R* **1986,** *288,* 877.
132. Sheats, J. E.; Czernuszewicz, R. S.; Dismukes, G. C.; Rheingold, A. L.; Petrouleas, V.; Stubbe, J.; Armstrong, W. H.; Beer, R. H.; Lippard, S. J. *J. Am. Chem. Soc.* **1987,** *109,* 1435.
133. Wieghardt, K.; Bossek, U.; Ventur, D.; Weiss, J. *J. Chem. Soc., Chem. Commun.* **1985,** 347.
134. Riggs-Gelasco, P. J.; Stemmler, T.; Penner-Hahn, J. E. *Coord. Chem. Rev.* **1995,** *144,* 245.
135. Waldo, G. S.; Yu, S. Y.; Penner-Hahn, J. P. *J. Am. Chem. Soc.* **1992,** *114,* 5869.
136. Fronko, R. M.; Penner-Hahn, J. E. *J. Am. Chem. Soc.* **1988,** *110,* 7554.
137. Waldo, G. S.; Penner-Hahn, J. E. *Biochemistry* **1995,** *34,* 1507.
138. Khangulov, S. V.; Voyevodskaya, N. V.; Varynin, V. V.; Grebenko, A. I.; Melik-Adamyan, V. R. *Biofizika* **1987,** *32,* 960.
139. Khangulov, S. V.; Goldfeld, M. G.; Gerasimenko, V. V.; Andreeva, N. E.; Barynin, V. V.; Grebenko, A. I. *J. Inorg. Biochem.* **1990,** *40,* 279.
140. Zheng, M.; Khangulov, S. V.; Dismukes, G. C.; Barynin, V. V. *Inorg. Chem.* **1994,** *33,* 382.
141. Kurtz, Jr., D. M. *JBIC* **1997,** *2,* 159.
142. Diesenhofer, J.; Epp, O.; Miki, K.; Huber, R.; Michel, H. *Nature* **1985,** *318,* 618.
143. Michel, J.; Diesenhofer, J. *Biochemistry* **1988,** *27,* 1.
144. Ort, D. R.; Yocum, C. F. In "Oxygenic Photosynthesis: The Light Reactions"; Ort, D. R., and Yocum, C. F., Eds.; Kluwer Academic Publishers: Boston, **1996,** 1.
145. Ädelroth, P.; Lindberg, K.; Andréasson, L.-E. *Biochemistry* **1995,** *34,* 9021.
146. Yocum, C. F. *Biochim. Biophys. Acta* **1991,** *1059,* 1.
147. Lindberg, K.; Andréasson, L.-E. *Biochemistry* **1996,** *35,* 14259.
148. Lindberg, K.; Vanngärd, T.; Andréasson, L. E. *Photosynth. Res.* **1993,** *38,* 401.
149. Barry, B. A.; Babcock, G. T. *Proc. Natl. Acad. Sci. U.S.A.* **1987,** *84,* 7099.
150. Gerken, S.; Brettel, K.; Schlodder, E.; Witt, H. T. *FEBS Lett.* **1988,** *237,* 69.
151. Joliot, P.; Barbieri, G.; Chabaud, R. *Photochem. Photobiol.* **1969,** *10,* 309.
152. "Bioenergetics in Photosynthesis"; Joliot, P., Kok, B., and Govindjee, Eds.; Academic Press: New York, 1975.
153. Kok, B.; Forbush, B.; McGloid, M. *Photochem. Photobiol.* **1970,** *11,* 457.
154. Sauer, K.; Yachandra, V. K.; Britt, R. D.; Klein, M. P. In "Manganese Redox Enzymes"; Pecoraro, V. L., Ed.; VCH Publishers: New York, 1992.
155. Yachandra, V. K.; Guiles, R. D.; McDermott, A. E.; Cole, J. L.; Britt, R. D.; Dexheimer, S. L.; Sauer, K.; Klein, M. P. *Biochemistry* **1987,** *26,* 5974.
156. Penner-Hahn, J. E.; Fronko, R. M.; Pecoraro, V. L.; Yocum, C. F.; Betts, S. D.; Bowlby, N. R. *J. Am. Chem. Soc.* **1990,** *112,* 2549.
157. MacLachlan, D. J.; Hallahan, B. J.; Ruffle, S. V.; Nugent, J. H. A.; Evans, M. C. W.; Strange, R. W.; Hasnain, S. S. *Biochem. J.* **1992,** *285,* 569.
158. George, G. N.; Prince, R. C.; Cramer, S. P. *Science* **1989,** *10,* 789.
159. DeRose, V. J.; Mukerji, I.; Latimer, M. J.; Yachandra, V. K.; Sauer, K.; Klein, M. P. *J. Am. Chem. Soc.* **1994,** *116,* 5239.
160. Dismukes, G. C.; Siderer, Y. *FEBS Lett.* **1980,** *121,* 78.

161. Dismukes, G. C.; Siderer, Y. *Proc. Natl. Acad. Sci. U.S.A.* **1981,** *78,* 274.
162. Cole, J.; Yachandra, V. K.; Guiles, R. D.; McDermott, A. E.; Britt, R. D.; Dexheimer, S. L.; Sauer, K.; Klein, M. P. *Biochim. Biophys. Acta* **1987,** *890,* 395.
163. Hansson, O.; Aasa, R.; Vaenngaard, T. *Biophys. J.* **1987,** *51,* 825.
164. Casey, J. L.; Sauer, K. *Biochim. Biophys. Acta* **1984,** *767,* 21.
165. Zimmermann, J.-L.; Rutherford, A. W. *Biochim. Biophys. Acta* **1984,** *767,* 160.
166. Beck, W. F.; de Paula, J. C.; Brudvig, G. W. *J. Am. Chem. Soc.* **1986,** *108,* 4018.
167. Kim, D. H.; Britt, R. D.; Klein, M. P.; Sauer, K. *Biochemistry* **1992,** *31,* 541.
168. Kim, D. H.; Britt, R. D.; Klein, M. P.; Sauer, K. *J. Am. Chem. Soc.* **1990,** *112,* 9389.
169. Haddy, A.; Dunham, W. R.; Sands, R. H.; Aasa, R. *Biochim. Biophys. Acta* **1992,** *1099,* 25.
170. Messinger, J.; Robblee, J. H.; Yu, W. O.; Sauer, K.; Yachandra, V. K.; Klein, M. P. *J. Am. Chem. Soc.* **1997,** *119,* 11349.
171. Messinger, J.; Nugent, J. H. A.; Evans, M. C. W. *Biochemistry* **1997,** *36,* 11055.
172. Åhrling, K. A.; Peterson, S.; Styring, S. *Biochemistry* **1997,** *36,* 13148.
173. Dexheimer, S. L.; Klein, M. P. *J. Am. Chem. Soc.* **1992,** *114,* 2821.
174. Campbell, K. A.; Peloquin, J. M.; Pham, D. P.; Debus, R. J.; Britt, R. D. *J. Am. Chem. Soc.* **1998,** *120,* 447.
175. Yachandra, V. K.; Guiles, R. D.; McDermott, A. E.; Cole, J. L.; DeRose, V. J.; Zimmermann, J. L.; Sauer, K.; Klein, M. P. *Physica B (Amsterdam)* **1989,** *158,* 78.
176. Boussac, A.; Zimmermann, J.-L.; Rutherford, A. W.; Lavergne, J. *Nature* **1990,** *347,* 303.
177. Gilchrist, M. L.; Ball, J. A.; Randall, D. W.; Britt, R. D. *Proc. Natl. Acad. Sci. U.S.A.* **1995,** *92,* 9545.
178. Tang, X.-S.; Randall, D. W.; Force, D. A.; Diner, B. A.; Britt, R. D. *J. Am. Chem. Soc.* **1996,** *118,* 7638.
179. Babcock, G. T.; Barry, B. A.; Debus, R. J.; Hoganson, C. W.; Atamian, M.; McIntosh, L.; Sithole, I.; Yocum, C. F. *Biochemistry* **1989,** *28,* 9557.
180. Force, D. A.; Randall, D. W.; Britt, R. D. *Biochemistry* **1997,** *36,* 12062.
181. Tommos, C.; Tang, X.-S.; Warncke, K.; Hoganson, C. W.; Styring, S.; McCracken, J.; Diner, B. A.; Babcock, G. T. *J. Am. Chem. Soc.* **1995,** *117,* 10325.
182. Tommos, C.; Babcock, G. T. *Acc. Chem. Res.* **1998,** *31,* 18.
183. Fontecave, M.; Pierre, J. C. *Bull. Soc. Chim. Fr.* **1996,** *133,* 653.
184. Hoganson, C. W.; Lydakis-Simantiris, N.; Tang, X.-S.; Tommos, C.; Warncke, K.; Babcock, G. T.; Diner, B. A.; McCracken, J.; Styring, S. *Photosyn. Res.* **1995,** *46,* 177.
185. Babcock, G. T. In "Photosynthesis: From Light to Biosphere"; Mathis, P., Ed.; Kluwer Academic Publishers: Netherlands, **1995,** *II,* 209.
186. Ahlbrink, R.; Haumann, M.; Cherepanov, D.; Bogershausen, O.; Mulkidjanian, A.; Junge, W. *Biochemistry* **1998,** *37,* 1131.
187. Tang, X.-S.; Diner, B. A.; Larsen, B. S.; Gilchrist, J.; M. L.; Lorigan, G. A.; Britt, R. D. *Proc. Natl. Acad. Sci. U.S.A.* **1994,** *91,* 704.
188. Wincencjusz, H.; Van Gorkom, H.; Yocum, C. F. *Biochemistry* **1997,** *36,* 3663.
189. Fine, P. L.; Frasch, W. D. *Biochemistry* **1992,** *31,* 12204.
190. Sandusky, P. O.; Yocum, C. F. *FEBS Lett.* **1983,** *162,* 339.
191. Latimer, M. J.; DeRose, V. J.; Mukerji, I.; Yachandra, V. K.; Sauer, K.; Klein, M. P. *Biochemistry* **1995,** *34,* 10898.
192. Tso, J.; Sivaraja, M.; Dismukes, G. C. *Biochemistry* **1991,** *30,* 4734.
193. Rutherford, A. W. *Trends Biochem. Sci.* **1989,** *14,* 227.
194. Ghanotakis, D. F.; Babcock, G. T.; Yocum, C. F. *FEBS Lett.* **1984,** *167,* 127.

195. DeRose, V. J.; Latimer, M. J.; Zimmerman, J. L.; Mukerji, I.; Yachandra, V. K.; Sauer, K.; Klein, M. P. *Chem. Phys.* **1995,** *194,* 443.
196. Sandusky, P. O.; Yocum, C. F. *Biochim. Biophys. Acta* **1986,** *849,* 85.
197. Radmer, R.; Ollinger, O. *FEBS Lett.* **1986,** *195,* 285.
198. Messinger, J.; Badger, M.; Wydrzynski, T. *Proc. Natl. Acad. Sci. U.S.A.* **1995,** *92,* 3209.
199. Brudvig, G. W.; Crabtree, R. H. *Proc. Natl. Acad. Sci. U.S.A.* **1986,** *83,* 4586.
200. Vincent, J. B.; Christou, G. *Inorg. Chim. Acta* **1987,** *136,* L41.
201. Kirk, M. L.; Chan, M. K.; Armstrong, W. H.; Solomon, E. I. *J. Am. Chem. Soc.* **1992,** *114,* 10432.
202. Larson, E.; Haddy, A.; Kirk, M. L.; Sands, R. H.; Hatfield, W. E.; Pecoraro, V. L. *J. Am. Chem. Soc.* **1992,** *114,* 6263.
203. Randall, D. W.; Gelasco, A.; Caudle, M. T.; Pecoraro, V. L.; Britt, R. D. *J. Am. Chem. Soc.* **1997,** *119,* 4481.
204. Baldwin, M. J.; Pecoraro, V. L. *J. Am. Chem. Soc.* **1996,** *118,* 11325.
205. Caudle, M. T.; Pecoraro, V. L. *J. Am. Chem. Soc.* **1997,** *119,* 3415.
206. Gardner, K. A.; Mayer, J. M. *Science* **1995,** *269,* 1849.
207. Blomberg, M. R. A.; Siegbahn, P. E. M.; Styring, S.; Babcock, G. T.; Akermark, B.; Korall, P. *J. Am. Chem. Soc.* **1997,** *119,* 8285.
208. Kitajima, N.; Osawa, M.; Tamura, N.; Moro-oka, Y.; Hirano, T.; Masaaki, H.; Nagano, T. *Inorg. Chem.* **1993,** *32,* 1879.
209. Kitajima, N.; Tolman, W. B. In "Progress in Inorganic Chemistry"; Karlin, K. D., Ed.; John Wiley & Sons, Inc.: New York, **1995,** *43,* 419.
210. Trofimenko, S. *Chem. Rev.* **1993,** *93,* 943.
211. Lah, M. S.; Chun, H. *Inorg. Chem.* **1997,** *36,* 1782.
212. Oki, A. R.; Bommarreddy, P. R.; Zhang, H.; Hosmane, N. *Inorg. Chim. Acta* **1995,** *231,* 109.
213. Adams, H.; Bailey, N. A.; Crane, J. D.; Fenton, D. E.; Latour, J.-M.; Williams, J. M. *J. Chem. Soc., Dalton Trans.* **1990,** 1727.
214. Di Vaira, M.; Mani, F. *J. Chem. Soc., Dalton Trans.* **1990,** 191.
215. Roesky, H. W.; Scholz, M.; Noltemeyer, M. *Chem. Ber.* **1990,** *123,* 2303.
216. Holleman, S. R.; Parker, O. J.; Breneman, G. L. *Acta. Cryst.* **1994,** *C50,* 867.
217. Andruh, M.; Huebner, K.; Noltemeyer, M.; Roseky, H.; W., *Z. Naturforsch.* **1993,** *48B,* 591.
218. Stolz, P.; Saak, W.; Strasdeit, H.; Pohl, S. *Z. Natursforsch.* **1989,** *44B,* 632.
219. Chen, X.; Long, G.; Willett, R. D.; Hawks, T.; Molnar, S.; Brewer, K. *Acta Cryst.* **1996,** *C52,* 1924.
220. Glerup, J.; Goodson, P. A.; Hodgson, D. J.; Michelsen, K.; Nielsen, K. M.; Weihe, H. *Inorg. Chem.* **1992,** *31,* 4611.
221. Riley, D. P.; Weiss, R. H. *J. Am. Chem. Soc.* **1994,** *116,* 387.
222. Riley, D. P.; Henke, S. L.; Lennon, P. J.; Weiss, R. H.; Neumann, W. L.; Rivers, W.; Aston, J. K. W.; Sample, K. R.; Rahman, H.; Ling, C. S.; Shieh, J. J.; Busch, D. H.; Szulbinski, W. *Inorg. Chem.* **1996,** *35,* 5213.
223. Burns, J. H.; Lumetta, G. J. *Acta Cryst.* **1991,** *C47,* 2069.
224. Deng, Y.; Burns, J. H.; Moyer, B. A. *Inorg. Chem.* **1995,** *34,* 209.
225. Othman, A. H.; Lee, K.-L.; Fun, H.-K.; Yip, B.-C. *Acta Cryst.* **1996,** *C52,* 602.
226. Chan, C.-W.; Che, C.-M.; Peng, S.-M. *Polyhedron* **1993,** *12,* 2169.
227. Brooker, S.; McKee, V. *Acta Cryst.* **1993,** *C49,* 441.
228. Bencini, A.; Biannchi, A.; Dapporto, P.; Garcia-España, E.; Marcelino, V.; Micheloni, M.; Paoletti, P.; Paola, P. *Inorg. Chem.* **1990,** *29,* 1716.

229. Deroche, A.; Morgenstern-Badarau, I.; Cesario, M.; Guilhem, J.; Keita, B.; Nadjo, L.; Houée-Levin, C. *J. Am. Chem. Soc.* **1996,** *118,* 4567.
230. Di Vaira, M.; Mani, F.; Stoppioni, P. *J. Chem. Soc., Dalton Trans.* **1992,** 1127.
231. Hagen, K. S. *Angew. Chem., Int. Ed. Engl.* **1992,** *31,* 764.
232. Gultneh, Y.; Farooq, A.; Karlin, K.; Liu, D. S.; Zubieta, J. *Inorg. Chim. Acta* **1993,** *211,* 171.
233. Knof, U.; Weyhermueller, T.; Wolter, T.; Wieghardt, K. *J. Chem. Soc., Chem. Commun.* **1993,** 726.
234. Bermejo, M. R.; Castineiras, A.; Garcia-Monteagudo, J. C.; Rey, M.; Sousa, A.; Watkinson, M.; McAuliffe, C. A.; Pritchard, R. G.; Beddoes, R. L. *J. Chem. Soc., Dalton Trans.* **1996,** 2935.
235. Jacobsen, E. N. In "Catalytic Asymmetric Synthesis"; Ojima, I., Ed.; VCH Publishers, Inc.: New York, **1993,** 159.
236. Pospisil; Jacobsen, E. N. *Chem. Eur. J.* **1996,** *2,* 974.
237. Pecoraro, V. L.; Butler, W. M. *Acta Cryst.* **1986,** *C42,* 1151.
238. Schake, A. R.; Schmitt, E. A.; Conti, A. J.; Streib, W. E.; Huffman, J. C.; Hendrickson, D. N.; Christou, G. *Inorg. Chem.* **1991,** *30,* 3192.
239. Shirin, Z.; Young, Jr., V. G.; Borovik, A. S. *J. Chem. Soc., Chem. Commun.* **1997,** 1967.
240. Aurangzeb, N.; Hulme, C. E.; McAuliffe, C. A.; Pritchard, R. G.; Watkinson, M.; Bermejo, M. R.; Sousa, A. *J. Chem. Soc., Chem. Commun.* **1994,** 2193.
241. Neves, A.; Vencato, I.; Erthal, S. M. D. *Inorg. Chim. Acta* **1997,** *262,* 77.
242. Eichhorn, D. M.; Armstrong, W. H. *J. Chem. Soc., Chem. Commun.* **1992,** 85.
243. Kitajima, N.; Komatsuzaki, H.; Hikichi, S.; Osawa, M.; Moro-oka, Y. *J. Am. Chem. Soc.* **1994,** *116,* 11596.
244. Larson, E. J.; Pecoraro, V. L. *J. Am. Chem. Soc.* **1991,** *113,* 3810.
245. Law, N. A.; Machonkin, T. E.; McGorman, J. P.; Larson, E. J.; Kampf, J. W.; Pecoraro, V. L. *J. Chem. Soc., Chem. Commun.* **1995,** 2015.
246. Saadeh, S. M.; Lah, M. S.; Pecoraro, V. L. *Inorg. Chem.* **1991,** *30,* 8.
247. Chandra, S. K.; Chakravorty, A. *Inorg. Chem.* **1992,** *31,* 760.
248. Chaudhuri, P.; Wieghardt, K. In "Progress in Inorganic Chememistry"; Lippard, S. J., Ed.; Wiley Interscience, **1987,** *35,* 329.
249. Quee-Smith, V. C.; DelPizzo, L.; Jureller, S. H.; Kerschner, J. L. *Inorg. Chem.* **1996,** *35,* 6461.
250. Schlager, O.; Wieghardt, K.; Nuber, B. *Inorg. Chem.* **1995,** *34,* 6456.
251. Du Bois, J.; Hong, J.; Carreira, E. M.; Day, M. W. *J. Am. Chem. Soc.* **1996,** *118,* 915.
252. Du Bois, J.; Tomooka, C. S.; Hong, J.; Carreira, E. M. *Acc. Chem. Res.* **1997,** *30,* 364.
253. Du Bois, J.; Tomooka, C. S.; Hong, J.; Carreira, E. M.; Day, M. W. *Angew. Chem., Int. Ed. Engl.* **1997,** *36,* 1645.
254. Buchler, J.; Dreher, W. C.; Lay, K.-L.; Lee, Y. J. A.; Scheidt, W. R. *Inorg. Chem.* **1983,** *22,* 888.
255. Collins, T. J.; Gordon-Wylie, S. W. *J. Am. Chem. Soc.* **1989,** *111,* 4511.
256. Collins, T. J.; Powell, R. D.; Slebodnick, C.; Uffelman, E. S. *J. Am. Chem. Soc.* **1990,** *112,* 899.
257. Fackler, N. L. P.; Zhang, S.; O'Halloran, T. V. *J. Am. Chem. Soc.* **1996,** *118,* 481.
258. Niemann, A.; Bossek, U.; Haselhorst, G.; Wieghardt, K.; Nuber, B. *Inorg. Chem.* **1996,** *35,* 906.

259. Tétard, D.; Rabion, A.; Verlhac, J.-B.; Guilhem, J. *J. Chem. Soc., Chem. Commun.* **1995,** 531.
260. Cheng, B.; Cukiernik, F.; Fries, P.; Marchon, J.-C.; Scheidt, W. R. *Inorg. Chem.* **1995,** *34,* 4627.
261. Cheng, B.; Fries, P. H.; Marchon, J.-C.; Scheidt, W. R. *Inorg. Chem.* **1996,** *35,* 1024.
262. Kipke, C. A.; Scott, M. J.; Ghodes, J. W.; Armstrong, W. H. *Inorg. Chem.* **1990,** *29,* 2193.
263. Kitajima, N.; Osawa, M.; Tanaka, M.; Moro-oka, Y. *J. Am. Chem. Soc.* **1991,** *113,* 8952.
264. Schardt, B. C.; Hollander, F. J.; Hill, C. L. *J. Am. Chem. Soc.* **1982,** *104,* 3964.
265. Schardt, B. C.; Hollander, F. J.; Hill, C. L. *J. Chem. Soc., Chem. Commun.* **1981,** 765.
266. Mikuriya, M.; Yamato, Y.; Tokii, T. *Bull. Chem. Soc. Jpn.* **1992,** *65,* 2624.
267. Mikuriya, M.; Yamato, Y.; Tokii, T. *Inorg. Chim. Acta* **1991,** *181,* 1.
268. Nishida, Y.; Oshino, N.; Tokii, T. *Z. Naturforsch.* **1988,** *43B,* 472.
269. Bonadies, J. A.; Kirk, M. L.; Lah, M. S.; Kessissoglou, D. P.; Hatfield, W. E.; Pecoraro, V. L. *Inorg. Chem.* **1989,** *28,* 2037.
270. Larson, E.; Haddy, A.; Kirk, M. L.; Sands, R. H.; Hatfield, W. E.; Pecoraro, V. L. *J. Am. Chem. Soc.* **1992,** *114,* 6263.
271. Kitajima, N.; Singh, U. P.; Amagai, H.; Osawa, M.; Moro-oka, Y. *J. Am. Chem. Soc.* **1991,** *113,* 7757.
272. Glerup, J.; Goodson, P. A.; Hazell, A.; Hazell, R.; Hodgson, D. J.; McKenzie, C. J.; Michelsen, K.; Rychlewska, U.; Toftlund, H. *Inorg. Chem.* **1994,** *33,* 4105.
273. Gelasco, A.; Pecoraro, V. L. *J. Am. Chem. Soc.* **1993,** *115,* 7928.
274. Zhang, Z. Y.; Brouca-Cabarreq, C.; Hemmert, C.; Dahan, F.; Tuchagues, J. P. *J. Chem. Soc., Dalton Trans.* **1995,** 1453.
275. Jensen, A. F.; Su, Z.; Hansen, N. K.; Larsen, F. K. *Inorg. Chem.* **1995,** *34,* 4244.
276. Manchanda, R.; Brudvig, G. W.; de Gala, S.; Crabtree, R. H. *Inorg. Chem.* **1994,** *33,* 5157.
277. Frapart, Y.-M.; Boussac, A.; Albach, R.; Anxolabehere-Mallart, E.; Deiroisse, M.; Verlhac, J.-B.; Blondin, G.; Girerd, J.-J.; Guilhem, J.; Cesario, M.; Rutherford, A. W.; Lexa, D. *J. Am. Chem. Soc.* **1996,** *118,* 2669.
278. Brewer, K. J.; Calvin, M.; Lumpkin, R. S.; Otvos, J. W.; Spreer, L. O. *Inorg. Chem.* **1989,** *28,* 4446.
279. Gelasco, A.; Kirk, M. L.; Kampf, J. W.; Pecoraro, V. L. *Inorg. Chem.* **1997,** *36,* 1829.
280. Larson, E.; Lah, M. S.; Li, X.; Bonadies, J. A.; Pecoraro, V. L. *Inorg. Chem.* **1992,** *31,* 373.
281. Gohdes, J. W.; Armstrong, W. H. *Inorg. Chem.* **1992,** *31,* 368.
282. Larson, E. J.; Riggs, P. J.; Penner-Hahn, J. E.; Pecoraro, V. L. *J. Chem. Soc., Chem. Commun.* **1992,** 102.
283. Baldwin, M. J.; Stemmler, T. L.; Riggs-Gelasco, P. J.; Kirk, M. L.; Penner-Hahn, J. E.; Pecoraro, V. L. *J. Am. Chem. Soc.* **1994,** *116,* 11349.
284. Torayama, H.; Nishide, T.; Asada, H.; Fujiwara, M.; Matsushita, T. *Polyhedron* **1998,** *17,* 105.
285. Torayama, H.; Nishide, T.; Asada, H.; Fujiwara, M.; Matsushita, T. *Chem. Lett.* **1996,** 387.
286. Wieghardt, K.; Bossek, U.; Nuber, B.; Weiss, J.; Bonvoisin, J.; Corbella, M.; Vitols, S. E.; Girerd, J. J. *J. Am. Chem. Soc.* **1988,** *110,* 7398.
287. Bossek, U.; Weyhermüller, T.; Wieghardt, K.; Nuber, B.; Weiss, J. *J. Am. Chem. Soc.* **1990,** *112,* 6387.

288. Arulsamy, N.; Glerup, J.; Hazell, A.; Hodgson, D. J.; McKenzie, C. J.; Toftlund, H. *Inorg. Chem.* **1994,** *33,* 3023.
289. Oberhausen, K. J.; O. B. R. J.; Richardson, J. F.; Buchanan, R. M.; Costa, R.; Latour, J.-M.; Tsai, H.-L.; Hendrickson, D. N. *Inorg. Chem.* **1993,** *32,* 4561.
290. Bertoncello, K.; Fallon, G. D.; Murray, K. S. *Polyhedron* **1990,** *9,* 2867.
291. Pessiki, P. J.; Khangulov, S. V.; Ho, D. M.; Dismukes, G. C. *J. Am. Chem. Soc.* **1994,** *116,* 891.
292. Pal, S.; Armstrong, W. H. *Inorg. Chem.* **1992,** *31,* 5417.
293. Wieghardt, K.; Bossek, U.; Zsoinai, L.; Huttner, G.; Blondin, G.; Girerd, J.-J.; Babonneau, F. *J. Chem. Soc., Chem. Commun.* **1987,** 651.
294. Bossek, U.; Saher, M.; Weyhermuller, T.; Wieghardt, K. *J. Chem. Soc. Chem. Commun.* **1992,** 1780.
295. Reddy, K. R.; Rajasekharan, M. V.; Padhye, S.; Dahan, F.; Tuchagues, J.-P. *Inorg. Chem.* **1994,** *33,* 428.
296. Bashkin, J. S.; Schake, A. R.; Vincent, J. B.; Chang, H.-R.; Li, Q.; Huffman, J. C.; Christou, G.; Hendrickson, D. N. *J. Chem. Soc., Chem. Commun.* **1988,** 700.
297. Caneschi, A.; Ferraro, F.; Gatteschi, D.; Melandria, M. C.; Rey, P.; Sessoli, R. *Angew. Chem., Int. Ed. Engl.* **1989,** *28,* 1365.
298. Bossek, U.; Hummel, H.; Weyhermuller, T.; Wieghardt, K.; Russell, S.; van der Wolf, L.; Kolb, U. *Angew. Chem., Int. Ed. Engl.* **1996,** *35,* 1552.
299. Coucouvanis, D.; Reynolds, R. A.; Dunham, W. R. *J. Am. Chem. Soc.* **1995,** *117,* 7570.
300. Nepveu, F.; Gaultier, N.; Korber, N.; Jaud, J.; Castan, P. *J. Chem. Soc., Dalton Trans.* **1995,** 4005.
301. Turner, P.; Gunter, M. J.; Hambley, T. W.; White, A. H.; Skelton, B. W. *Inorg. Chem.* **1992,** *31,* 2295.
302. Chen, X.-M.; Tong, Y.-X.; Xu, Z.-T.; Mak, C. W. T. *J. Chem. Soc., Dalton Trans.* **1995,** 4001.
303. Ménage, S.; Vitols, S. E.; Bergerat, P.; Codjovi, E.; Girerd, J.-J.; Guillot, M.; Solans, X.; Calvet, T. *Inorg. Chem.* **1991,** *30,* 2666.
304. Hodgson, D. J.; Schwartz, B. J.; Sorrell, T. N. *Inorg. Chem.* **1989,** *28,* 2226.
305. Chang, H.-R.; Diril, H.; Nilges, M. J.; Zhang, X.; Potenza, J. A.; Schugar, H. J.; Hendrickson, D. N.; Isied, S. S. *J. Am. Chem. Soc.* **1988,** *110,* 625.
306. Diril, H.; Chang, H.-R.; Zhang, X.; Larsen, S. *J. Am. Chem. Soc.* **1987,** *109,* 6207.
307. Wesolek, M.; Meyer, D.; Osborn, J. A.; De Cian, A.; Fischer, J.; Derory, A.; Legoll, P.; Drillon, M. *Angew. Chem., Int. Ed. Engl.* **1994,** *33,* 1592.
308. Yu, S. B.; Wang, C. P.; Day, E. P.; Holm, R. H. *Inorg. Chem.* **1991,** *30,* 4067.
309. Ishimura, Y.; Inoue, K.; Koga, N.; Iwamura, H. *Chem. Lett.* **1994,** 1693.
310. Cortés, R.; Lezama, L.; Pizzaro, J. L.; Arriotura, M. I.; Solans, X.; Rojo, T. *Angew. Chem., Int. Ed. Engl.* **1994,** *33,* 2488.
311. Cortés, R.; Pizzaro, J. L.; Lezama, L.; Arriotura, M. I.; Rojo, T. *Inorg. Chem.* **1994,** *33,* 2697.
312. Caudle, M. T.; Kampf, J. W.; Kirk, M. L.; Rasmussen, P. G.; Pecoraro, V. L. *J. Am. Chem. Soc.* **1997,** *119,* 9297.
313. Auger, N.; Girerd, J.-J. *J. Am. Chem. Soc.* **1990,** *112,* 448.
314. Pal, S.; Chan, M. K.; Armstrong, W. H. *J. Am. Chem. Soc.* **1992,** *114,* 6398.
315. Vincent, J. B.; Chang, H.-R.; Folting, K.; Huffman, J. C.; Christou, G.; Hendrickson, D. N. *J. Am. Chem. Soc.* **1987,** *109,* 5703.
316. Bakie, A. R. E.; Hursthouse, M. B.; New, L.; Thornton, P.; Whit, P. G. *J. Chem. Soc., Chem. Commun.* **1980,** 684.

317. Bhula, R.; Gainsford, G. J.; Weatherburn, D. C. *J. Am. Chem. Soc.* **1988,** *110,* 7550.
318. Reynolds, R. A.; Yu, W. O.; Dunham, W. R.; Coucouvanis, D. *Inorg. Chem.* **1996,** *35,* 2721.
319. Kessissoglou, D. P.; Kirk, M. L.; Bender, C. A.; Lah, M. S.; Pecoraro, V. L. *J. Chem. Soc., Chem. Commun.* **1989,** 84.
320. Kitajima, N.; Osawa, M.; Imai, S.; Fujisawa, K.; Moro-oka, Y. *Inorg. Chem.* **1994,** *33,* 4613.
321. Rardin, R. L.; Bino, A.; Poganiuch, P.; Tolman, W. B.; Liu, S.; Lippard, S. J. *Angew. Chem., Int. Ed. Engl.* **1990,** *29,* 812.
322. Baldwin, M. J.; Kampf, J. W.; Kirk, M. L.; Pecoraro, V. L. *Inorg. Chem.* **1995,** *34,* 5252.
323. Wang, S.; Tsai, H.-L.; Hagen, K. S.; Hendrickson, D. N.; Christou, G. *J. Am. Chem. Soc.* **1994,** *116,* 8376.
324. Hendrickson, D. N.; Christou, G.; Schmitt, E. A.; Libby, E.; Bashkin, J. S.; Wang, S.; Tsai, H. L.; Vincent, J. B.; Boyd, P. D. W.; Huffman, J. C.; Folting, K.; Li, Q. Y.; Streib, W. E. *J. Am. Chem. Soc.* **1992,** *114,* 2455.
325. Aubin, S. M. J.; Wemple, M. W.; Adams, D. M.; Tsai, H.-L.; Christou, G.; Hendrickson, D. N. *J. Am. Chem. Soc.* **1996,** *118,* 7746.
326. Mikuriya, M.; Hashimoto, Y.; Kawamori, A. *Chem. Lett.* **1995,** 1095.
327. Wemple, M. W.; Tsai, H.-L.; Folting, K.; Hendrickson, D. N.; Christou, G. *Inorg. Chem.* **1993,** *32,* 2025.
328. Wang, S.; Tsai, H.-L.; Libby, E.; Folting, K.; Streib, W. E.; Hendrickson, D. N.; Christou, G. *Inorg. Chem.* **1996,** *35,* 7578.
329. Brooker, S.; McKee, V.; Shepard, W. B. *J. Chem. Soc., Dalton Trans.* **1987,** 2555.
330. Wieghardt, K.; Bossek, U.; Gebert, W. *Angew. Chem., Int. Ed. Engl.* **1983,** *22,* 328.
331. Bashkin, J. S.; Chang, H.-R.; Streib, W. E.; Huffman, J. C.; Hendrickson, D. N.; Christou, G. *J. Am. Chem. Soc.* **1987,** *109,* 6502.
332. Bouwman, E.; Bocar, M. A.; Libby, E.; Huffman, J. C.; Folting, K.; Christou, G. *Inorg. Chem.* **1992,** *31,* 5185.
333. Gelasco, A.; Askenas, A.; Pecoraro, V. L. *Inorg. Chem.* **1996,** *35,* 1419.
334. Chan, M. K.; Armstrong, W. H. *J. Am. Chem. Soc.* **1991,** *113,* 5055.
335. Kawasaki, H.; Kusumoki, M.; Hayashi, Y.; Suzuki, M.; Munezawa, K.; Suenaga, M.; Senda, H.; Uehara, A. *Bull. Chem. Soc. Jpn.* **1994,** *67,* 1310.
336. Philouze, C.; Blondin, G.; Girerd, J.-J.; Guilhem, J.; Pascard, C.; Lexa, D. *J. Am. Chem. Soc.* **1994,** *116,* 8557.
337. Jeffery, J. C.; Thornton, P.; Ward, M. D. *Inorg. Chem.* **1994,** *33,* 3612.
338. Chan, M. K.; Armstrong, W. H. *J. Am. Chem. Soc.* **1990,** *112,* 4985.
339. Cotton, F. A.; Wilkinson, G. *Advanced Inorganic Chemistry* (John Wiley & Sons, New York, 1988).
340. Weil, J. A.; Bolton, J. R.; Wertz, J. E. *Electron Paramagnetic Resonance: Elementary Theory and Practical Applications* (John Wiley & Sons, New York, 1994).
341. Bencini, A.; Gatteschi, D. *Electron Paramagnetic Resonance of Exchange Coupled Systems* (Springer-Verlag, New York, 1989).
342. de Paula, J. C.; Beck, W. F.; Brudvig, G. W. *J. Am. Chem. Soc.* **1986,** *108,* 4002.
343. de Paula, J. C.; Brudvig, G. W. *J. Am. Chem. Soc.* **1985,** *107,* 2643.
344. Åhrling, K.; Pace, R. J. *Biophys. J.* **1995,** *68,* 2081.
345. Bonvoisin, J.; Blondin, G.; Girerd, J. J.; Zimmermann, J. L. *Biophys. J.* **1992,** *61,* 1076.
346. Zheng, M.; Dismukes, G. C. *Inorg. Chem.* **1996,** *35,* 3307.

347. Tang, X. S.; Gilchrist, M. L.; Lorigan, G. A.; Larson, B.; Britt, R. D.; Diner, B. A. *J. Am. Chem. Soc.* **1993,** *115,* 2382.
348. Britt, R. D.; Zimmermann, J.-L.; Sauer, K.; Klein, M. P. *J. Am. Chem. Soc.* **1989,** *111,* 3522.
349. Randall, D. W.; Sturgeon, B. E.; Ball, J. A.; Lorigan, G. A.; Chan, M. K.; Klein, M. P.; Armstrong, W. H.; Britt, R. D. *J. Am. Chem. Soc.* **1995,** *117,* 11780.
350. Khangulov, S. V.; Voyevodskaya, N. V.; Varynin, V. V.; Grebenko, A. I.; Melik-Adamyan, V. R. *Biofizika* **1987,** *32,* 1044.
351. Khangulov, S.; Sivaraja, M.; Barynin, V. V.; Dismukes, G. C. *Biochemistry* **1993,** *32,* 4912.
352. Waldo, G. S.; Fronko, R. M.; Penner-Hahn, J. E. *Biochemistry* **1991,** *30,* 10486.
353. Kirby, J. A.; Robertson, A. S.; Smith, J. P.; Thompson, A. C.; Cooper, S. R.; Klein, M. P. *J. Am. Chem. Soc.* **1981,** *103,* 5528.
354. Kirby, J. A.; Goodin, D. B.; Wydrzynski, T.; Robertson, A. S.; Klein, M. P. *J. Am. Chem. Soc.* **1981,** *103,* 5537.
355. Guiles, R. D.; Zimmermann, J.-L.; McDermott, A. E.; Yachandra, V. K.; Cole, J. L.; Dexheimer, S. L.; Britt, R. D.; Wieghardt, K.; Bossek, U.; Sauer, K.; Klein, M. P. *Biochemistry* **1990,** *29,* 471.
356. Berthomieu, C.; Boussac, A. *Biochemistry* **1995,** *34,* 1541.
357. Guiles, R. D.; Yachandra, V. K.; McDermott, A. E.; Cole, J. L.; Dexheimer, S. L.; Britt, R. D.; Sauer, K.; Klein, M. P. *Biochemistry* **1990,** *29,* 486.
358. Klein, M. P.; Sauer, K.; Yachandra, V. K. *Photosyn. Res.* **1993,** *38,* 265.
359. Yachandra, V. K.; DeRose, V. J.; Latimer, M. J.; Mukerji, I.; Sauer, K.; Klein, M. P. *Photochem. Photobiol.* **1991,** *53,* 98S.
360. Rompel, A.; Andrews, J. C.; Cinco, R. M.; Wemple, M. W.; Christou, G.; Law, N. A.; Pecoraro, V. L.; Sauer, K.; Yachandra, V. K.; Klein, M. P. *J. Am. Chem. Soc.* **1997,** *119,* 4465.
361. Roelofs, T. A.; Liang, W.; Latimer, M. J.; Cinco, R. M.; Rompel, A.; Andrews, J. C.; Sauer, K.; Yachandra, V. K.; Klein, M. P. *Proc. Natl. Acad. Sci. U.S.A.* **1996,** *93,* 3335.
362. Riggs-Gelasco, P. J.; Mei, R.; Yocum, C. F.; Penner-Hahn, J. E. *J. Am. Chem. Soc.* **1996,** *118,* 2387.
363. Arndt, D. In "Manganese Compounds as Oxidizing Agents in Organic Chemistry"; Lee, D. G., Ed.; Open Court Publishing Company: La Salle, IL, 1981.
364. Snider, B. B. *Chem. Rev.* **1996,** *96,* 339.
365. Jacobsen, E. N. In "Comprehensive Organometallic Chemistry II: A Review of the Literature 1982–1994"; Hegedus, L. S., Ed.; Elsevier Science, Inc.: Tarrytown, NY, **1995,** *12,* 1097.
366. Katsuki, T. *Coord. Chem. Rev.* **1995,** *140,* 189.
367. Katsuki, T. *J. Mol. Catal. A-Chem.* **1996,** *113,* 87.
368. Groves, J. T.; Nemo, T. E.; Myers, R. S. *J. Am. Chem. Soc.* **1979,** *101,* 1032.
369. Groves, J. T.; Haushalter, R. C.; Nakamura, M.; Nemo, T. E.; E. B. J., *J. Am. Chem. Soc.* **1981,** *103,* 2884.
370. "Cytochrome P450: Structure, Mechanism, and Biochemistry"; Ortiz de Montellano, P. R., Ed.; Plenum Press: New York, 1995.
371. Jørgensen, K. A. *Chem. Rev.* **1989,** *89,* 431.
372. Jørgensen, K. A.; Schiøtt, B. *Chem. Rev.* **1990,** *90,* 1483.
373. Meunier, B. *Chem. Rev.* **1992,** *92,* 1411.
374. Meunier, B., Ed., *J. Mol. Catal. A-Chem.* **1996,** *113.*

375. Stern, M. K.; Groves, J. T. In "Manganese Redox Enzymes"; Pecoraro, V. L., Ed.; VCH Publishers, Inc.: New York, **1992,** 233.
376. Groves, J. T.; Stern, M. K. *J. Am. Chem. Soc.* **1983,** *105,* 5791.
377. Groves, J. T.; Nemo, T. E. *J. Am. Chem. Soc.* **1983,** *105,* 5786.
378. Groves, J. T.; Stern, M. K. *J. Am. Chem. Soc.* **1987,** *109,* 3812.
379. Srinivasan, K.; Michaud, P.; Kochi, J. K. *J. Am. Chem. Soc.* **1986,** *108,* 2309.
380. Samsel, E. G.; Srinivasan, K.; Kochi, J. K. *J. Am. Chem. Soc.* **1986,** *107,* 7606.
381. Srinivasan, K.; Kochi, J. K. *Inorg. Chem.* **1985,** *24,* 4671.
382. Feichtinger, D.; Plattner, D. A. *Angew. Chem., Int. Ed. Engl.* **1997,** *36,* 1718.
383. Zhang, W.; Loebach, J. L.; Wilson, S. R.; Jacobsen, E. N. *J. Am. Chem. Soc.* **1990,** *112,* 2801.
384. Jacobsen, E. N.; Zhang, W.; Muci, A. R.; Ecker, J. R.; Deng, L. *J. Am. Chem. Soc.* **1991,** *113,* 7063.
385. Jacobsen, E. N.; Zhang, W.; Güler, M. L. *J. Am. Chem. Soc.* **1991,** *113,* 6703.
386. Irie, R.; Ito, Y.; Katsuki, T. *Synlett* **1991,** *3,* 265.
387. Irie, R.; Noda. K.; Ito, Y.; Matsumoto, N.; Katsuki, T. *Tetrahedron Lett.* **1990,** *31,* 7345.
388. Irie, R.; Noda, K.; Ito, Y.; Katsuki, T. *Tetrahedron Lett.* **1991,** *32,* 1055.
389. Tokunaga, M.; Larrow, J. F.; Fumistoshi, K.; Jacobsen, E. N. *Science* **1997,** *277,* 936.
390. Linker, T. *Angew. Chem., Int. Ed. Engl.* **1997,** *36,* 2060.
391. Finney, N. S.; Pospisil, P. J.; Chang, S.; Palucki, M.; Konsler, R. G.; Hansen, K. B.; Jacobsen, E. N. *Angew. Chem., Int. Ed. Engl.* **1997,** *36,* 1720.
392. Linde, C.; Arnold, M.; Norrby, P.-O.; Akermark, B. *Angew. Chem., Int. Ed. Engl.* **1997,** *36,* 1723.
393. Fu, H.; Look, G. C.; Zhang, E. N.; Jacobsen, E. N.; Wong, C.-H. *J. Org. Chem.* **1991,** *56,* 6497.
394. Sharpless, K. B.; Teranishi, A. Y.; Backvall, J.-E. *J. Am. Chem. Soc.* **1977,** *99,* 3120.
395. Norrby, P.-O.; Linde, C.; Åkermark, J. *J. Am. Chem. Soc.* **1995,** *117,* 11035.
396. Yamada, T.; Imagawa, K.; Mukaiyama, T. *Chem. Lett.* **1992,** 2109.
397. Collman, J. P.; Zhang, X.; Lee, V. J.; Uffelman, E. S.; Braumann, J. *Science* **1993,** *261,* 1404.
398. Lai, T.-S.; Kwong, H.-L.; Che, C.-M.; Peng, S.-M. *J. Chem. Soc., Chem. Commun.* **1997,** 2373.
399. Halterman, R. L.; Jan, S.-T. *J. Org. Chem.* **1991,** *56,* 5253.
400. Groves, J. T.; Han, Y.-Z. In "Cytochrome P450: Structure, Mechanism, and Biochemistry"; Ortiz de Montellano, P. R., Ed.; Plenum Press: New York, **1995,** 3.
401. Beckman, J. S. *Chem. Res. Toxicol.* **1996,** *9,* 836.
402. Beal, M. F. *Neuroscientist* **1997,** *3,* 21.
403. Hunt, J. A.; Lee, J. B.; Groves, J. T. *Chem. Biol.* **1997,** *4,* 845.
404. Marla, S. S.; Lee, J.; Groves, J. T. *Proc. Natl. Acad. Sci. U.S.A.* **1997,** *94,* 14423.
405. Groves, J. T.; Takahashi, T.; Butler, W. M. *Inorg. Chem.* **1983,** *22,* 884.
406. Chang, C. J.; Low, D. W.; Gray, H. B. *Inorg. Chem.* **1997,** *36,* 270.
407. Bottomley, L. A.; Neeley, F. L. *Inorg. Chem.* **1997,** *36,* 5435.
408. Dehnicke, K.; Strahle, J. *Angew. Chem., Int. Ed. Engl.* **1992,** *31,* 955.
409. Groves, J. T.; Takahashi, T. *J. Am. Chem. Soc.* **1983,** *105,* 2073.
410. Bellesia, F.; Ghelfi, F.; Pagnoni, U. M.; Pinetti, A. *J. Chem. Res. (S)* **1989,** 360.
411. Bellesia, F.; Ghelfi, F.; Pagnoni, U. M.; Pinetti, A. *J. Chem. Res. (S)* **1989,** 108.
412. Bellesia, F.; Ghelfi, F.; Pagnoni, U. M.; Pinetti, A. *Synth. Commun.* **1991,** *21,* 489.
413. Bellesia, F.; Ghelfi, F.; Pagnoni, U. M.; Pinetti, A. *J. Chem. Res. (S)* **1991,** 284.

414. Bellesia, F.; Ghelfi, F.; Pagnoni, U. M.; Pinetti, A. *Gazz. Chim. Italiana* **1993,** *123,* 289.
415. Bellesia, F.; Ghelfi, F.; Pagnoni, U. M.; Pinetti, A. *J. Chem. Res. (S)* **1990,** 188.
416. Kurosawa, K.; Yamaguchi, K. *Bull. Chem. Soc. Jpn.* **1981,** *54,* 1757.
417. Donnelly, K. D.; Fristad, W. E.; Gellerman, B. J.; Peterson, J. R.; Selle, B. J. *Tetrahedron Lett.* **1984,** *25,* 607.
418. Markó, I. E.; Richardson, P. F. *Tetrahedron Lett.* **1991,** *32,* 1831.
419. Richardson, P. F.; Markó, I. E. *Synlett,* **1991,** 733.
420. Uemara, S.; Okazaki, H.; Onoe, A.; Okano, M. *Bull. Chem. Soc. Jpn.* **1978,** *51,* 3568.
421. Tanner, D. D.; Gidley, G. C. *J. Org. Chem.* **1968,** *33,* 38.
422. Poutsma, M. L. *J. Am. Chem. Soc.* **1965,** *87,* 4285.
423. Markó, I. E.; Richardson, P. R.; Bailey, M.; Maguire, A. R.; Coughlan, N. *Tetrahedron Lett.* **1997,** *38,* 2339.
424. Huynh, V.-B.; Crawford, R. L. *FEMS Microbiol. Lett.* **1985,** *28,* 119.
425. Saadeh, S. M. Ph.D. Thesis, University of Michigan, 1992.
426. Policar, C.; Artaud, I.; Mansuy, D. *Inorg. Chem.* **1996,** *35,* 210.
427. Riley, D. P.; Lennon, P. J.; Neumann, W. L.; Weiss, R. H. *J. Am. Chem. Soc.* **1997,** *119,* 6522.
428. Weiss, R. H.; Flickinger, A. G.; Rivers, W. J.; Hardy, M. M.; Aston, K. W.; Ryan, U. S.; Riley, D. P. *J. Biol. Chem.* **1993,** *268,* 23049.
429. Beyer, W. F. J.; Fridovich, I. *Arch. Biochem. Biophys.* **1989,** *271,* 149.
430. Beyer, W. F. J.; Fridovich, I. *Methods Enzym.* **1990,** *186,* 242.
431. Darr, D.; Zarilla, K. A.; Fridovich, I. *Arch. Biochem. Biophys.* **1987,** *258,* 351.
432. Rush, J. D.; Maskos, Z.; Koppenol, W. H. *Arch. Biochem. Biophys.* **1991,** *289,* 97.
433. Matsushita,T.; Shono, T. *Bull. Chem. Soc. Jpn.* **1981,** *54,* 3743.
434. Baudry, M.; Etienne, S.; Bruce, A.; Palucki, M.; Jacobsen, E.; Malfroy, B. *Biochem. Biophys. Res. Commun.* **1993,** *192,* 964.
435. Doctorow, S. R.; Huffman, K.; Marcus, C. B.; Musleh, W.; Bruce, A.; Baudry, M.; Malfroy, B. Academic Press: New York, **1997,** *38,* 247.
436. Rajan, R.; Rajaram, R.; Nair, B. U.; Ramasami, T.; Mandal, S. K. *J. Chem. Soc., Dalton Trans.* **1996,** 2019.
437. Frasch, W. D.; Mei, R. *Biochim. Biophys. Acta* **1987,** *891,* 8.
438. Mathur, P.; Crowder, M.; Dismukes, G. C. *J. Am. Chem. Soc.* **1987,** *109,* 5227.
439. Pessiki, P. J.; Dismukes, G. C. *J. Am. Chem. Soc.* **1994,** *116,* 898.
440. Gelasco, A.; Bensiek, S.; Pecoraro, V. L. *Inorg. Chem.* **1998,** *37,* 3301.
441. Sakiyama, H.; Okawa, H.; Isobe, R. *J. Chem. Soc., Chem. Commun.* **1993,** 882.
442. Sakiyama, H.; Tamaki, H.; Kodera, M.; Matsumoto, N.; Okawa, H. *J. Chem. Soc., Dalton Trans.* **1993,** 591.
443. Naruta, Y.; Maruyama, K. *J. Am. Chem. Soc.* **1991,** *113,* 3595.
444. Naruta, Y.; Sasayama, M. *J. Chem. Soc., Chem. Commun.* **1994,** 2667.
445. Naruta, Y.; Sasayama, M.-A.; Ichihara, K. *J. Mol. Cat. A* **1997,** *117,* 115.
446. Larson, E. J.; Pecoraro, V. L. *J. Am. Chem. Soc.* **1991,** *113,* 7809.
447. Stibrany, R. T.; Gorun, S. M. *Angew. Chem., Int. Ed. Engl.* **1990,** *29,* 1156.
448. Mathews, J. H.; Dewey, L. H. *J. Phys. Chem.* **1913,** *17,* 211.
449. Ashmawy, F. M.; McAuliffe, C. A.; Parish, R. V.; Tames, J. *J. Chem. Soc., Chem. Commun.* **1984,** 14.
450. Ashmawy, F. M.; McAuliffe, C. A. *J. Chem. Soc., Dalton Trans.* **1985,** 1391.
451. Watkinson, M.; Whiting, A.; McAuliffe, C. A. *J. Chem. Soc., Chem. Commun.* **1994,** 2141.

452. Fujiwara, M.; Matsushita, T.; Shono, T. *Polyhedron* **1985,** *4,* 1895.
453. Matsushita, T.; Fujiwara, M.; Shono, T. *Chem. Lett.* **1981,** 631.
454. Matsushita, T.; Hirata, Y.; Shono, T. *Bull. Chem. Soc. Jpn.* **1982,** *55,* 108.
455. Naruta, Y.; Sasayama, M.; Sasaki, T. *Angew. Chem., Int. Ed. Engl.* **1994,** *33,* 1839.
456. Limburg, J.; Brudvig, G. W.; Crabtree, R. H. *J. Am. Chem. Soc.* **1997,** *119,* 2761.
457. Lind, J.; Shen, X.; Ericksen, T. E.; Merényi, G. *J. Am. Chem. Soc.* **1990,** *112,* 479.
458. McMillen, D. F.; Golden, D. M. *Ann. Rev. Phys. Chem.* **1982,** *33,* 493.
459. Thorp, H. H.; Sarneski, J. E.; Brudvig, G. W.; Crabtree, R. H. *J. Am. Chem. Soc.* **1989,** *111,* 9249.
460. Cooper, S. R.; Calvin, M. *J. Am. Chem. Soc.* **1977,** *99,* 6623.
461. Shank, M.; Barynin, V.; Dismukes, G. C. *Biochemistry* **1994,** *33,* 15433.
462. Vainshtein, B. K.; Melik-Adamyan, W. R.; Barynin, V. V.; Vagin, A. A. In "Progress in Bioorganic Chemistry and Molecular Biology"; Ovchinnikov, Y. A., Ed.; Elsevier Science Publishers: New York, **1984,** 117.
463. Nagata, T.; Mizukami, J. *J. Chem. Soc., Dalton Trans.* **1995,** 2825.
464. Nishida, Y.; Akamatsu, T.; Kazuyoshi, T.; Sakamoto, M. *Polyhedron* **1994,** *13,* 2251.
465. Dave, B. C.; Czernuszewicz, R. S. *Inorg. Chim. Acta.* **1994,** *227,* 33.
466. Higuchi, C.; Sakiyama, H.; Okawa, H.; Fenton, D. E. *J. Chem. Soc., Dalton Trans.* **1995,** 4015.
467. Riggs-Gelasco, P. J. Ph.D. Thesis, University of Michigan, 1995.
468. Defrance, S.; Meunier, B.: Séris, J.-L. *New J. Chem.* **1992,** *16,* 1015.
469. Tangoulis, V.; Malamatari, D. A.: Soulti, K.; Stergiou, V.; Raptopoulou, C. P.; Terzis, A.; Kabanos, T. A.; Kessissoglou, D. P. *Inorg. Chem.* **1996,** *35,* 4974.
470. Cheng, B.; Scheidt, W. R. *Acta Cryst.* **1996,** *C52,* 361.
471. Stephenson, G. R. In "Advanced Asymmetric Synthesis"; Stephenson, G. R., Ed.; Chapman and Hall: New York, **1996,** 367.
472. Vincent, J. B.; Tsai, H.-L.; Blackman, A. G.; Wang, S.; Boyd, P. D. W.; Folting, K.; Huffman, J. C.; Lobovsky, E. B.; Hendrickson, D. N.; Christou, G. *J. Am. Chem. Soc.* **1993,** *115,* 12353.
473. Yu, S.-B.; Lippard, S. J.; Shewky, I.; Bino, A. *Inorg. Chem.* **1992,** *31,* 3502.
474. Mikuriya, M.; Fujii, T.; Tokii, T.; Kawamori, A. *Bull. Chem. Soc. Jpn.* **1993,** *66,* 1675.
475. Diril, H.; Chang, H.-R.; Nilges, M. J.; Zhang, X.; Potenza, J. A.; Schugar, H. J.; Isied, S. S.; Hendrickson, D. N. *J. Am. Chem. Soc.* **1989,** *111,* 5102.
476. Kessissoglou, D. P.; Butler, W. M.; Pecoraro, V. L. *Inorg. Chem.* **1987,** *26,* 495.
477. Riggs-Gelasco, P. J.; Rui, M.; Ghanotakis, D. F.; Yocum, C. F.; Penner-Hahn, J. E. *J. Am. Chem. Soc.* **1996,** *118,* 2400.
478. Michaud-Soret, I.; Jacquamet, L.; Debaecker-Petit, N.; Le Pape, L.; Barynin, V. V.; Latour, J.-M. *Inorg. Chem.* **1998,** *37,* 3874.